Zeolite Resources in Wyoming

Robert W. Gregory, Jacob D. Carnes, and Davin A. Bagdonas

Report of Investigations No. 72 • 2016

WYOMING STATE GEOLOGICAL SURVEY
Thomas A. Drean, Director and State Geologist

Director and State Geologist Thomas A. Drean

Design and layout by:
Christina D. George

Cover photo: Outcrops of Tertiary rocks exposed along Beaver Rim, Fremont County, including the Wagon Bed, White River, and Split Rock Formations.

Left: Lacustrine (lake bed) outcrops of the Green River Formation in Middle Firehole Canyon east of Flaming Gorge Reservoir (looking west), Sweetwater County. Much of southwest Wyoming was covered by a vast lake (Lake Gosiute) during early to middle Eocene time (55-38 million years ago), and numerous natural zeolite deposits eventually formed in Eocene rocks of this and similar Eocene lakes.

Zeolite Resources in Wyoming

Wyoming State Geological Survey (WSGS) Report of Investigations No. 72, 2016

Citation: Gregory, R.W., Carnes, J.D., and Bagdonas, D.A., 2016, Zeolite resources in Wyoming: Wyoming State Geological Survey Report of Investigations 72, 65 p.

For additional information about the WSGS or to order publications and maps, log on to http://www.wsgs.wyo.gov, call 307-766-2286, ext. 224, or email wsgs-info@wyo.gov.

Zeolite Resources in Wyoming

Wyoming State Geological Survey
Report of Investigations No. 72
2016

Robert W. Gregory, Jacob D. Carnes, and Davin A. Bagdonas

Wyoming State Geological Survey, Laramie, Wyoming 82071

Table of Contents

List of Figures

List of Tables

ABSTRACT

Natural zeolites are hydrous, aluminosilicate minerals that typically contain alkali and alkaline earth metals, and occur in a variety of geologic settings. There are several groups of natural zeolites with differing chemical and physical properties, but unlike other minerals, nearly all are porous at the molecular level. Due to their large void volume, natural zeolites are low density minerals, reducing handling and processing costs. They are known as molecular sieves due to their molecular-level porosity, which gives them the unique ability to remove and exchange ions and molecules from fluids and gases based on size, shape, and electric charge. Natural zeolites also exhibit a high degree of reversible hydration, making them reusable, with treatment, for extended periods of time.

The unique properties and characteristics of natural zeolites make them useful in a variety of industrial agricultural applications requiring molecular sieves, ion exchange processes, and adsorption. Similar materials are designed for specific applications, but natural zeolites offer the advantage of lower production costs and higher volumes available in natural deposits. Natural zeolites occur in large quantities in Wyoming, primarily in the Washakie Basin. Additional deposits occur at the margins of the Wind River Basin and the Bighorn Basin. Depositional settings favorable for zeolite formation occurred over much of the Tertiary in Wyoming, particularly lacustrine systems such as the Eocene Green River Formation and its time equivalents. Volcanism during much of that same time supplied the aluminosilicate and alkalic ash fall components from which natural zeolites typically form.

This investigation is an attempt to verify previously reported occurrences as well as explore additional favorable locations for natural zeolite deposits. Additionally, X-ray diffraction, multi-element geochemistry, and microscopic examination will aid future research and exploration, and lead to an expansion of the development of Wyoming's natural zeolite resources.

INTRODUCTION

Background

Natural zeolites comprise a group of industrial minerals with a diverse range of applications. The unique characteristics of zeolites make them useful in a long list of applications, including agriculture, hazardous waste containment, odor control, water and air purification, cement manufacturing, and many specialized uses. These minerals present a development opportunity for Wyoming because (1) Wyoming hosts deposits of natural zeolites in minable quantities, (2) most zeolites currently used by industry are synthetic and therefore more costly to utilize than natural zeolites, and (3) the utility of zeolites is expanding in a variety of areas and continues to prove useful as new applications are demonstrated. While synthetic zeolites can be made with greater phase purity and uniformity, many applications do not require such high standards and thus make natural zeolites more attractive given their lower production costs.

The Swedish mineralogist Axel Fredrik Cronstedt, in 1756, observed steam emanating from the mineral stilbite [$Ca(Al_2Si_7O_{18})•7H_2O$] upon rapid heating and concluded that it must contain water within its crystal structure. He coined the term *zeolite*, which in Greek loosely translates to *boiling stones*. Many zeolite minerals will exhibit this frothing upon heating (Mumpton, 1978).

Natural zeolites are hydrated aluminosilicate minerals of alkali and alkaline earth elements, most commonly sodium, potassium, and calcium. As tectosilicates, zeolites have framework structures that interconnect cavities ranging from 3 to 10 angstroms (Å) (Tchernev, 2006). These channels are filled with water, and their walls hold exchangeable cations (Gottardi and Galli, 1985). The channel "walls" (the crystal atomic lattice) in a three-dimensional volume of zeolite represents a vast area (in two dimensions) on which cation exchange can take place. The channeled structure of zeolites results in their high cation exchange capacity (CEC). The high CEC of zeolites applies to liquids, gases, and vapors. Cation exchange occurs at normal atmospheric pressures and temperatures (less than 100°C; Gottardi and Galli, 1985). Since the internal channels are relatively large, they allow smaller molecules and cations to enter the mineral framework and become adsorbed, while larger components are excluded and remain in the gas or liquid exposed to the zeolite. For example, smaller organic molecules can be separated from larger ones using zeolites. Other methods of separation may be ineffective due to similar properties of such materials (Flanigen and Mumpton, 1977). Because of this filtering ability, zeolites are often referred to as molecular sieves. They are capable of almost complete reversible dehydration (Deer and others, 1967). The chemically inert nature of zeolites leads to properties that are desirable in industrial minerals: they are non-toxic, biologically neutral, and environmentally stable.

Synthetic zeolites for specific applications gained popularity in the 1950s, and their research and development is ongoing. Presently, there are more than 150 synthetic zeolite framework structures and more than 60 natural zeolite minerals known (Proceedings of the National Academy of Sciences website, March 2016).

Small amounts of natural zeolites occur in many igneous rocks. All zeolites of economic potential are sedimentary in nature and largely formed by the devitrification and alteration of tuffaceous deposits (Bramlette and Posnjak, 1933). These deposits originated as pyroclastic ejecta, primarily as volcanic ash. Subsequent burial and diagenesis caused zeolite mineralization within sedimentary beds of early Tertiary age (65-25 Ma) in the Rocky Mountain region. Hay (1978) and Surdam and Sheppard (1978) provide detailed descriptions of natural zeolite formation. The reader is also referred to Hay and Sheppard (1977), Iijima (1980), Gottardi (1989), and Lander and Hay (1993) for good technical reviews and discussions of zeolite genesis.

In addition to the mentioned references on zeolite genesis, there are several other general sources on zeolites. Natural zeolite structure and chemistry are well covered by Gottardi and Galli (1985), while those aspects of synthetic zeolites can be found in Breck (1974). Additional sources for explanations of the origin, properties, and uses of zeolites are also available by Mumpton (1977), Sand and Mumpton (1978), and Kallo and Sherry (1988). The International Natural Zeolite Association holds conferences every four years, and its "Book of Abstracts" is an exceptional source for trends in zeolite research. Scientific periodicals covering zeolites include "Zeolites" and "Clays and Clay Minerals."

Scope and results of project

The Wyoming State Legislature, in 2014, allocated $252,488 to the Wyoming State Geological Survey (including $94,488 in Abandoned Mine Lands funds) to investigate the state's iron, lithium, rare earth elements (REE), and natural zeolite mineral resources. The AML money was designated to REE, and this investigation was allotted $102,960.

Primary goals of this investigation are to examine and sample known or reported zeolite occurrences referred to in previous studies in Wyoming, including King and Harris (2002), graduate theses such as Bay (1969) and others referenced herein. Along with summaries of previous investigations, we examined areas with favorable rock units or geologic settings, or both, and depositional histories, with the focus of documenting new zeolite mineral occurrences. All samples collected during the course of this study were analyzed using X-ray diffraction (XRD) to identify zeolite minerals by comparing diffractogram patterns with those of known natural zeolite mineral species. Samples with identifiable zeolite phases were subsequently analyzed for major, minor, and trace elements, and whole rock geochemistry. Samples were also selected for thin section examination and photography, or scanning electron microscope (SEM) analysis. Multi-element geochemistry is an invaluable resource as it can reveal the existence of rock characteristics that may be of value in the future despite the lack of a present application or value.

The scope of this investigation precluded a complete reconnaissance of all possible zeolite occurrences within tuffaceous or igneous rocks in Wyoming. However, we have attempted to sample a wide variety of locations and as many as possible given the time, funding, and seasonal constraints of such an endeavor. Should additional finds be made in conjunction with other current or future the WSGS investigations and mapping projects, we will continue to add all such information to our sample databases.

This investigation provides the reader with detailed insight into the nature of zeolite minerals and their potential applications, and perhaps development opportunities at some point in the future. Data, including sample locations, geochemical analyses, and geologic depositional setting, will expand the potential for development opportunities in areas of interest based on some of the associated information gathered along with that of zeolite minerals. Products of this investigation include this written report with maps, photographs of sample sites, samples, and photographs of samples under the microscope and in thin section. All field descriptions, photographs, raw XRD data, and geochemical analytical data will be made available online by way of our Wyoming Database of Geology (Wyo-DOG, currently in development) with free access via the WSGS website at http://www.wsgs.wyo.gov/.

Samples and analyses

Samples collected during the course of this investigation are only intended as a quick check of a potentially zeolitic-bearing rock formation (or a bed within a formation) and as such are not necessarily representative of the entire rock unit. Grab samples neither confirm nor deny the existence of economic concentrations of zeolite minerals. A more detailed and systematic sampling protocol would be necessary to make estimates of zeolite concentrations across a large area. The grab sample only indicates the character of that volume of rock sampled. Every possible attempt was made to sample that which appears representative of any given outcrop.

In addition to hand samples and petrographic observations, samples were crushed and pulverized with a hammer mill and mortar/pestle, respectively, then scanned by XRD (Rigaku MiniFlex II desktop diffractometer, with the following parameters: 30 kV, 15 mA, 0.02° step width, and 1.02 seconds/step scan speed). Geochemical analyses on samples collected for this study were performed by ALS Chemex, Inc., of Reno, Nevada. Major element oxides were

analyzed by inductively coupled plasma atomic emission spectrometry (ICP-AES), and multi-element suites were analyzed by inductively coupled plasma mass spectrometry (ICP-MS). With effective preparation, these methods have shown to be reliable as reconnaissance analytical tools, and accurate to within 1/100th of a percent for whole rock analyses and 10 parts per billion for most elements within the multi-element suites of analyses. Geochemical analyses are presented in Appendix 2 (tables 6, 7, and 8).

Zeolite applications

Zeolites are used in some of society's most crucial sectors. The following subsections touch on only a fraction of the current and potential beneficial uses of natural zeolites. While this investigation targets natural zeolites in Wyoming, some of the applications described below currently are better filled by synthetic zeolites. Much ongoing research is geared toward the possible substitution of lesser expensive natural zeolites for synthetic versions. An excellent resource for additional reading into applications and ongoing research and development is the International Natural Zeolite Association's "Book of Abstracts" accompanying the group's quadrennial international conferences.

Virta and Flanagan (2014) list several current uses of natural zeolites. The top five accounted for nearly 80 percent of usage in 2014 and are, in order of decreasing tonnage used, animal feed, odor control, water purification, pet litter, and wastewater treatment. Following the top five are, in order of decreasing tonnage used, gas absorption and adsorption, fertilizer carriers, oil absorbents, desiccants, catalysis, fungicide and pesticide carriers, aquaculture, and cement. See Appendix 1 for brief summaries of some research areas in which natural zeolites are applied and utilized.

Natural zeolite production and prices

Virta and Flanagan (2014) report that approximately 3 million metric tons (tonnes) of natural zeolite was produced globally in 2014, most of which was mined in China. Thirty-seven countries are believed to produce natural zeolite, the top eight of which are listed in table 1. Other nations reportedly producing natural zeolite in 2014 included Korea, Turkey, Cuba, Jordan, Mexico, and Indonesia, in decreasing order of tonnage produced (Virta and Flanagan, 2014).

Production in the United States ranked third among all countries in 2014, with 64,100 tonnes from eight mines in six western states (fig. 1; Virta and Flanagan, 2014). The most recent domestic clinoptilolite production was from, in decreasing order of total production, New Mexico, Texas, Idaho, California, and Oregon. Additionally, Virta and Flanagan (2014) report Arizona produced chabazite and accounted for the lowest tonnage among producing states.

Table 1. The top eight natural zeolite producing countries in 2014. Data from Virta and Flanagan, 2014.

Country	Production (thousand tonnes)
China	1,800 - 2,200 est.
Republic of Korea	230
United States	64.1
Turkey	40 - 50 est.
Cuba	44.0
Jordan	13.0
Mexico	2.0 - 2.5 est.
Indonesia	1.5

Figure 1. Locations of recent zeolite mining operations in the United States (Modified after Eyde and Holmes, 2006; data from Virta and Flanagan, 2014).

Wyoming has one historic commercial natural zeolite deposit, the Fort LaClede deposit in southeastern Sweetwater County (King and Harris, 2002). According to Wyoming State Department of Revenue ad valorem documents, 12,020 tons of clinoptilolite came from the mine in 2002. Eyde and Holmes (2006) report that in the 1980s, small amounts of clinoptilolite-chabazite were mined by

U.S. Energy Corporation for use in an experimental sewage treatment plant in Riverton, Wyoming. They do not cite the amount mined or the location of the mine, other than at Beaver Rim.

Natural zeolite prices vary between $110 and $440 per tonne but average about $165 per tonne, depending on purity and contractual negotiations (Virta and Flanagan, 2014).

Zeolite mining

Natural zeolite mining in the United States is carried out by surface pit operations (figs. 2 and 3). There is typically a minor amount of overburden to remove before reaching deposits ranging from a few tens up to several hundred feet in thickness. Mining operations are not complex; large masses are either stripped or blasted when necessary, and thicker deposits are often mined by bench methods. Systematic drilling and sampling programs are both crucial elements in defining the extent and quality of the overall deposit. The milling process includes crushing, screening, sizing, and packaging. Depending on the end product desired, fine grinding (-60 to +325 mesh) and even ultrafine or micron (μ) sized grinding may be used (1 – 10μ; 1μ = 1/1,000th of a millimeter). Particle sizes as fine as 1μ are used in such applications as paper filler (Holmes, 1994). Most mines offer their finished products – some pretreated – for sale in bulk or in smaller quantities as retail products such as pet litter, algae control for aquariums, spill control and cleanup.

Figure 2. Clinoptilolite quarry near Winston, New Mexico, operated by St. Cloud Mining Company.

Figure 3. Clinoptilolite quarry near Death Valley Junction, California, (Ash Meadows Zeolite LLC).

GEOLOGY OF NATURAL ZEOLITES

Natural zeolites have been known since 1756 when the Swedish mineralogist Axel Fredrik Cronstedt coined the term *zeolite* from the Greek words for boiling and stone. Cronstedt collected some curious crystals from a copper mine and noticed that upon heating with a blowpipe, the minerals exhibited a peculiar frothing. That was the result of water being driven out of the void spaces within the minerals' crystalline molecular framework. He would name that particular mineral stilbite (table 2).

Mineralogy

The unique value of zeolites is derived from their abilities of adsorption, desorption, and reversible hydration and dehydration. Natural zeolites are hydrated aluminosilicate minerals of alkali and alkaline earth elements (Sheppard, 1976). Their aluminosilicate base structure (fig. 4) consists of an oxygen atom shared by two tetrahedra of silicon or aluminum in the form $(AlSi)O_4$. In three dimensions, the arrangement translates to a framework structure of voids interconnected by channels of uniform diameter (fig. 5). On a molecular scale, this results in a highly porous and nearly infinite surface area. Breck (1974) offers an extensive list of tables containing detailed chemical and physical properties of many natural and a few synthetic zeolites.

Chemical properties

Chemically, the arrangement of aluminum and silicon results in a net negative charge of the overall structure

Table 2. Some of the common natural zeolite minerals, chemical formulas, and select properties. Modified after Harris (1995), Sand and Mumpton (1978), and Breck (1974).

Mineral Name	Chemical Formula (from Harris, 1993)	Crystal System	void volume %	specific gravity
Analcime (a.k.a. Analcite)	$Na(AlSi_2O_6)•H_2O$	cubic	18	2.24 - 2.29
Chabazite	$(Ca,Na_2)_2[Al_4Si_8O_{24}]•13H_2O$	hexagonal-rhombohedral	47	2.05 - 2.1
Clinoptilolite	$(Na_2,K_2,Ca)[Al_3Si_{10}O_{24}]•8H_2O$	monoclinic	39	2.16
Dachiardite	$(Ca,Na_2\ K_2)_5[Al_{10}Si_{38}O_{96}]•24H_2O$	monoclinic, orthorhombic	34	2.16
Epistilbite	$Ca_3([Al_6Si_{18}O_{48}]•16H_2O$	monoclinic	25	2.21
Erionite	$(Na_2,K_2,Ca)_{4.5}[Al_9Si_{27}O_{72}]•27H_2O$	hexagonal	35	2.02 - 2.08
Faujasite	$(Ca,Na_2)[Al_2Si_4O_{12}]•8H_2O$	cubic	47	1.91
Ferrierite	$(K,Na)_2(Mg)[Al_3Si_{15}O_{36}](OH)•9H_2O$	orthorhombic	0	2.14 - 2.21
Gismondine (a.k.a. Gismondite)	$(Ca,Na_2\ K_2)[Al_2Si_2O_8]•4H_2O$	monoclinic	46	2.27
Gonnardite	$Na_2Ca[(Al,Si)_5O_{10}]_2•7H_2O$	orthorhombic	31	2.25
Harmotome	$Ba[Al_2Si_6O_{16}]•6H_2O$	tetragonal	31	2.35
Heulandite	$(Ca,Na_2)[Al2Si_7O_{18}]•6H_2O$	monoclinic	39	2.1 - 2.2
Laumontite	$Ca[Al_2Si_4O_{12}]•4H_2O$	monoclinic	34	2.2 - 2.3
Mordenite	$(Na_2,\ K_2,Ca)[Al_2Si_{10}O_{24}]•6H_2O$	orthorhombic	28	2.12 - 2.15
Natrolite	$Na_2[Al_2Si_3O_{10}]•4H_2O$	orthorhombic	23	2.23
Phillipsite	$(Ca,Na_2K_2)_{2.5}[Al_5Si_{11}O_{32}]•10H_2O$	monoclinic	31	2.15 - 2.2
Scolecite	$Ca[Al_2Si_3O_{10}]•3H_2O$	monoclinic	31	2.27
Stilbite	$Ca_2Na[Al_5Si_{13}O_{36}]•16H_2O$	monoclinic	39	2.16
Thomsonite	$Ca_2,Na[(AlSi)_5O_{20}]•6H_2O$	orthorhombic	32	2.3
Yugawaralite	$Ca[Al_2Si_5O_{14}]•4H_2O$	monoclinic	27	2.2

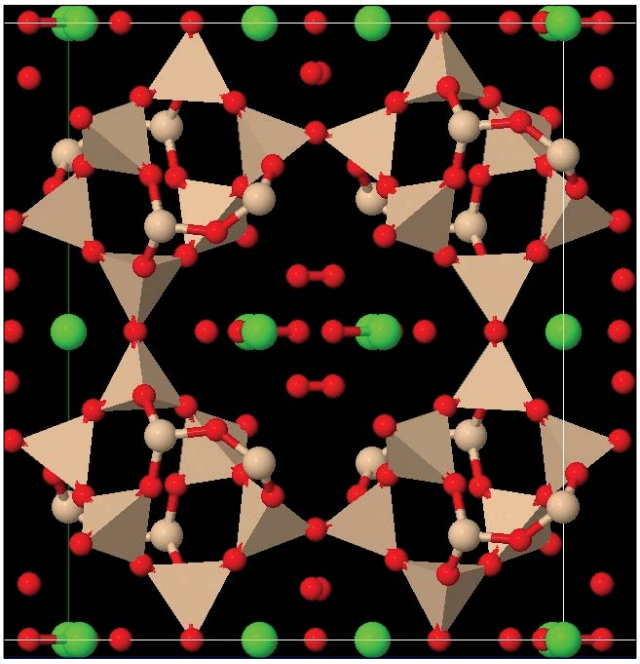

Figure 4. Unit cell of clinoptilolite showing tetrahedra (beige). Each tetrahedra is made up of four oxygen atoms (red spheres) and one silicon atom (beige spheres – one is concealed in the center of each tetrahedron). Green spheres represent exchangeable cations (typically Ca, K, Na).

where, in general, the greater the aluminum content in the framework structure, the more negative the overall charge and the higher the capacity for exchange with positively charged cations or molecules. The negative charge of the framework is balanced by the exchangeable alkali and alkaline earth cations of calcium, potassium, sodium and less commonly, magnesium. The most common and widely used natural zeolite minerals are listed in table 2. Also listed are their general chemical formulas, crystal system, and void (pore) volume (after Breck, 1974). Lower cation exchange capacities can be the result of cations or other particles larger in diameter than the channel widths becoming trapped within the framework during the formation of the zeolite minerals, thereby reducing the potential number of sites for future exchanges. To some degree, this can be countered by fine grinding to very small zeolite particle sizes.

The mineralogical framework of natural zeolites determines chemical properties such as *adsorption/desorption*, *cation exchange*, and completely reversible *dehydration*. These properties are derived from a given zeolite mineral's crystal structure, its physical framework geometry, and the type and number of alkaline or alkaline earth cations in its formula (Eyde and Holmes, 2006). Adsorption is the adherence of an atom, cation, or molecule to a solid

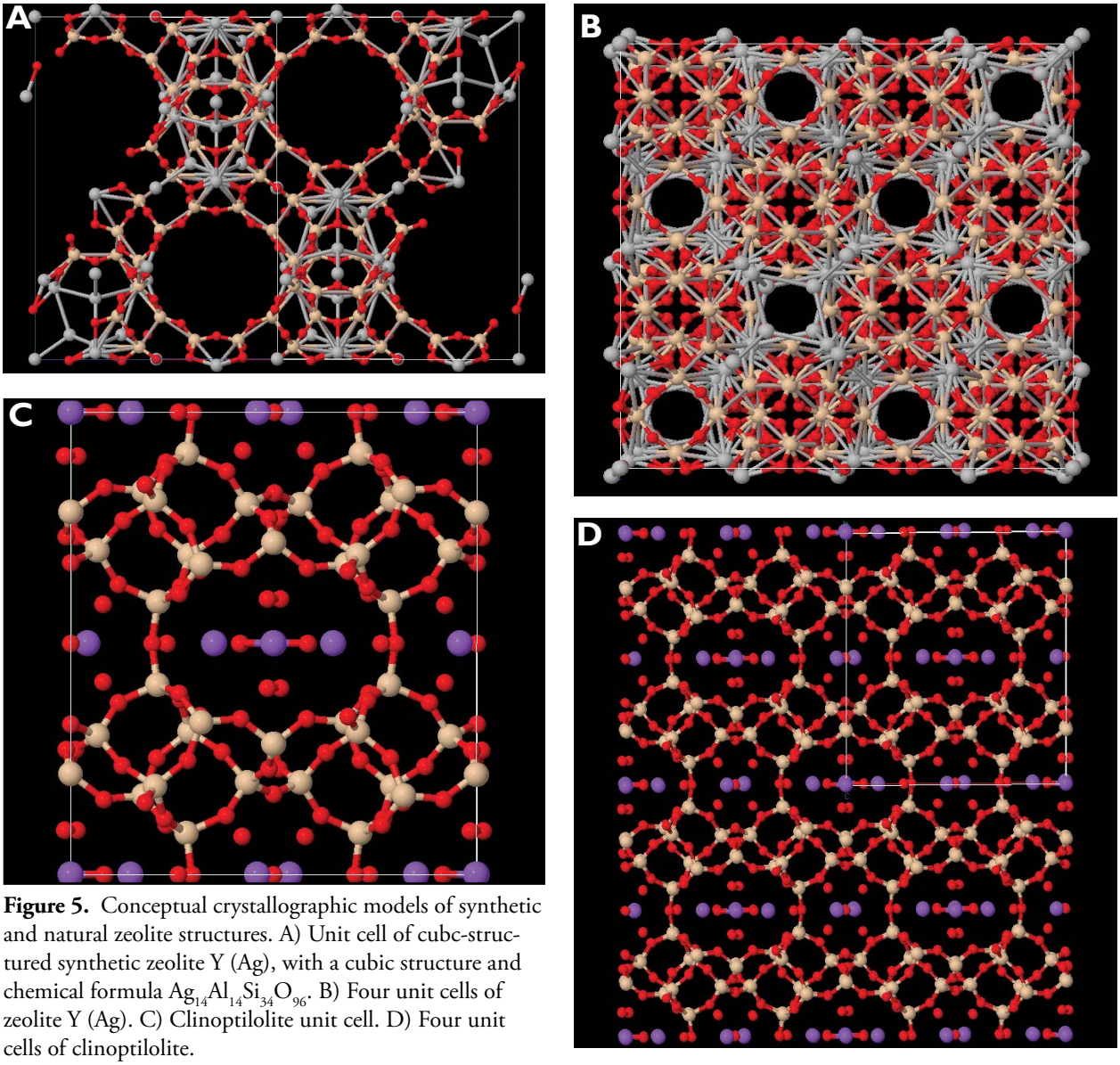

Figure 5. Conceptual crystallographic models of synthetic and natural zeolite structures. A) Unit cell of cubc-structured synthetic zeolite Y (Ag), with a cubic structure and chemical formula $Ag_{14}Al_{14}Si_{34}O_{96}$. B) Four unit cells of zeolite Y (Ag). C) Clinoptilolite unit cell. D) Four unit cells of clinoptilolite.

surface within the zeolite framework. Within that framework, water molecules form hydration spheres around cations such as calcium, sodium or potassium (Ca, Na, K). When the zeolite becomes dehydrated, either naturally or by heating, those cations typically are removed (desorbed) along with the water, resulting in an abundance of negatively charged tetrahedral sites within the framework. To balance the net negative charge of the framework, positively charged cations are then readily attracted and adsorbed to the negatively charged sites with the introduction of a different fluid or gas. The interconnectivity of the channels and cavities in zeolites translates to a rather large effective surface area. For example, chabazite, one of the more porous natural zeolites, has a surface area as much as 600 square meters per gram of the mineral (Vaughn, 1978).

The size of the interconnected channels between the aluminosilicate tetrahedra limits the size of the ion or molecule that can enter and be adsorbed (Harris, 1995). For example, chabazite, erionite, and mordenite have slightly larger channel widths and thus could capture larger molecules than those with tighter apertures (Harris, 1995). A fluid containing two types of compounds, one a much smaller molecule than the other, can sieve out the larger molecules, thus effectively removing the smaller of the two from the fluid. Due to the larger sizes of hydrocarbon molecules, the petroleum industry makes greater use of specially synthesized zeolites, which can be made with larger channel widths. Among the natural zeolites, calcium-rich minerals generally have larger channel widths than their sodium-

and potassium-rich counterparts; the potassic varieties having the smallest of the three (Deer and others, 1967).

Most natural zeolites can be almost completely dehydrated and rehydrated with no deleterious effects on their crystalline integrity. Whereas minerals such as clays may exhibit a collapse in their structure upon heating, most zeolites remain intact and thus can be heated to temperatures well beyond the boiling point of water. This results in their ability to completely dehydrate, maximizing their capacity for cation exchange. There are limits to the amount of heat they can withstand and in general, the higher the silica content, the higher temperature to which they can be heated; mordenite and clinoptilolite remain stable until approximately 650°C.

Physical properties

Natural zeolites are extensively tested as to their efficacy for a particular application for such physical characteristics as particle morphology, crystal habit, specific gravity, density, color, degree of crystallinity, chemical purity, and color. An excellent reference for physical and chemical properties of natural zeolites is Breck (1974). While a particular zeolite may be ideally suited for wastewater treatment, it may be largely useless for certain other purposes, and thus a thorough evaluation process precedes any large scale use (Eyde and Holmes, 2006). Typically, natural zeolites are earthy or chalky in appearance, finely crystalline, and light colored in white, gray, blue, and green (fig. 6). Due to their porous nature, zeolites have low specific gravity; most are between 2.0-2.3 grams per cubic centimeter (g/cm^3) and are noticeably lighter than surrounding rocks (table 2). They fracture semi-conchoidally and have a Mohs hardness range of 3.5 to 5. Clay minerals, such as montmorillonite, illite, and kaolinite, are commonly associated with zeolites and are sometimes mistaken for them. However, zeolites are harder (3.5-5 compared to 1-2 for clays) and will not swell and shrink when hydrated and dehydrated. Another notable difference between natural zeolites and clays is the lower specific gravity; most clays have little to no void space and feel noticeably denser (up to 3.0 g/cm^3).

Figure 6. Hand specimens of natural zeolite (clinoptilolite).

While natural zeolites have characteristic properties such as low density, hardness, and color, identifying them must be done using more sophisticated methods. Physical characteristics can be useful tools in identifying suspected zeolite deposits, but the best way to make an identification is by XRD. Natural zeolites in sedimentary rocks are in most cases derived from tuffs, which are consolidated volcanic ash fall deposits. Tuffs themselves often exhibit the same physical characteristics as natural zeolites (fig. 7). The difference is whether the tuff has been zeolitized, the process by which silicon, aluminum, oxygen, and other cations become arranged as an ordered mineral. There are several geologic settings in which zeolites can originate and will be discussed in subsequent sections.

Figure 7. Outcrops of non-zeolitic tuff beds in the northern Granite Mountains area, eastern Fremont County.

XRD is used to identify zeolites and their associated minerals. In practice, the peaks from a sample diffractogram are compared with those of a known zeolite standard pattern. Since every mineral species has its own unique orderly internal atomic arrangement, each mineral will have its own diffraction pattern, distinct from all other minerals. The diffraction pattern of an unidentified sample can be compared to that of known mineral species for identification. XRD is one of the most accurate methods of positively identifying zeolite minerals, but does require careful and time-consuming sample preparation and analysis in a laboratory. Software programs with extensive *search and match* capabilities have greatly advanced the mineral identification process in the last several years. For this investigation, JADE® Version 9.6 was used along with PDF-4 Minerals, a database compiled by the International Centre for Diffraction Data (ICDD), for search and match purposes.

Natural zeolite deposit types

Following Cronstedt's work, zeolites became increasingly well known as accessory minerals in the fractures, vugs, and other cavities within basaltic rocks where they often form remarkably euhedral crystals (fig. 8).

The abundance of building block components such as aluminum and silicon in volcanic ash, along with alkalis and alkaline earth cations, results in the common occurrence of zeolites in basaltic rocks and much more common and abundant occurrences in tuffaceous sedimentary rocks. Natural zeolite deposits form most commonly by the alteration and devitrification of aluminosilicate glass and minerals associated with volcanic ash fall deposits. The interaction of pore waters with the volcanic components in favorable physiochemical environments has resulted in large economic deposits of natural zeolites, the most common being analcime, chabazite, clinoptilolite, erionite, heulandite, laumontite, mordenite, and phillipsite (Harris, 1993). Sedimentary natural zeolite deposits are generally classified based on the geologic setting of their origin. Sheppard (1973) describes five sedimentary environments in which most natural zeolites form: (1) hydrothermal and hot spring, (2) burial metamorphic, (3) weathering, (4) open system, and (5) closed system.

Hydrothermal and hot spring zeolite occurrences are common, but not economic. There are well-known occurrences documented in cores from active geothermal areas within Yellowstone National Park (King and Harris, 2002). Due to the lack of mineral exploration in the park, only a

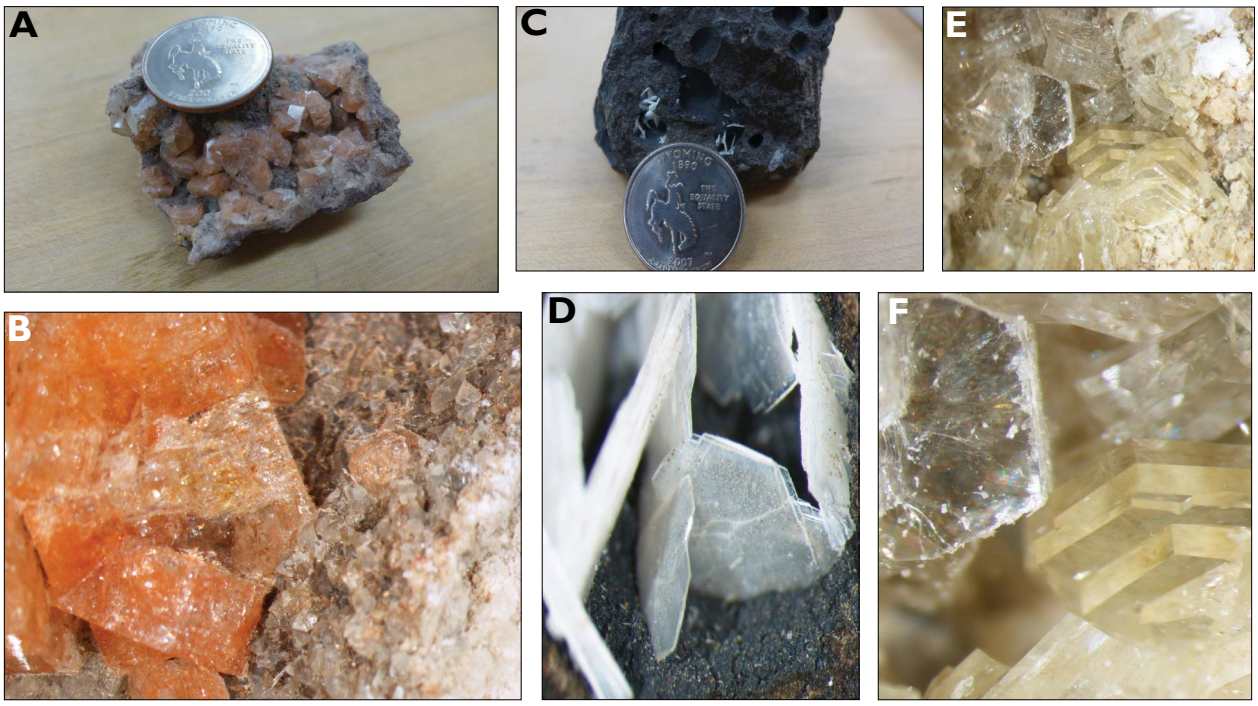

Figure 8. Rare large euhedral crystals of natural zeolite. A) Chabazite (nominal formula $Ca_2Al_4Si_8O_{24}$•$12H_2O$) from Nova Scotia. B) Close-up of a chabazite; width of view is 11 mm. C) Basalt-hosted ferrierite (nominal formula $[Na,K,Mg]_2[Si,Al]_{18}O_{36}$•$9H_2O$) from British Columbia. D) Close-up of the basalt-hosted ferrierite; width of view is 4.3 mm. E) Clinoptilolite in basalt from Malheur County, Oregon, (nominal formula $[Na_2,K_2,Ca][Al_3Si_{10}O_{24}]$•$8H_2O$); image is 8.3 mm across. F) Close-up of the clinoptilolite; image is 5.5 mm across.

few occurrences are known, but natural zeolites are likely far more common than what is thus far documented. Zeolite mineralization in this type of setting is typically zoned vertically, and generally correlates with depth and thus increasing temperature (Sheppard, 1973). Other examples of hydrothermally generated natural zeolite occurrences include wairakite from Wairakei, New Zealand (Steiner, 1953), and in Onikobe, Japan (Seki and others, 1969).

Very low grade burial metamorphism can form a succession of natural zeolite minerals such as laumontite, heulandite, analcime, and wairakite (Coombs and others, 1959). Typical settings for such occurrences are thick sequences of volcaniclastics up to several thousand feet thick in deep marine environments (Sheppard, 1973). The chemistry of the protolith is the main determining factor in which minerals form, but all minerals of the zeolite metamorphic facies form at low pressures (<0.5 GPa) and temperatures (<250°C). Higher pressures and temperatures result in higher grade mineral assemblages such as those of the prehnite-pumpellyite or greenschist facies (fig. 9).

Weathering within a few feet of the surface can result in zeolite formation under certain conditions. Soils of alkaline and saline chemistry are necessary for this to happen, and these occurrences are not of economic significance (Sheppard, 1973).

Commercial deposits of natural zeolites are all from the last two of the geologic settings mentioned above, the open- and closed-system types (Sheppard, 1973). The notion of *open* versus *closed* refers to whether the depositional environment experiences an influx of fresh surface or groundwater. Open systems are affected by either streams on the surface flowing into and out of a lake in which zeolite precursor components exist, or by subsurface hydrologic flow. Closed systems are generally found in relatively shallow saline alkaline lakes of higher pH than that of open systems, which favor the devitrification of aluminosilicate components. Both systems generally exhibit mineralogical zoning; vertical zoning is more typical in open systems with zeolitization more intense with depth, particularly those with thicker accumulations of tuffaceous material, whereas saline alkaline lakes are usually zoned laterally, with zeolites more common toward the depositional center of the lake (Sheppard, 1973). Wyoming contains zeolite deposits formed in both system types. Commercial deposits of clinoptilolite found in the Adobe Town Member of the Eocene Washakie Formation (Surdam and Sheppard, 1978) formed in a closed system within a hypersaline alkaline lake setting. The Oligocene White River Formation locally hosts zeolite minerals formed in an open system in which the permeability of the formation allowed ample time for zeolite-forming reactions between groundwater and rhyolitic tuffaceous rocks (Lander and Hay, 1993).

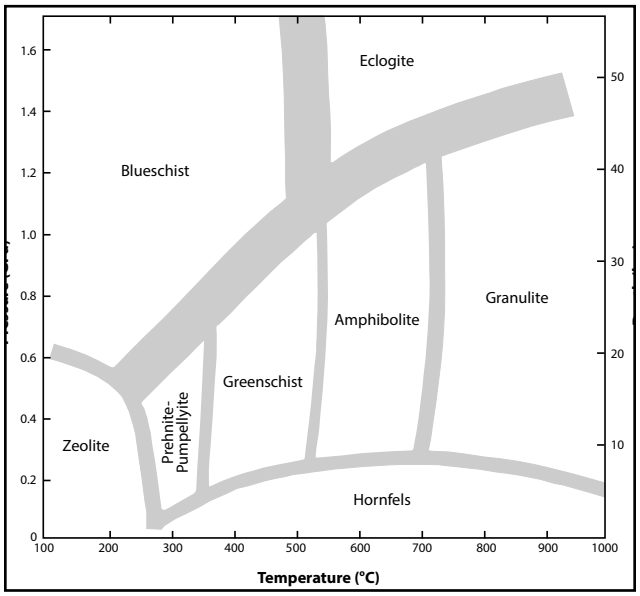

Figure 9. Pressure-temperature diagram showing the approximate (and gradational) boundaries between the various metamorphic facies (modified after Winter, 2001).

Locations of natural zeolite deposits

Commercial natural zeolite deposits in the United States are largely restricted to the western states, excluding Alaska and Hawaii, although there are some potentially economic deposits in Alaska as well as along the Alabama-Mississippi border (Eyde and Holmes, 2006). Paleogene strata (Paleocene, Eocene, and Oligocene) deposited during a period of regional back arc volcanism produced most zeolitized strata in Wyoming. The Laramide orogeny and crustal shortening had ceased by the end of Paleocene period during a subsequent episode of magmatism (Snoke, 1993). Laramide deformation had created tremendous topographic relief, and vast lacustrine systems developed in many of the intermontane expanses such as the Greater Green River Basin (fig. 10). In Wyoming, volcanic centers associated with regional Paleogene magmatism are the Absaroka, Black Hills, and the Rattlesnake Hills volcanic provinces. Igneous rocks emplaced by these volcanic systems vary from calc-alkalic to alkalic (Snoke, 1993). Pyroclastic material, including vast amounts of vitric ash rich in calcium, potassium, and sodium from these and similar volcanic systems in the western states, was ejected and disseminated across the region periodically between approximately 62-38 Ma (Snoke, 1993).

Zeolitization from vitric material in saline and alkaline settings is well known (Surdam and Sheppard, 1978). The abundance of volcanic ash available during the Eocene

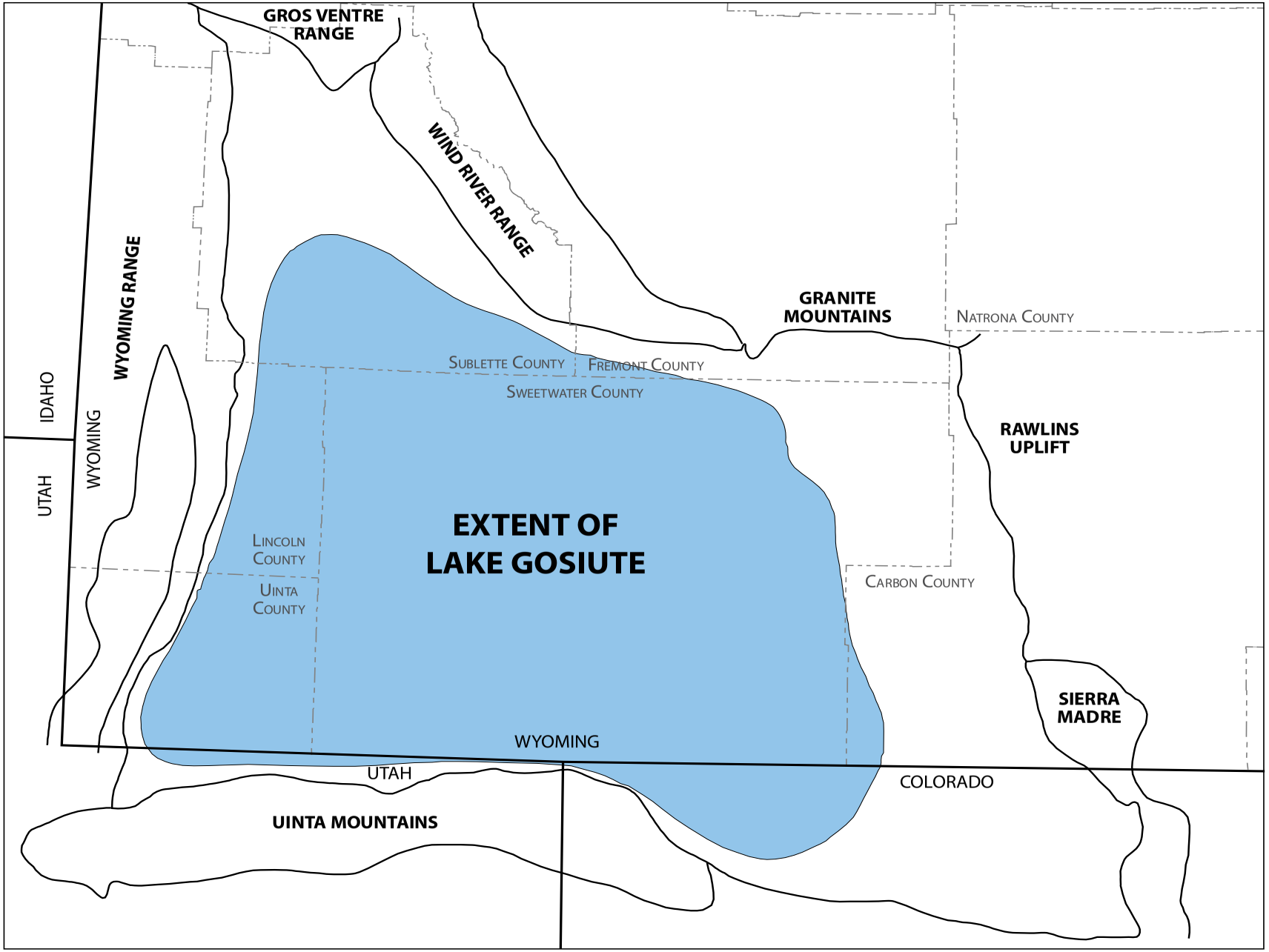

Figure 10. Maximum extent of the Eocene Lake Gosiute during deposition of the Green River Formation (modified from Sullivan, 1980).

(Green River Formation, Wagon Bed Formation, and other time equivalents) and the existence of predominantly closed-system saline and alkaline lake settings resulted in numerous natural zeolite occurrences and commercial-grade deposits in the Rocky Mountain region including Wyoming. Additionally, younger rocks (Oligocene White River Formation) developed favorable settings for the zeolitization of tuffaceous sediments (Lander and Hay, 1993). The greater Green River Basin, particularly the Washakie Basin, hosts the majority of natural zeolite deposits in Wyoming (fig. 11). Additional small deposits occur at the margins of the Wind River and Bighorn Basins. Minor occurrences are also found in the southern margin of the Powder River and northeastern Shirley Basins.

The following sections include both reviews of known or reported Wyoming natural zeolite occurrences and investigations of additional tuffaceous regimes for zeolite occurrences. The rock formation names referred to in the text are depicted in the stratigraphic columns in figure 12.

WYOMING NATURAL ZEOLITE OCCURRENCES

Southwest Wyoming

Washakie Basin

The Washakie Basin occupies an area of roughly 2,500 square miles in south-central Wyoming. It is situated generally between the Rock Springs Uplift to the west and the Muddy Creek valley to the east. The Muddy Creek drainage generally marks the geographic low between the eastern Washakie Basin and Atlantic Rim and the foothills of the Sierra Madre Range. During nearly all of the Eocene this basin was dominated by lakes and fluvial depositional systems. The Wasatch, Green River, and Washakie

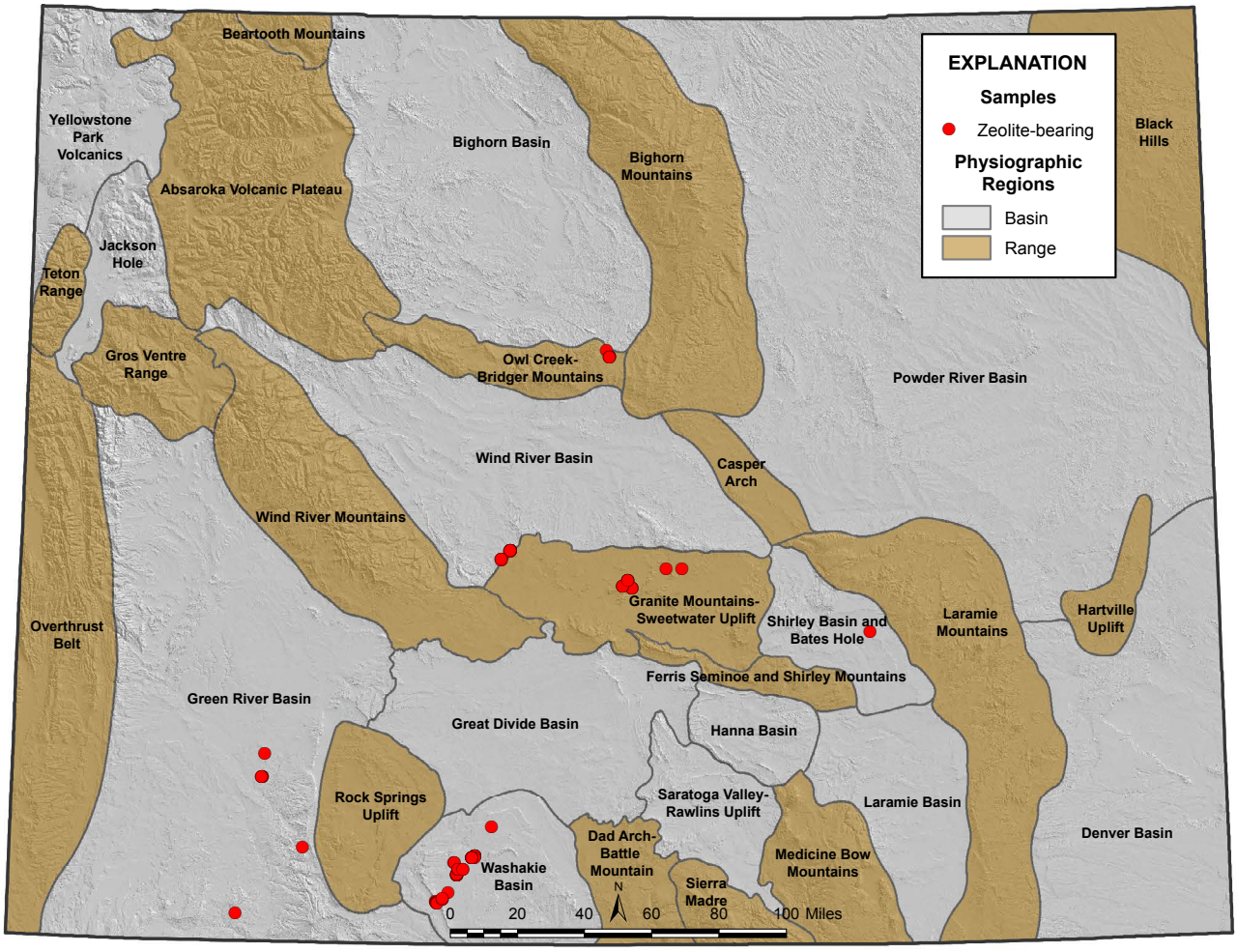

Figure 11. Map of Wyoming showing locations of zeolite occurrences discussed in this report. Additional occurrences and their lcoations can be found in Appendix 1 and in King and Harris (1990, 2002).

Formations make up the vast majority of exposed rock units in the basin, along with quaternary surficial deposits, most of which are eolian sand deposits. Most of the Eocene units in southwest Wyoming contain abundant vitric ash material, particularly the younger units of the Washakie Formation and its time-equivalent Bridger Formation, which is in the western portion of the Greater Green River Basin (fig. 11).

Eocene units of the Washakie Basin in Sweetwater County host significant zeolite occurrences (e.g. King and Harris, 2002). Johannsen (1914) first recognized zeolites in the Washakie Formation in the eastern portion of the Washakie Basin. Zeolitic host rocks of the Washakie Formation are best exposed along the margins, particularly in the north and west portions of the Washakie Basin. The Washakie Formation is split into the lower Kinney Rim and upper Adobe Town members (Roehler, 1973a). The Kinney Rim member of the Washakie Formation is a nearly 275 m (900 ft) thick succession of fluvial rocks, composed of interbedded gray, green, and red mudstones, gray to gray-green, very fine- to fine-grained sandstones, and minor thin limestones and tuffs (Roehler, 1973a). The Adobe Town Member of the Washakie Formation unconformably overlies the Kinney Rim Member and is a 700 m (2,300 ft) thick succession of alternating beds of green, gray, and red tuffaceous mudstone, and gray, fine- to coarse-grained, tuffaceous to arkosic sandstone; minor

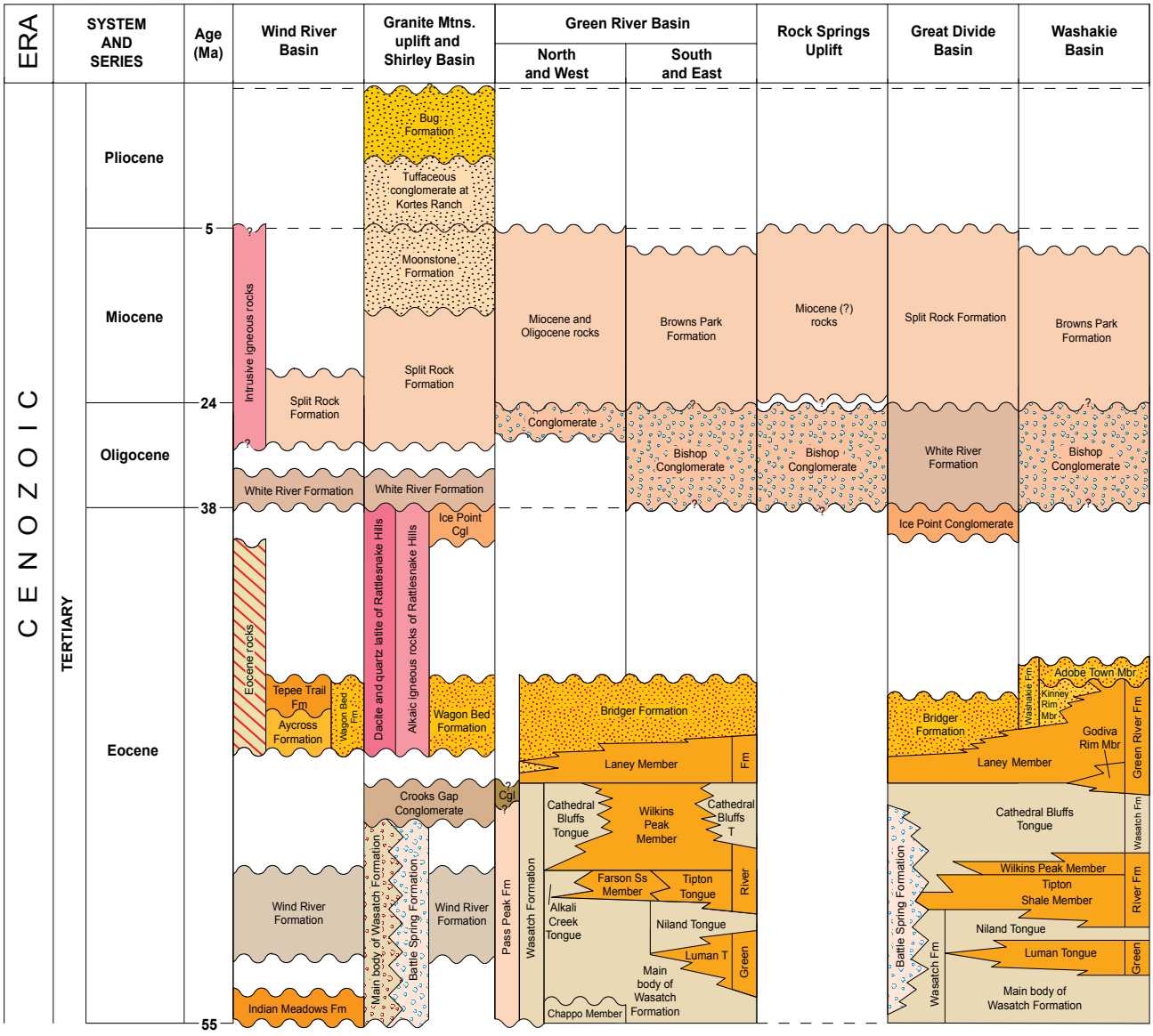

Figure 12. Stratigraphic columns listing the zeolite-bearing formations discussed in this report (modified from Love and others, 1993; Love and Christensen, 1985, 2014).

beds of tuff, siltstone, and conglomerate are also present (Roehler, 1973a). This unit crops out over much of the central portion of the Washakie Basin and is partially overlain by Quaternary surficial sand dune deposits (Roehler, 2004).

Washakie Formation - Adobe Town Member

Approximately 27.5 m (90 ft) above the base of the Adobe Town Member is a zeolitic tuff to tuffaceous sandstone with a characteristic robin's-egg-blue color (bed 579 of Roehler, 1973a). This tuff to tuffaceous sandstone is an important marker bed that can be recognized over a wide area in the Washakie Basin (fig. 13). The robin's-egg-blue marker bed is as much as 3.7 m (12 ft) thick (Curry and Santini, 1986), within an approximately 30.5 m (100 ft) succession of zeolitic tuff and tuffaceous sandstone that begins approximately 7.6 m (25 ft) above the base of the Adobe Town Member (fig. 14). Zeolite minerals in this succession include clinoptilolite, heulandite, and mordenite (Roehler, 1973a).

The inactive Fort LaClede zeolite quarry lies in section 1, T. 16 N., R. 98 W. (fig. 15). The bed that is quarried from this location lies just above a robin's-egg-blue platy tuff and reportedly contains up to 90 percent clinoptilolite (Curry and Santini, 1986).

At the west margin of Washakie Basin, the Adobe Town Member is exposed in a succession of thin outcrops dipping less than 10 degrees to the northeast. Analcime, clinoptilolite, and heulandite are present in small amounts in tuffs, tuffaceous sandstones, and tuffaceous mudstones (samples collected near Kinney Rim Road, labeled on some maps as Sweetwater County Road 19; fig. 16). The Adobe Town Member thickens from about 24.4 m (80 ft) to about 42.7 m (140 ft) from west to east (Roehler, 1973b).

In addition to the tuffaceous succession that includes the robin's-egg-blue marker bed, Roehler (1973a) identified four other thick tuffaceous units in the Kinney Rim Member and the Adobe Town Member; King and Harris (2002) remark that these tuffaceous rocks are presumably zeolitic, but this statement has not previously been confirmed. The two tuffaceous units in the Adobe Town Member are a 2.4 m (8 ft) thick chalk-white biotite tuff marker bed, approximately 348 m (1,140 ft) above the base of the Adobe Town Member (bed 637), and a 2.7 m (9 ft) thick, white, finely bedded tuff marker bed, approximately 555 m (1,820 ft) above the base of the Adobe Town Member (bed 664). In the areas visited during this investigation, the two beds of the Adobe Town Member were either not present due to erosion, burial by quaternary sands, or barren with respect to zeolite mineralization (see discussion of the Kinney Rim Member below).

Lower Iron Pipe Draw areas, secs. 11 and 12, T. 16 N., R. 98 W., Sweetwater County

A review of Wyoming ad valorem tax records reveals that 12,020 short tons of material were mined in 2002, with no prior or subsequent production. The quarry is approximately 2.2 miles south of the historic Fort LaClede ruins in sec. 25, T. 17 N., R. 98 W., SE1/4, SE1/4. The nearly monomineralic bed there is reportedly between 65 and 90 percent clinoptilolite (Harris, 1993) and varies in thickness from less than 1 m up to about 4 m (3-13 ft)(Curry and Santini, 1986). The main bed appears thickest in the vicinity of the quarry but thins laterally and becomes increasingly interbedded with zeolitic sandstones, siltstones, and mudstones. Samples collected in this area commonly contained clinoptilolite and heulandite (figs. 17-18).

Zeolite mineralization at the Fort LaClede quarry is associated with the robin's-egg-blue colored tuff in the Adobe Town Member of the Eocene Washakie Formation (Roehler, 1973a; King and Harris, 2002). The blue tuff here is about 5-6 m (15-20 ft) thick and weathers to dull white. The zeolitic tuff overlies tan, massive, medium-grained, zeolitized tuffaceous lithic quartz sandstone; this sandstone is about 0.3-1 m (1-3 ft) thick. Tan to buff tuffaceous sandstone overlies the blue tuff.

From the basal Adobe Town Member of the Washakie Formation, clinoptilolite and minor amounts of possible heulandite were identified in several samples of tuff and tuffaceous sandstone collected above and below the robin's-egg-blue marker bed at several locations. Approximately one mile southwest of the Fort LaClede zeolite quarry an 11 m (36 ft) thick succession of beds was sampled, and nearly all beds contained clinoptilolite and minor heulandite, and one bed contained analcime (fig. 19). Most beds are less than 2 m (7 ft) thick with interbedded tuffaceous sandstone, siltstone, and minor limestone (fig. 20). Zeolite-bearing beds include brown, yellowish gray, tan, and bluish-gray biotite tuff; blue-green (robin's-egg-blue) platy tuff; tan, green-yellowish gray sandy tuff; and light green tuffaceous sandstone (fig. 21). Many of these beds are white to buff inside but rusty colored on weathered surfaces, commonly stained and spotted with secondary iron-oxide mineralization, typically hematite, with local patchy limonite (figs. 22 and 23).

Eagle Nest Draw (South), sec. 28, T. 16 N., R. 98 W., Sweetwater County

Eagle Nest Draw contains an intermittent stream that flows to the northeast and lies southwest of the Fort LaClede quarry and the nearby locations described above. Approximately 5 miles southwest of the quarry, outcrops of the lower Adobe Town Member of the Washakie Formation

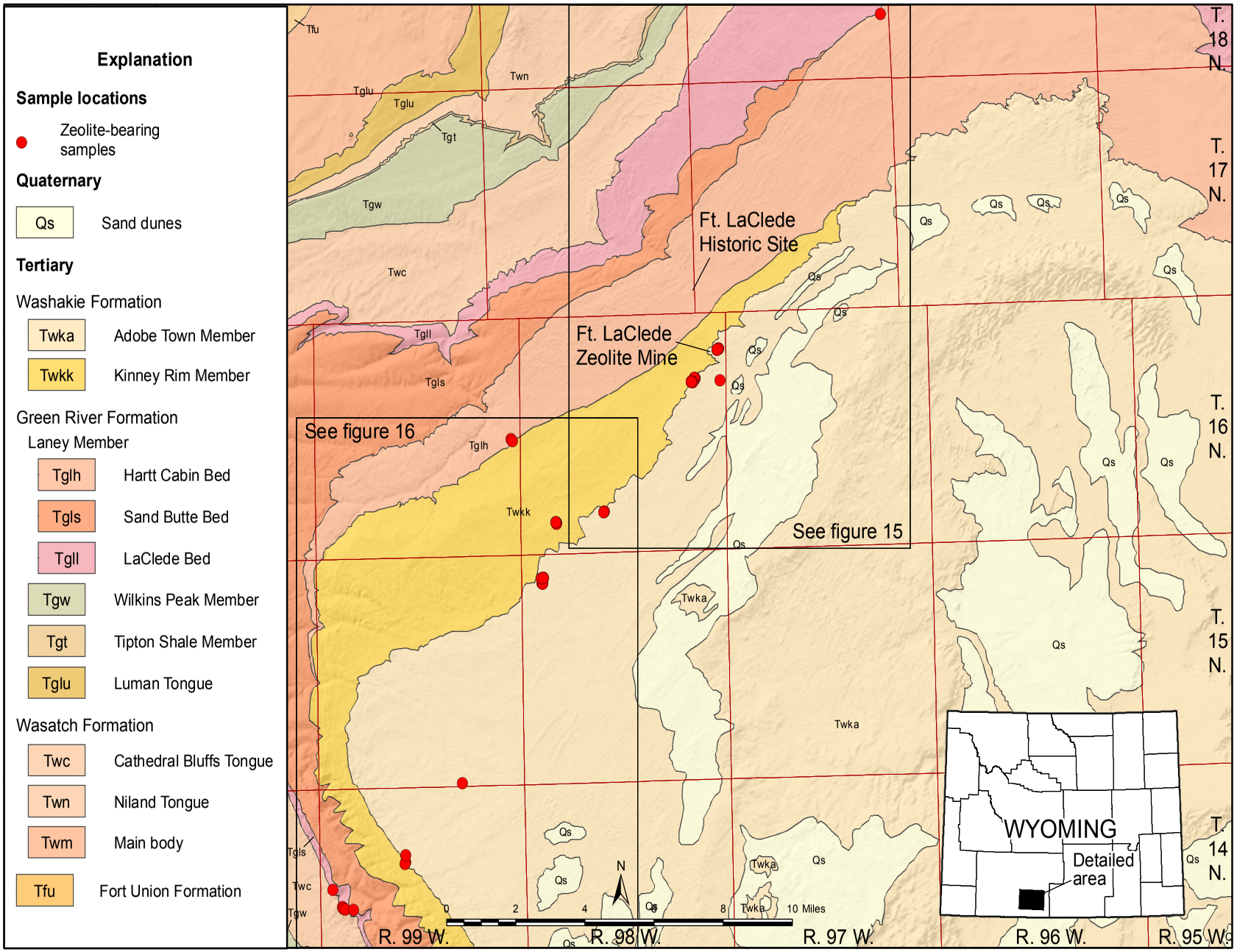

Figure 13. Geologic map of the Washakie Basin showing locations of zeolite-bearing samples collected during this investigation. Map modified from Love and Christensen (1985, 2014 release).

Figure 14. Outcrops of the Adobe Town Member of the Washakie Formation, including the robin's-egg-blue tuff marker bed. This photo was taken in sec. 12, T. 16 N., R. 98 W., Sweetwater County, south of the Fort LaClede zeolite quarry.

are fairly well exposed on ridges along the southeast side of the draw. Two samples were collected here, both containing clinoptilolite and one containing a minor heulandite component. The tuff bed at this locality is approximately 1.5 m (5 ft) thick, white to buff in color, largely homogeneous but is speckled with very small (< 0.5 mm) flakes of brown to black biotite as well as minor iron-oxide staining (fig. 24). This location may be near the contact with the underlying Kinney Rim Member, however, that contact appears to be concealed by quaternary fluvial deposits.

Lower Adobe Town Member, East of Bitter Creek Road (County Rd. 19) sec. 6, T. 15 N., R. 98 W., Sweetwater County

This location is similar to the two previously described sites, as there are numerous clinoptilolite-bearing tuff or tuffaceous sandstone beds, including a blue-green tuffaceous sandstone. Most of the tuffs are tan to yellow to light to medium brown, biotitic, and form resistant ridges interbedded with similarly colored tuffaceous mudstones (figs. 25 and 26).

Lower Adobe Town Member, East of Kinney Rim, sec. 9, T. 15 N., R. 99 W., Sweetwater County

This location is approximately 1.2 miles east of the high point of Kinney Rim along Bitter Creek Road (Sweetwater County Road 19). The lower-most units of the Adobe Town Member are fairly well exposed in gently northeast-dipping outcrops. Clinoptilolite is present in two samples near the base of the member; Sample 20141105JC-5 (fig. 27) is grayish-blue to blue-green sandy biotite tuff to muddy tuffaceous sandstone, and Sample 20141105JC-6 is a green, fine- to medium-grained biotite-rich, well indurated tuffaceous sandstone lying approximately 85 m (280 ft) northeast of Sample 20141105JC-5. Approximately 285 m (934 ft) north of Sample 20141105JC-5 is an analcime-bearing blue-green, muddy, poorly indurated, medium-grained tuffaceous sandstone.

Bitter Creek Road, sec. 35, T. 15 N., R. 99 W., Sweetwater County

Bed 620 of Roehler (1973a) is described as a tan, limy, silty, hard, finely laminated tuff. A clinoptilolite-bearing sample of tuff (20141105BG-3; fig. 28) was collected at this location and loosely matches Roehler's description of bed 620, but was generally blocky rather than laminated, and not silty or limy. Based on Roehler's 2004 map, this is most likely bed 620; the gentle dip of the Adobe Town Member in the area would place bed 637 (the nearest tuff to bed 620) well to the east of this location.

Washakie Formation - Kinney Rim Member

The Adobe Town and the Kinney Rim Members of the Washakie Formation are separated in the western parts of the Washakie Basin by an unconformity, while in the east and southeast, the Kinney Rim Member is truncated or interfingers with the Laney Shale Member of the Green River Formation (Roehler, 1973a). Roehler points out that the contact between the two members is marked by a series of medium brown sandstones; below the contact the rocks are similar to but noticeably less vitric than those of the overlying Adobe Town Member and its tuffaceous marker beds. At the base of the Kinney Rim Member is a 1.5 m (5 ft) thick, white, ridge forming limey tuff to tuffaceous limestone (bed 515) and a 2.1 m (7 ft) thick white, hard silty tuff approximately 88 m (290 ft) above the base of the Kinney Rim Member (bed 540). Samples were collected from or near both of these beds during the course of this investigation.

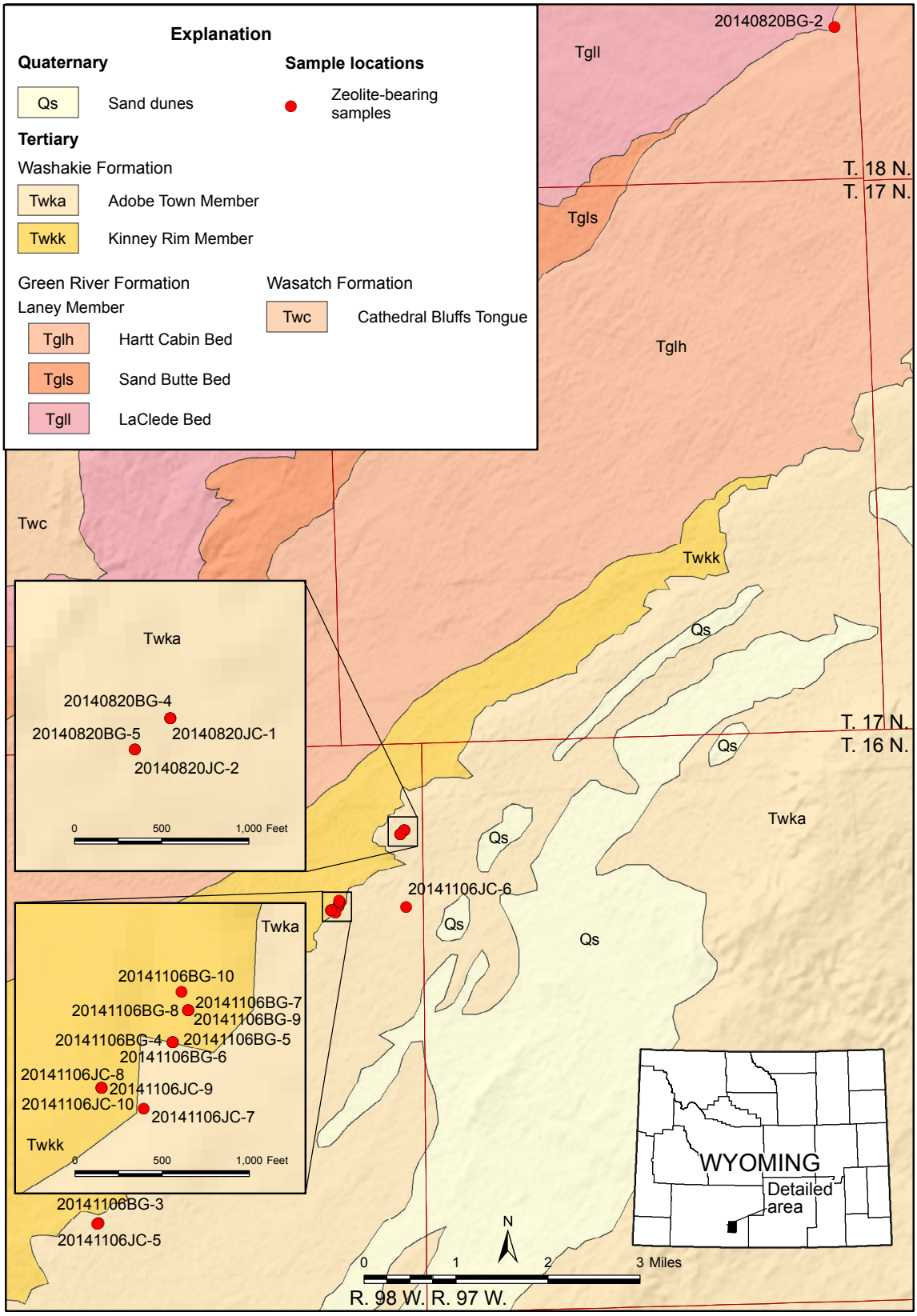

Figure 15. Locations of zeolite-bearing samples collected in the northern portions of the Washakie Basin. Map modified from Roehler (2004).

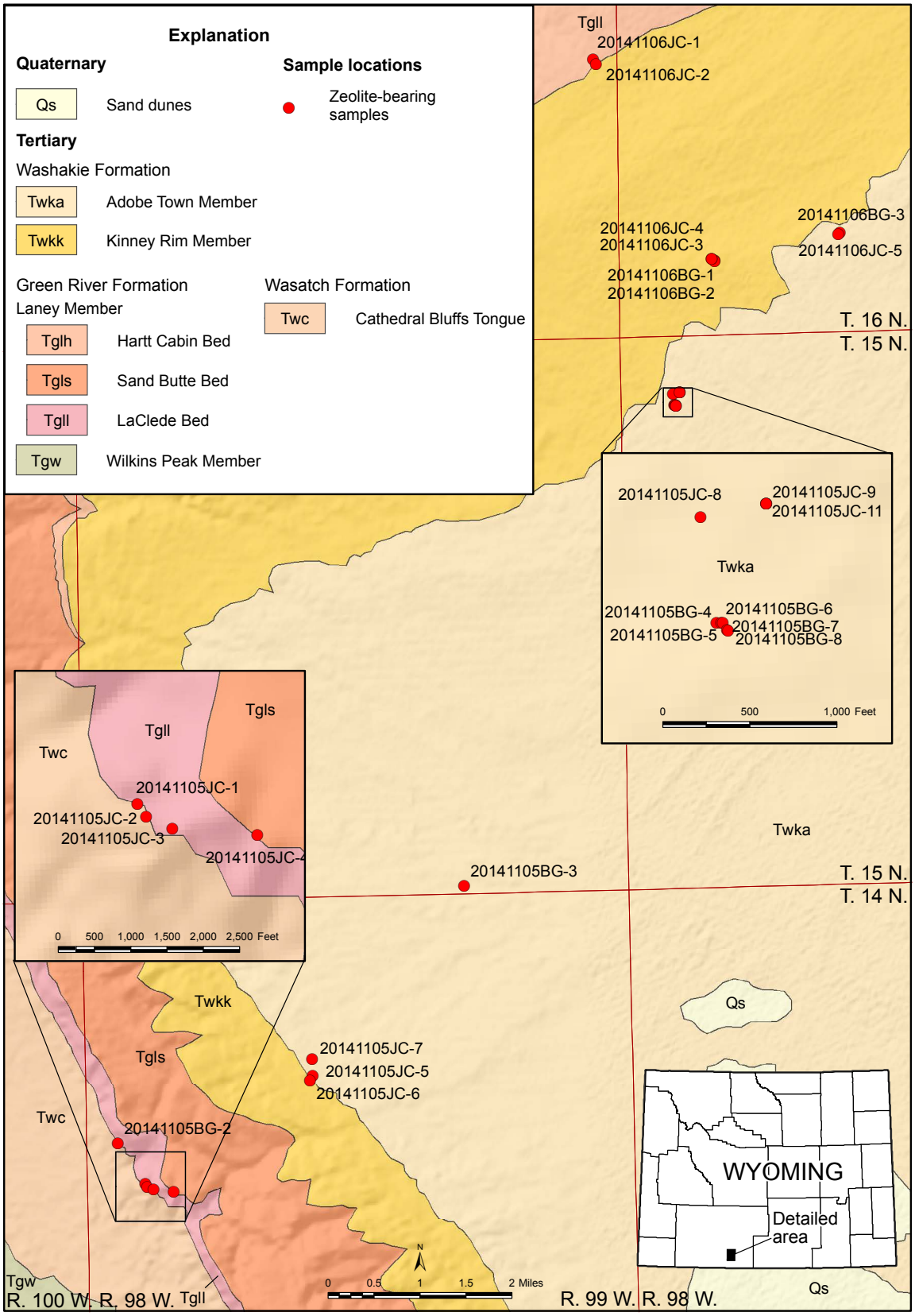

Figure 16. Locations of zeolite-bearing samples collected in the western portions of the Washakie Basin. Map modified from Roehler (2004).

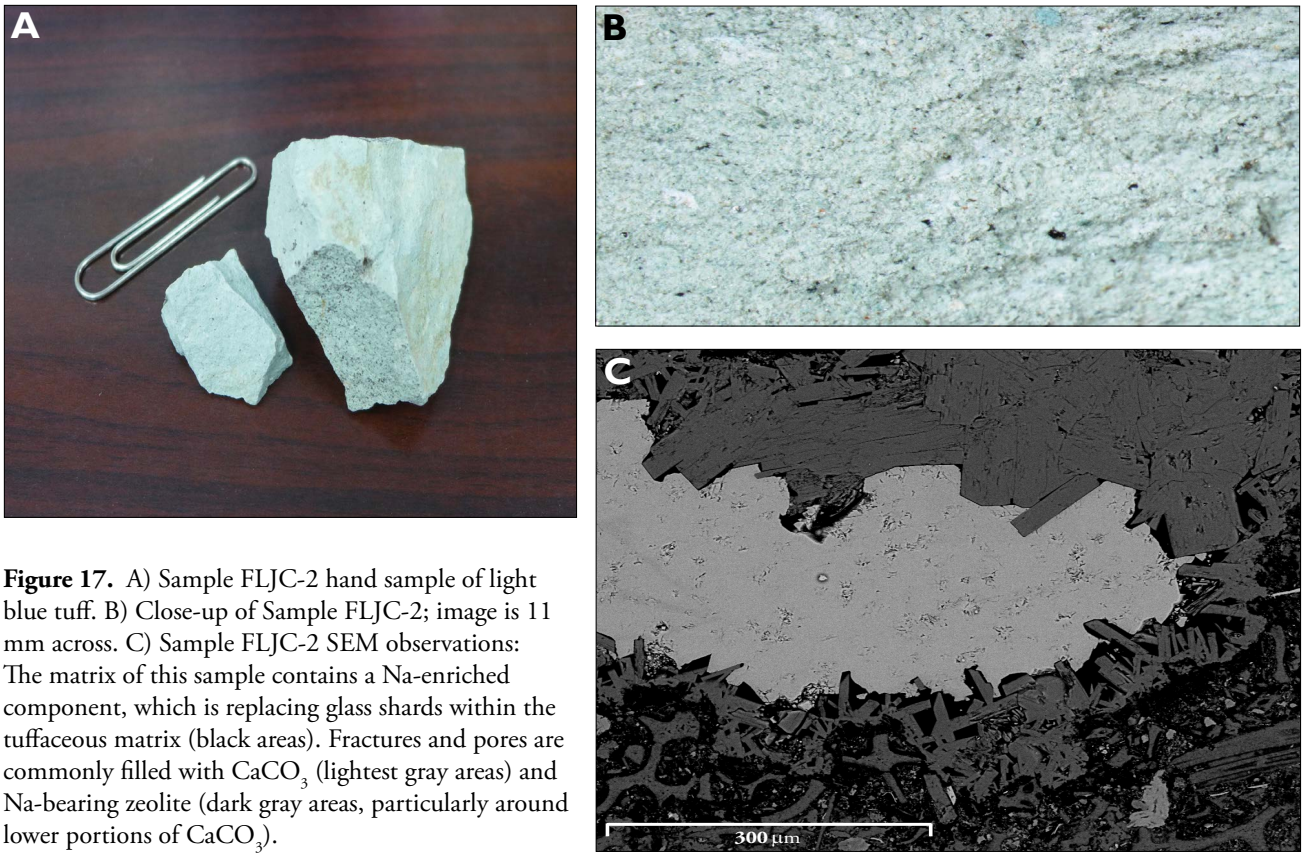

Figure 17. A) Sample FLJC-2 hand sample of light blue tuff. B) Close-up of Sample FLJC-2; image is 11 mm across. C) Sample FLJC-2 SEM observations: The matrix of this sample contains a Na-enriched component, which is replacing glass shards within the tuffaceous matrix (black areas). Fractures and pores are commonly filled with $CaCO_3$ (lightest gray areas) and Na-bearing zeolite (dark gray areas, particularly around lower portions of $CaCO_3$).

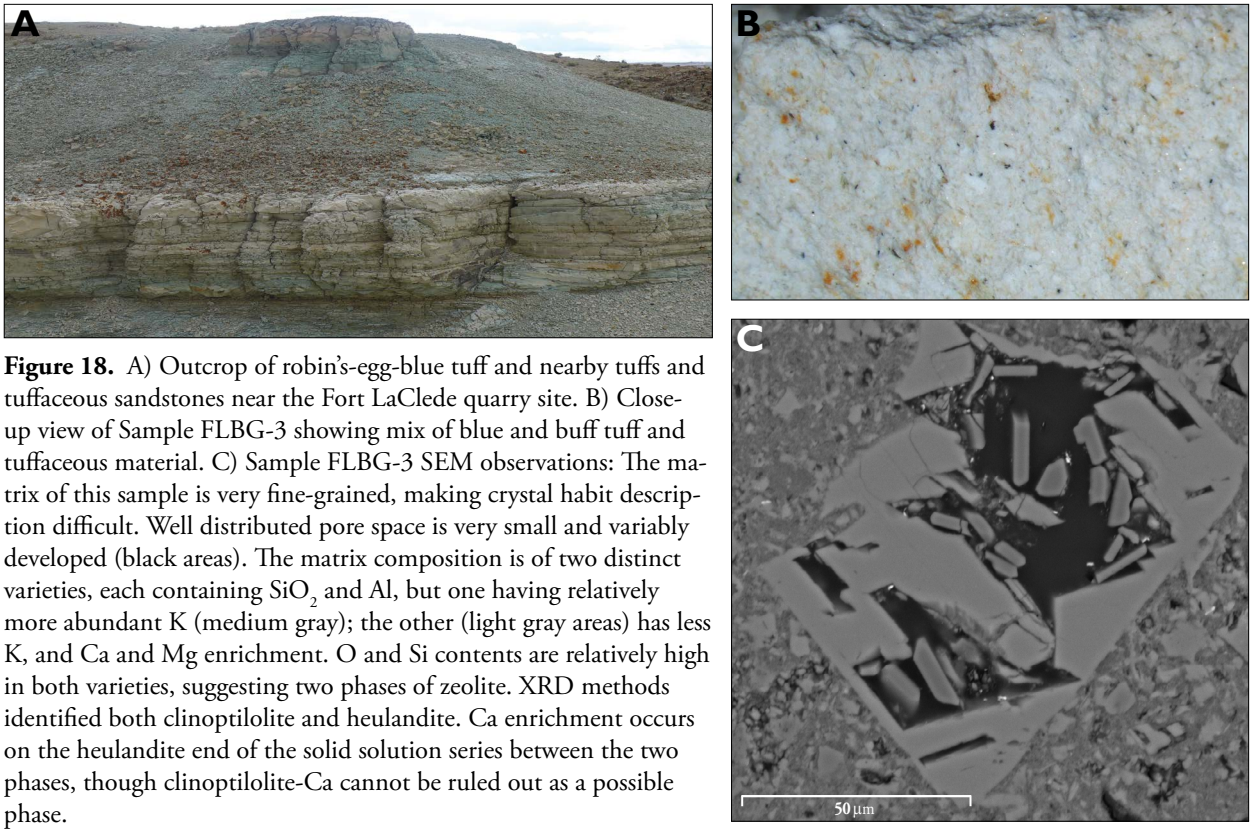

Figure 18. A) Outcrop of robin's-egg-blue tuff and nearby tuffs and tuffaceous sandstones near the Fort LaClede quarry site. B) Close-up view of Sample FLBG-3 showing mix of blue and buff tuff and tuffaceous material. C) Sample FLBG-3 SEM observations: The matrix of this sample is very fine-grained, making crystal habit description difficult. Well distributed pore space is very small and variably developed (black areas). The matrix composition is of two distinct varieties, each containing SiO_2 and Al, but one having relatively more abundant K (medium gray); the other (light gray areas) has less K, and Ca and Mg enrichment. O and Si contents are relatively high in both varieties, suggesting two phases of zeolite. XRD methods identified both clinoptilolite and heulandite. Ca enrichment occurs on the heulandite end of the solid solution series between the two phases, though clinoptilolite-Ca cannot be ruled out as a possible phase.

Figure 19. Outcrop of robin's-egg-blue tuff and adjacent rocks in the Adobe Town Member of the Washakie Formation near the Fort LaClede quarry. The robin's-egg-blue tuff here consists of blue to white zeolitic tuff; Sample 20141106JC-8 is of the robin's-egg-blue tuff. The tuff overlies green, fine-grained, platy, tuffaceous, zeolitic sandstone, represented by Sample 20141106JC-9. Overlying the tuff is tan to yellow to light blue biotite tuff represented by Sample 20141106JC-10. The robin's-egg-blue tuff hosts heulandite and clinoptilolite, the underlying sandstone hosts heulandite, and the overlying biotite tuff hosts analcime.

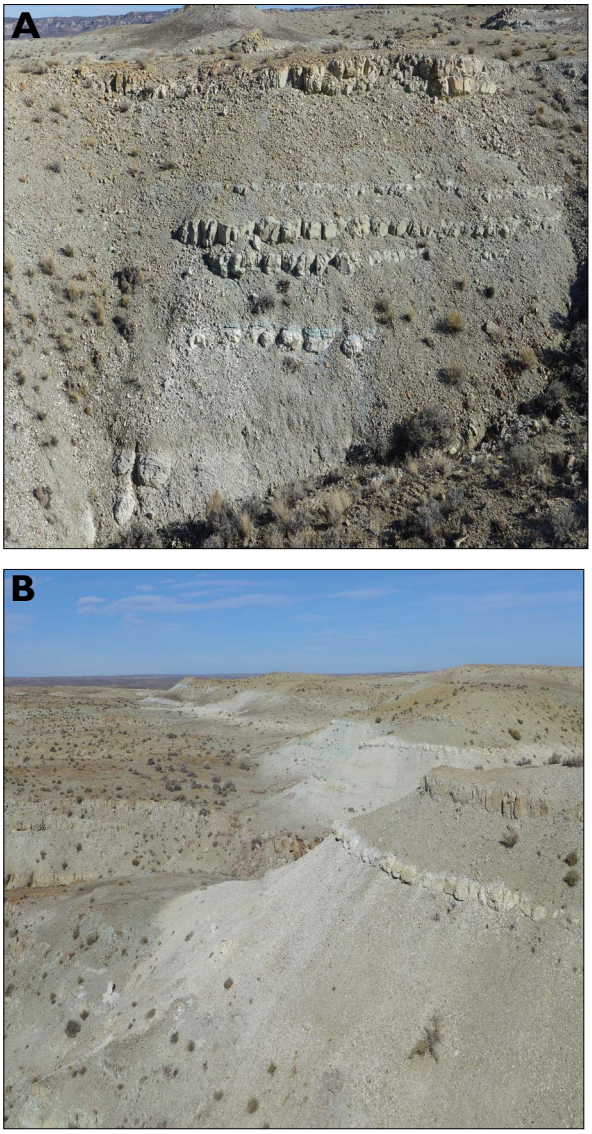

Figure 20. Outcrops of the robin's-egg-blue tuff of the Adobe Town Member of the Washakie Formation, W1/2 section 12, T. 16 N., R. 98 W., Sweetwater County. A) This photo is an example of the interbedded tan to buff tuff and tuffaceous sandstone beds along with a thin robin's-egg-blue bed. B) Looking northeast, generally along strike of the robin's-egg-blue tuff sequence.

Upper Iron Pipe Draw, secs. 13 and 24, T. 16 N., R. 99 W., Sweetwater County

Analcime was identified in float samples from an area of poorly exposed outcrop of white to light gray calcareous tuff and tuffaceous mudstone. The samples appear to be consistent with bed 515 of Roehler (1973a). Samples 20141105JC-1 and 20141105JC-2 were collected about 100 m (330 ft) apart in sections 13 and 24, respectively.

Upper Eagle Nest Draw, sec. 32, T. 16 N., R. 98 W., Sweetwater County

Stratigraphically higher and approximately 2.5 miles southeast of the Iron Pipe Draw location, several samples contained clinoptilolite and analcime. This site is likely near the top of the Kinney Rim Member and is situated in section 32, T.16N. – R.98W., (figs. 29 and 30).

Green River Formation - Laney Member

The Laney Member of the Green River Formation crops out at the margins of the Washakie Basin with the excep-

Figure 21. Outcrops of robin's-egg-blue tuff showing the subtle difference between the blocky buff and generally platy blue zeolitic tuff beds in the W1/2 section 12, T. 16 N., R. 98 W., Sweetwater County.

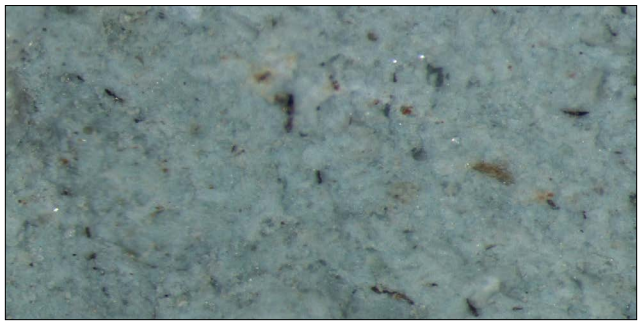

Figure 22. Close-up view of robin's-egg-blue tuff similar to that in figure 21 (different sample location). This sample exhibits local vuggy porosity and sparse iron oxide staining; width of view is 3 mm.

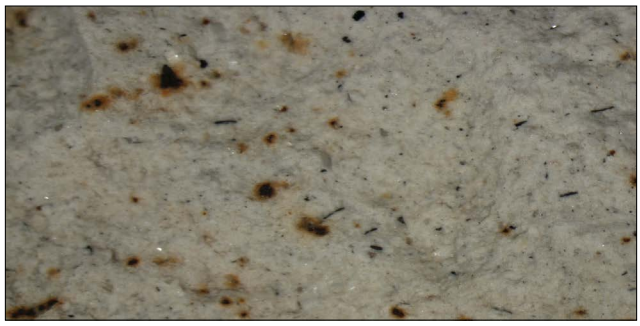

Figure 23. Close-up view of a white zeolitic tuff (sampled near the robin's-egg-blue tuff) showing patchy iron oxide staining, probably due to the breakdown of biotite; width of view is 11 mm.

Figure 24. A) Zeolitic tuff (Sample 20141106BG-3) collected from the lower part of the Adobe Town Member near Eagle Nest Draw in SE1/4 SW1/4 sec. 28, T. 16 N., R. 98 W. B) Close-up showing scattered biotite laths and iron oxide staining.

tion of the southern portion, where it and the Washakie Formation are unconformably overlain by the Miocene Browns Park Formation. Some of the Laney Member beds host analcime, clinoptilolite, and mordenite (Bradley, 1945; Roehler, 1972).

The positively identified zeolites are within a prominent buff colored tuff marker bed that ranges from 1.5 to 18.3 m (5 to 60 ft) in thickness (Roehler, 1972). Roehler (1973b) reports at least seven additional tuffaceous units in the Laney Member; these units have not previously been identified as zeolitic, though King and Harris (2002) state that the presence of zeolites in these sediments is likely. Roehler (1973b) subdivides the Laney Member into three rock-stratigraphic units named the LaClede Bed, the Sand Butte Bed, and the Hartt Cabin Bed, listed oldest to youngest. This investigation sampled reported zeolitic units within the lowermost of these, the LaClede Bed of Roehler (1973b). These horizons of the Green River Formation formed in Lake Gosiute, known for its fluctuating size, depth, and chemical stratification. The LaClede Bed on Kinney Rim is approximately 137 m (450 ft) thick and consists of mostly oil shales (fig. 31; Roehler, 1973b).

Figure 25. Outcrop of the Adobe Town Member of the Washakie Formation. The top of the outcrop is capped by a resistant tan to yellow, well indurated biotite tuff. The tan to yellow tuff overlies a less resistant tan to yellow mudstone, which in turn overlies resistant white biotite tuff and a thin lens of blue-green, medium-grained tuffaceous sandstone, which is poorly visible in the photograph. Sample 20141105JC-10 is from the capping tan to yellow tuff. Sample 20141105JC-9 is of the blue-green sandstone, and Sample 20141105JC-11 is from the white tuff; these two samples were collected from approximately the same stratigraphic level. Both of the tuffs and the sandstone host clinoptilolite and heulandite.

Figure 26. A series of interbedded zeolitic tuffs and tuffaceous mudstones within the robin's-egg-blue tuff outcrops. A) Locations of several samples collected, all of which contained clinoptilolite and/or minor heulandite. B) Outcrop of Sample 20141105BG-7, hosting clinoptilolite and minor heulandite. C) Outcrop of Sample 20141105BG-8, which also hosts clinoptilolite and minor heulandite.

Figure 27. Grayish-blue to blue-green, sandy, biotite tuff to muddy tuffaceous sandstone in the Adobe Town Member of the Washakie Formation. The sandstone hosts clinoptilolite and heulandite. This is the site of Sample 20141105JC-5. The stratigraphic position of this unit is similar to that of the robin's-egg-blue tuff at the Fort LaClede quarry.

Kinney Rim near Bitter Creek Road, secs. 18 and 19, T. 14 N., R. 99 W., Sweetwater County

Our results of LaClede Bed samples collected in this vicinity are consistent with Roehler's (1972) generalized map showing authigenic silicate mineral facies in the western and northern portions of the Washakie Basin based on depth, and thus water salinity and alkalinity. Several samples collected at Kinney Rim contained only analcime and a minor amount of heulandite.

Laney Wash, south of Delaney Rim, sec. 25, T. 18 N., R. 97 W., Sweetwater County

This site is approximately 27 miles northeast of the Kinney Rim location and contains clinoptilolite. The sample was collected from what appears to be near the base of the LaClede Bed. This location lies in the vicinity of Roehler's (1972) boundary between zones 1 and 2, of zeolite barren, and clinoptilolite and mordenite, respectively.

Green River Basin

Green River Formation - Wilkins Peak Member

Figure 28. Outcrop of a blocky clinoptilolite-bearing tuff (Sample 20141105BG-3) believed to be from bed 620 of Roehler (1973a).

Middle Firehole Canyon area, sec. 34, T. 17 N., R. 106 W., Sweetwater County

Minor alteration of feldspar to analcime and sericite is reportedly present in sandstone of the Wasatch Formation in Firehole Basin (Vine and Tourtelot, 1973). The Wasatch Formation in this area (fig. 32) is a succession of interbedded hematite-stained arkose, calcareous arkose, shale, and mudstone. The Wasatch is generally overlain by (but locally interfingers with) the Wilkins Peak Member of the Green River Formation, which hosts analcime in other parts of the Green River Basin (King and Harris, 2002). Several samples were collected from suspected tuffaceous sandstones, siltstones, and mudstones of the Wilkins Peak Member. One sample of greenish gray to yellowish brown sandy non-calcareous mudstone tested positive for analcime (fig. 33).

Bridger Formation

Twin Buttes area, sec. 7, T. 13 N., R. 109 W., Sweetwater County

The Twin Buttes are two prominent erosional remnants of the Eocene Bridger Formation approximately 10 miles west of Flaming Gorge Reservoir and visible in the area from many miles in most directions. Each butte is unconformably overlain by small outcrops of Oligocene Bishop Conglomerate.

Sheppard (1971a, 1971b) reports tuffs and tuffaceous sandstones in the Bridger Formation near Twin Buttes host clinoptilolite. Murphey and Evanoff (2008) provide the most detailed description of the Bridger Formation within the Bridger Basin; additionally, their work produced ten 1:24,000 scale bedrock maps covering the Bridger Basin

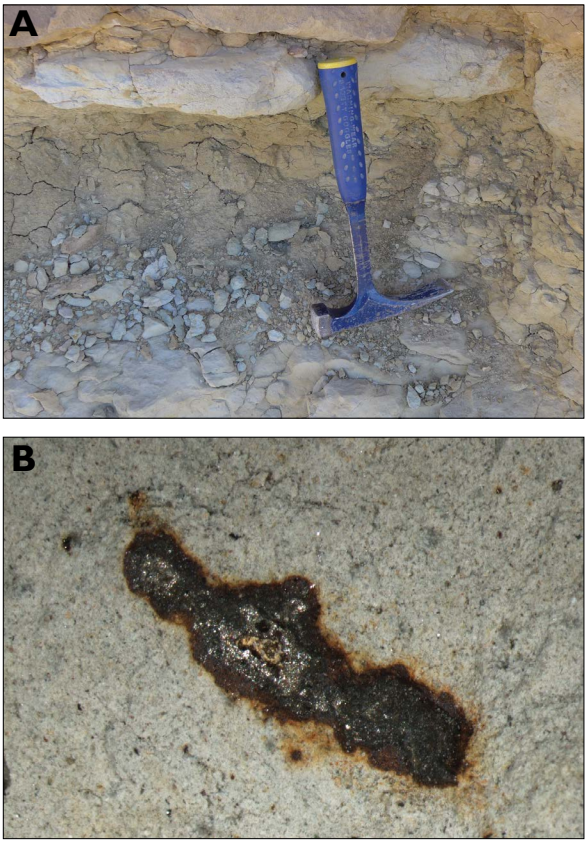

Figure 29. A) Outcrop in a drainage of a soft, sandy analcime-bearing tuff (Sample 20141106BG-1), approximately 1.5 m (5 ft) thick. B) Close-up (11 mm width of view) showing irregularly shaped cavities filled with hematite and secondary euhedral quartz crystals.

(Murphey and Evanoff, 2008). Except for limestones, the Bridger Formation sediments are largely volcanoclastic (Murphey and Evanoff, 2008). One unit, the Henrys Fork tuff, is continuous across the entire Bridger Basin. The Henrys Fork tuff is typically about 1 m (3 ft) thick and forms a ledge. Murphey and others (1999) found that the Henrys Fork tuff has a K-Ar age of 46.92 +/- 0.44 Ma.

Clinoptilolite in a seemingly minor amount was found in a sample of yellowish gray sandy calcareous believed to be from the Henrys Fork tuff (fig. 34). The site is consistent with the location of the Henrys Fork tuff (Brand and others, 2007).

Blue Rim sec. 35, T. 22 N., R. 108 W., to sec. 30, T. 21 N., R. 107 W., Sweetwater County

Blue Rim is in the northeastern part of the Green River Basin, approximately 20 miles northwest of the town of Green River. The area is named for its distinctive light blue layers of tuffaceous sandstones and mudstones easily

Figure 30. Outcrop of a (minor) clinoptilolite- and heulandite-bearing tuffaceous sandstone (Sample 20141106BG-2) with similar iron oxide mineralization to that of Sample 20141106BG-1. Boles and Surdam (1979) suggested that the presence of heulandite may indicate an influx of fresh water into a saline lake system, of which the increased sand component may also be indicative.

seen in aerial images. The rim itself is a north-northwest trending erosional escarpment that spans approximately 6 miles from sec. 35, T. 22 N., R. 108 W., to sec. 30, T. 21 N., R. 107 W. The Blue Rim escarpment exposes sediments within the upper portion of unit A of the Bridger Formation (Matthew, 1909; Kistner, 1973), which forms badlands topography along Blue Rim (fig. 35). The escarpment is west-southwest facing, and regional dip in the area is up to 1.5° to the southwest, meaning that the slope is notably retreating updip (Kistner, 1973).

With the exception of minor but persistent lacustrine limestone beds, the Bridger Formation at Blue Rim is composed of fluvial deposits (Kistner, 1973). At Blue Rim, the upper unit A of the Bridger Formation overlies the lacustrine Opal Tongue of the Laney Member of the Green River Formation (Kistner, 1973). The Opal Tongue forms a ledge at the base of Blue Rim and overlies the lower portion of unit A of the Bridger Formation. Surdam (1972) reported that tuff and tuffaceous sandstone in the Bridger Formation near Blue Rim host clinoptilolite.

Upper Big Island Wash, sec. 7, T. 21 N., R. 108 W., Sweetwater County

Location number 71 of King and Harris (2002) mentions clinoptilolite in tuffs and tuffaceous sandstones in Eocene Bridger Formation in the Blue Rim area of northwest Sweetwater County, originally reported by Surdam (1972). Clinoptilolite was identified in a sample of gray non-calcareous tuffaceous sandstone with patchy yellow surface staining one in the western half of this section (fig. 36). The sample is predominantly quartz sandstone, along

Figure 31. Thin oil shales of the Laney Member of the Green River Formation at Kinney Rim, SW1/4 sec. 18, T. 14 N., R. 99 W., Sweetwater County. The presence of oil shales may suggest a change in water chemistry from inhospitable hypersaline-alkaline to fresher water more supportive of organisms (Surdam and Parker, 1972). Fluctuating water chemistry is likely responsible for the periodic nature of zeolite-bearing versus organic-rich strata.

with lesser amounts of potassium feldspar and still lesser clinoptilolite.

Stevens Flat, sec. 16, T. 20 N., R. 108 W., Sweetwater County

The contact between the Bridger Formation and the underlying Laney Member of the Green River Formation is gradational and inconspicuous in this area of the basin (fig. 37). We collected three samples containing minor amounts of clinoptilolite, presumably near the base of the Bridger Formation. King and Harris (2002) suggest that this location was possibly mistaken for the Blue Rim location described by Surdam (1972). Current field investigations contradict this assertion. Wolfbauer (1972) reported the presence of clinoptilolite in the Opal tuff of the Bridger Formation near Stevens Flat but did not provide an exact location. Kistner (1973) later gave the legal location of the Opal tuff (called the "White Tuff" in his 1973 M.S. thesis) sample at Stevens Flat in sec. 17, T. 20 N., R. 108 W. We sampled tuffaceous sediments approximately 0.5 – 1 mile east of Wolfbauer's (1972) sample locations hosted minor heulandite and clinoptilolite,but seemingly less than 20 percent as Kistner (1973) reported. Our samples are from gray to light yellow to light bluish gray, locally yellow stained, biotitic tuffaceous sandstone (fig. 38).

Central Wyoming

There are several zeolite-rich deposits in this region of Wyoming, although they are only considered marginally economic at best, mostly due to the beds' lack of sufficient thickness, low zeolite content, excessive overburden, or a combination thereof. During this investigation, we

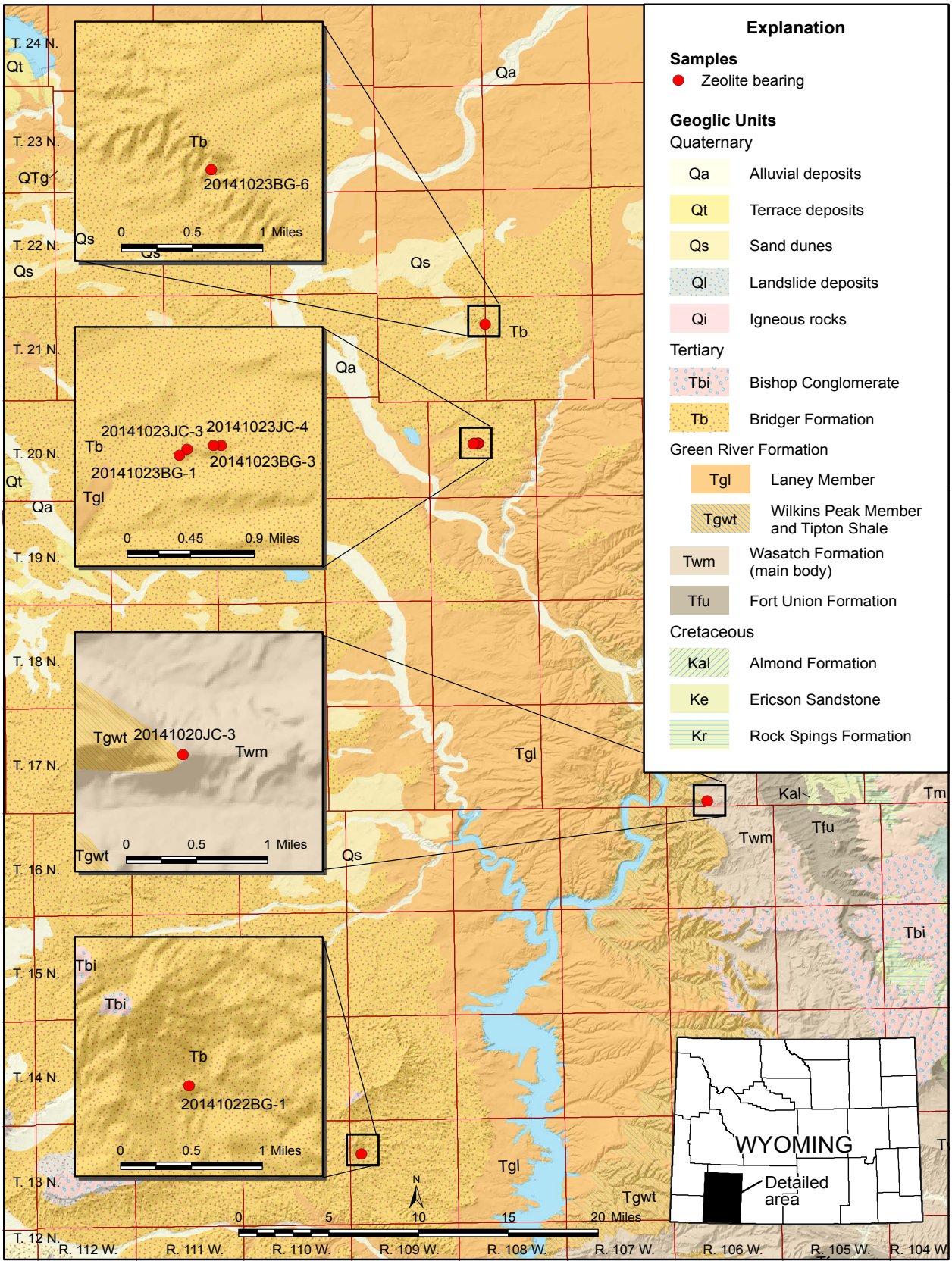

Figure 32. Geologic map of part of the western Green River Basin, showing sample sites in western Sweetwater County, Wyoming. Map modified from Love and Christiansen (1985, 2014 release).

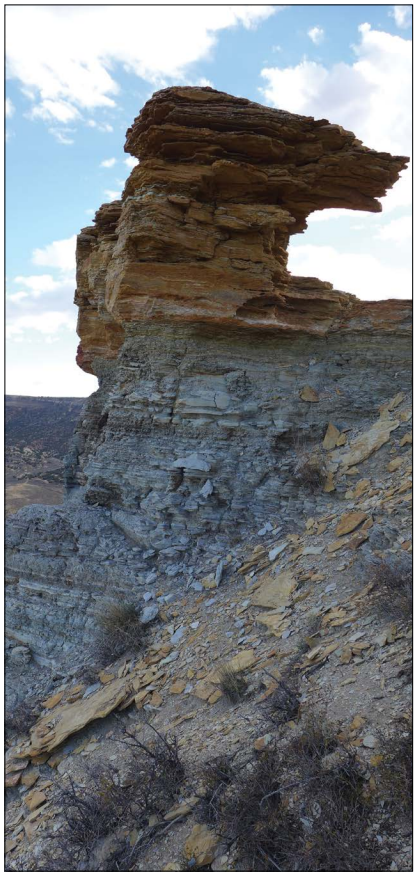

Figure 33. Outcrops of interbedded red thinly bedded mudstone, and greenish-gray to yellowish-brown thinly bedded to shaley mudstone in the lower Wilkins Peak Member of the Green River Formation in the Firehole Canyon area. Sample 20141020JC-3 is of the greenish-gray to yellowish-brown thin-bedded to shaley mudstone and hosts analcime.

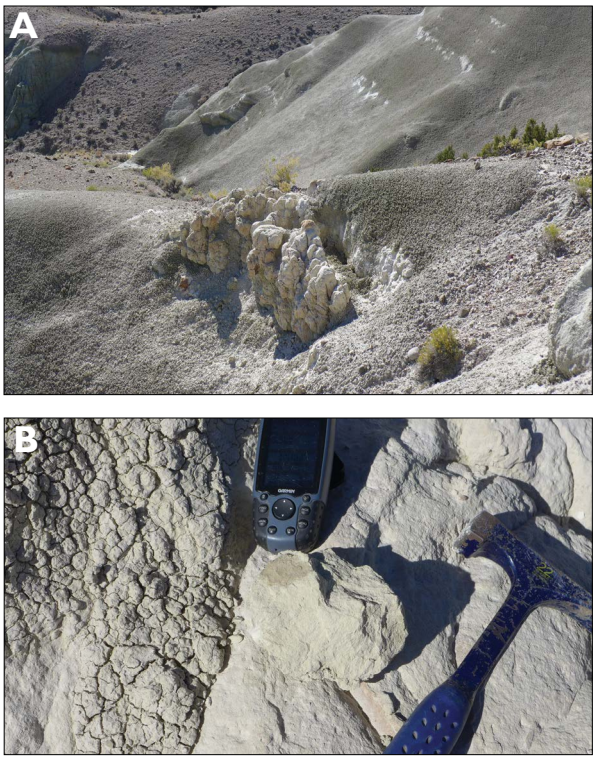

Figure 34. A) Outcrop of the Henrys Fork tuff on the southeast slope of the south Twin Butte. The tuff is a persistent marker bed in the area. B) Sample 20141022BG-1, taken from the Henrys Fork tuff.

examined known or reported occurrences in and around the Wind River Basin, primarily Eocene rocks of similar age to those described above, but also in rocks of Triassic, Miocene, and Pliocene ages.

Wind River Basin

This investigation identified no significant zeolite occurrences in the interior of the Wind River Basin. However, several previous workers have described potential zeolite occurrences and other probable locations for zeolite. Abundant tuffs occur in the western and northern most portions of the basin within the Wind River Formation and younger overlying units. King and Harris (2002) note several minor occurrences in central Wyoming that were not prioritized for this investigation (table 3).

Beaver Rim

Beaver Rim, also known as Beaver Divide, is an escarpment resulting primarily from the erosion of Oligocene and younger sediments that once covered the majority of the Wind River Basin. The resistance of conglomerate and sandstone in the lower White River Formation controls the rate of exposure and subsequent erosion of the pre-Oligocene rocks below. The escarpment that forms Beaver Rim extends northeastward from the Green Cove area (T. 30 N., R. 96 W.) in southern Fremont County past Sand Draw oil field (T. 32 N., R. 95 W.), and then meanders generally eastward toward the Rattlesnake Hills in southwestern

Figure 35. The erosional escarpment of the Bridger Formation at Blue Rim. Tuffs, tuffaceous sandstone, and bentonitic claystones and mudstones weather and erode to form a badlands topography. In the distance is the Big Island trona mine (OCI Inc.). This view of Big Island Wash is to the southwest and was taken in the W1/2 of sec. 7, T. 21 N., R. 107 W., northwest Sweetwater County.

Natrona County (T. 33 N., R. 88 W.). The name Beaver Rim is widely recognized, while the name Beaver Divide is more descriptive with respect to the region's drainage systems. Streams to the north and northwest flow into the Wind River, and those to south and southeast flow into the Sweetwater River.

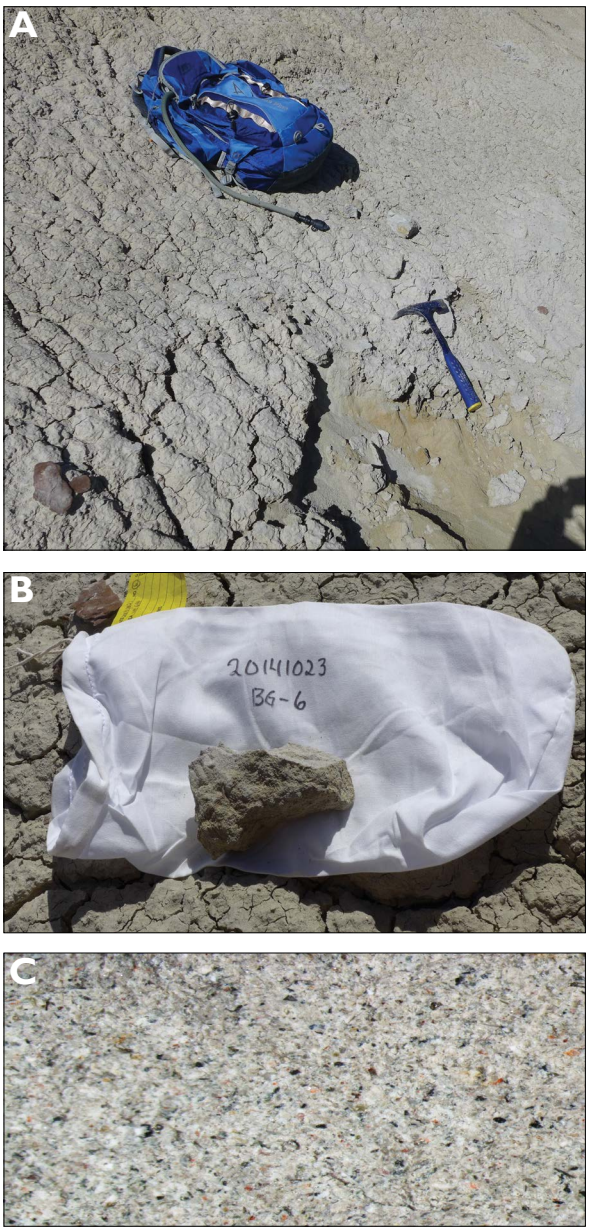

Figure 36. A) Bentonitic mudstone with subtle tuffaceous sandstone, Blue Rim area. B) Minor clioptilolite is present in this sample as part of the tuffaceous matrix in this sandstone. C) Detrital and authigenic grains with interstitial minor clinoptilolite-bearing matrix; width of view is 11 mm.

Figure 37. Outcrop of the Opal Tongue at Stevens Flat. In the foreground is bluish gray, weakly calcareous, clinoptilolite-bearing mudstone, with minor pelecypod fossils. This is the location of Sample 20141023JC-4. The bluish-gray mudstone is overlain by gray, fine-grained tuffaceous, heulandite-bearing sandstone with minor biotite and cast fossils. The gray tuffaceous sandstone is represented by Sample 20141023JC-3.

Figure 38. Interbedded tuffaceous sandstones and mudstones of the Opal Tongue of the Bridger Formation at Stevens Flat, sec. 16, T. 20 N., R. 108 W., western Sweetwater County.

Table 3. Miscellaneous natural zeolite occurrences in central Wyoming. Numbers in parentheses refer to select minor occurrences in King and Harris (2002); WRR = Wind River (Indian) Reservation.

Location Name (Location Number)	Legal Location	County	Geologic Unit	Zeolite(s) Present	Reference
Sand Draw oil and gas field area (21)	sec. 1, T. 32 N., R. 95 W.	Fremont	Wagon Bed Formation	Clinoptilolite	Boles, 1968; Boles and Surdam, 1971
South of Wagon Bed Spring (21)	sec. 3, T. 31 N., R. 95 W.	Fremont	Wagon Bed Formation	Erionite	Boles, 1968; Boles and Surdam, 1971
Green Cove area (21)	secs. 2 and 3, T. 30 N., R. 96 W.	Fremont	Wagon Bed Formation	Chabazite, phillipsite	Boles, 1968; Boles and Surdam, 1971
Halfway Draw tuff member (23)	sec. 2, T. 33 N., R. 96 W.	Fremont	Wind River Formation	Clinoptilolite	Love, 1970
Crowheart Butte (24)	sec. 23, T. 4 N., R. 3 W. (WRR)	Fremont	Wind River Formation	Clinoptilolite	Boles and Surdam, 1973
Ethete (25)	sec. 20, T. 1 N., R. E. (WRR)	Fremont	Mowry Shale	Analcime	Slaughter and Early, 1965
Maverick Springs (26)	T. 6 N., R. 3 W. (WRR)	Fremont	Mowry Shale	Analcime	Slaughter and Early, 1965
Dubois area (28)	T. 40 N., R. 105 W.	Fremont	Popo Agie Member	Analcime	Keller, 1952
Popo Agie Member type section (29)	sec. 3, T. 32 N., R. 100 W.	Fremont	Popo Agie Member	Analcime	Keller, 1952
Maverick Springs Dome (30)	T. 6 N., R. 3 W., (WRR)	Fremont	Popo Agie Member	Analcime	Keller, 1952
Circle Ridge Dome (31)	sec. 6, T. 6 N., R. 2 W., (WRR)	Fremont	Popo Agie Member	Analcime	Keller, 1952
Derby Dome (32)	Tps. 31 N. and 32 N., R. 98 W.	Fremont	Popo Agie Member	Analcime	Keller, 1952
Red Grade (33)	sec. 13, T. 5 N., R. 6 W., (WRR)	Fremont	Popo Agie Member	Analcime	High and Picard, 1965
Hudson Dome (34)	sec. 24, T. 2 S., R. 1 E., (WRR)	Fremont	Popo Agie Member	Analcime	High and Picard, 1965
Dallas Dome (35)	sec. 13, T. 32 N., R. 99 W.	Fremont	Popo Agie Member	Analcime	High and Picard, 1965
Red Canyon (36)	sec. 36, T. 31 N., R. 99 W.	Fremont	Popo Agie Member	Analcime	High and Picard, 1965
Stratigraphic section no. 8 (37)	NW ¼, sec. 18, T. 6 N., R. 2 E., (WRR)	Fremont	Mowry Shale	Analcime	Davis, 1967a,b
West of Horse Creek Road (38)	sec. 11, T. 42 N., R. 107 W.	Fremont	Mowry Shale	Analcime	Davis, 1967a,b
Kidd Ranch (54)	sec. 23, T. 39 N., R. 82 W.	Natrona	Mowry Shale	Analcime	Slaughter and Early, 1965; Davis, 1971a,b, 1976
Casper area (55)	secs., 30 and 31, T. 33 N., R. 80 W.	Natrona	Mowry Shale	Analcime	Slaughter and Early, 1965; Davis, 1971a,b, 1976
Stratigraphic section no. 6 (56)	sec. 32, T. 39 N., R. 85 W.	Natrona	Mowry Shale	Analcime	Davis, 1967a

Wagon Bed Formation

The Eocene Wagon Bed Formation crops out along most of the length of Beaver Rim in Fremont and western Natrona Counties. Van Houten (1964) provided a detailed description of the stratigraphy of the Wagon Bed Formation across its outcrop length. West of the Conant Creek anticline, Wagon Bed Formation is divided into five stratigraphic units; east of Muskrat Basin, the Wagon Bed is divided into six units (Van Houten, 1964). Only the lowest (unit 1) is correlative from east to west. In the area between Conant Creek anticline and Muskrat Basin, the Wagon Bed is only divided into unit 1 and an upper undifferentiated succession. The Wagon Bed Formation in general contains a succession of mostly persistent sandstone, siltstone, and mudstone beds of variable thicknesses, and with significant volcanic material and bentonitic clays (Van Houten, 1964). Significant zeolite mineralization has only been recognized in the Wagon Bed Formation west of the Conant Creek anticline (Van Houten, 1964; King and Harris, 2002).

During this investigation samples were collected from as many tuffaceous units as possible in both the western (fig. 39) and eastern areas of Wagon Bed Formation outcrops along Beaver Rim. In Wagon Bed outcrops below Beaver Rim west of Conant Creek anticline, zeolite minerals are most common in unit 3 (Van Houten, 1964), although scattered occurrences are also reported from units 4 and 5.

In the Wagon Bed Spring area, all five units described by Van Houten (1964) are exposed. Only those taken from unit 3 (of Van Houten, 1964) contained zeolite minerals, although zeolite occurrences are also reported from unit 4 (fig. 40).

Wagon Bed Spring, secs. 33 and 34, T. 32 N., R. 95 W., Fremont County

Wagon Bed Spring is in the SW¼ sec. 34, T. 32 N., R. 95 W. immediately west of Wyoming Highway 135 where it crosses Beaver Rim. Most of the Wagon Bed Formation is well exposed at Wagon Bed Spring. Following the stratigraphic divisions of Van Houten (1964), unit 1 consists of ledge forming, interbedded greenish-gray mudstone, and sandstone. Unit 2 is composed of bluish-gray mudstone, interbedded with bluish-gray arkosic sandstone. Unit 3 is a tan to white succession of interbedded tuff, tuffaceous mudstone, and tuffaceous arkosic sandstone. Unit 4 in the Wagon Bed Spring area is poorly exposed, and is composed dominantly of green, glauconitic mudstone. Unit 5 consists of ridge forming greenish gray to red arkosic sandstone, interbedded with mudstone and minor gray to tan tuff. Slump and landslide deposits are common in the lower half of Beaver Rim at Wagon Bed Spring. Zeolites (clinoptilolite or heulandite, or both) are present in tuffs throughout unit 3 at this location.

The Wagon Bed Formation here is overlain by buff to gray, tuffaceous arkosic sandstone of the White River Formation. White River Formation samples collected from the Wagon Bed Spring locality are not zeolitic.

In this area, we sampled units 2, 3, 4, and 5 based on spatial relationships and descriptions by Van Houten (1964). Clinoptilolite and heulandite are the most commonly associated zeolite minerals in this area (Van Houten, 1964). All samples contained clinoptilolite, and all but one also contained minor amounts of heulandite. Samples collected from the lower part of unit 3 consisted of weakly to moderately sandy biotite tuff, with common, local rusty brown to pale yellow iron-oxide staining, and scattered vugs. Tuffaceous layers commonly crop out along with interbedded sandstone, siltstone, and claystone (figs. 41 and 42). Most homogeneous tuff beds are less than 2 m (6 ft) thick. About 3 m stratigraphically higher in unit 3, in a succession of interbedded tuff and arkosic sandstone, a sample of white to light yellow, limonite-stained biotite tuff contained clinoptilolite and heulandite. Near the top of unit 3, minor amounts of clinoptilolite and heulandite were also identified in a tuffaceous siltstone. Minor slumping is common in the area and has displaced some outcrops (fig. 43).

Government Slide Draw area, sec. 18, T. 31 N., R. 95 W., Fremont County

At this location, samples were collected near the base and near the top of unit 3 (Van Houten, 1964). Figure 44 shows an outcrop of the Wind River Formation overlain by units 1, 2, and 3 of Van Houten (1964). A sample of white to very light gray, iron oxide-stained tuff near the base of unit 3 contained heulandite, while an orange to rusty colored tuff approximately 9 m (30 ft) higher in the section contained erionite (fig. 45). Higher in the section, approximately 8 m (26 ft), a sample from a thin bed of white to greenish gray, vuggy, weakly iron-stained tuff contained clinoptilolite and heulandite (fig. 46).

White River Formation

In the western area of Beaver Rim, Van Houten (1964) describes bentonitic and tuffaceous yellow-gray to grayish orange mudstone, lenses of arkose and conglomerate, and beds of vitric tuff in the Big Sand Draw Sandstone Lentil and overlying Beaver Divide Conglomerate Member. Limestone beds, some of which persist for several miles, are common in the upper porous sandstone sequence. They occur most abundantly 31-61 m (100-200 ft) above the base of the sequence. Although there are no known zeolite

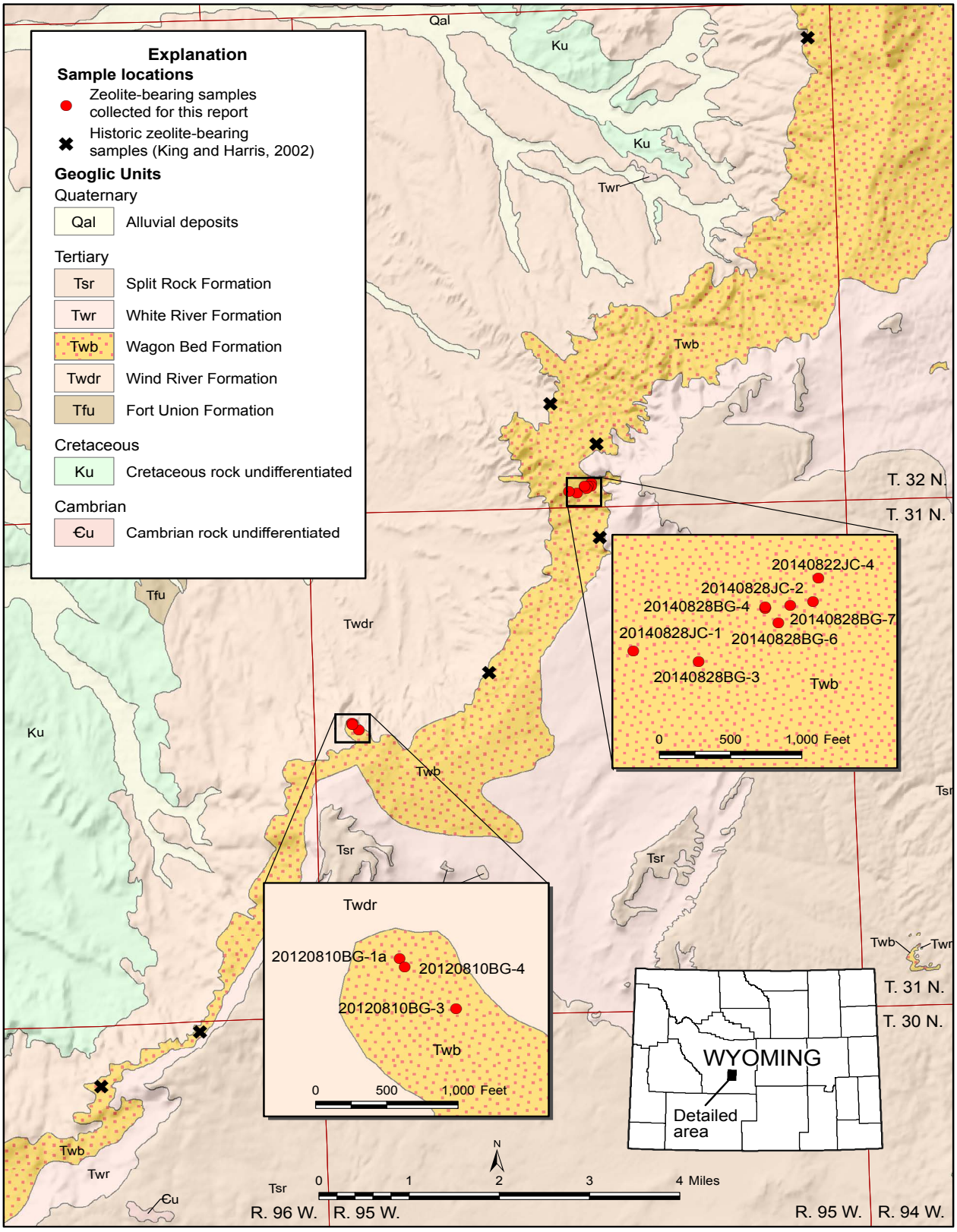

Figure 39. Geologic map of the western Beaver Rim (Beaver Divide) area, Fremont County, showing sample locations for this investigation and also general locations (centroids) of areas discussed in King and Harris (2002). Map modified from Johnson and Sutherland, 2009.

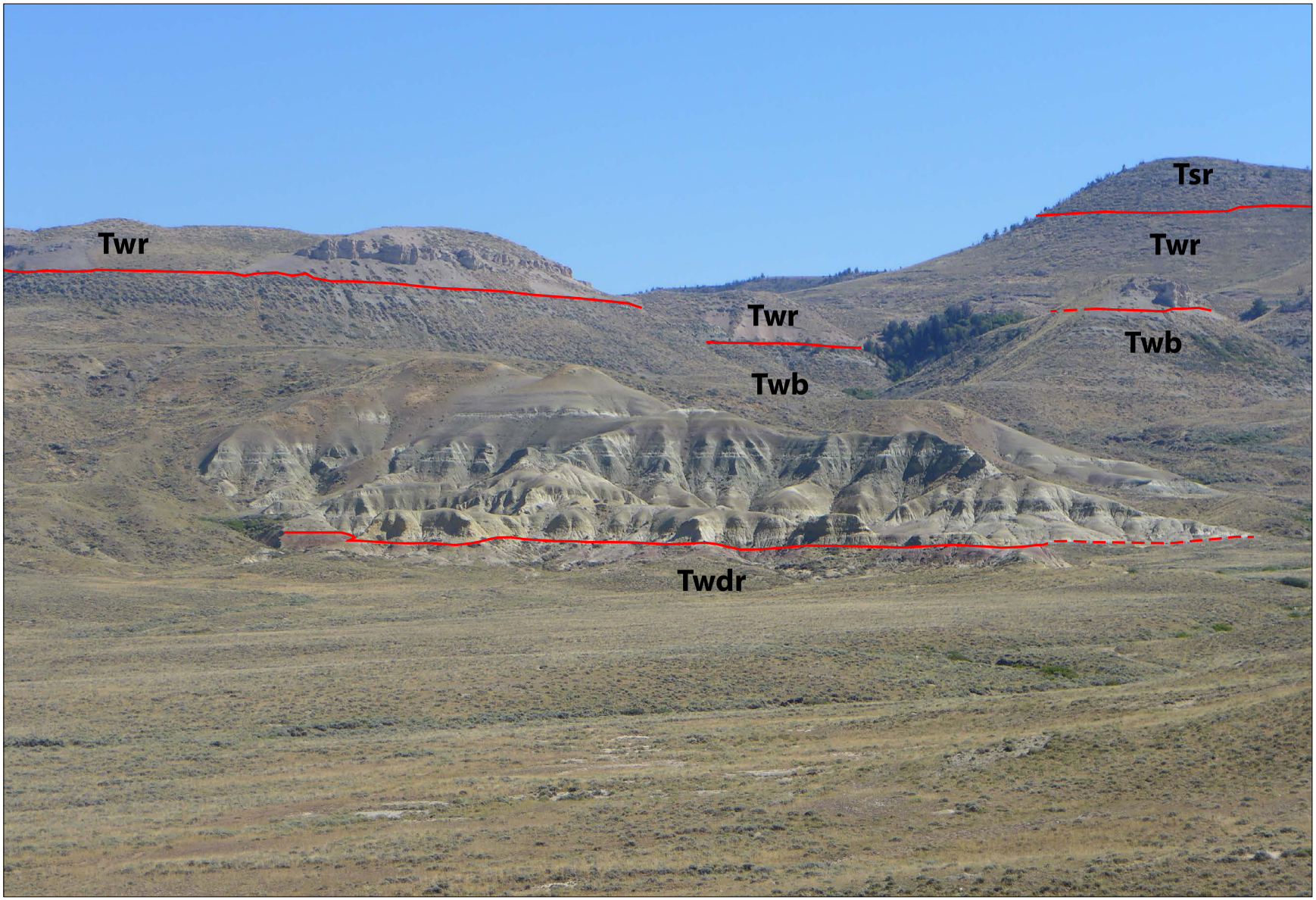

Figure 40. Exposures of the Eocene Wind River (Twdr), Wagon Bed (Twb), the Oligocene White River (Twr), and the Miocene Split Rock (Tsr) Formations at Wagon Bed Spring, secs. 33 and 34, T. 32 N., R. 95 W., Fremont County. The contacts between these units are disconformities. This is the Wagon Bed Formation type section (Van Houten, 1964).

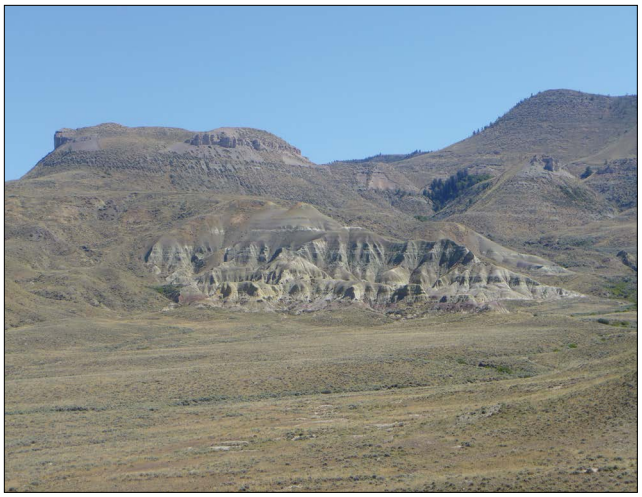

Figure 41. Outcrop of white to light tan to yellow zeolitic biotite tuff from unit 3 of the Wagon Bed Formation (Van Houten, 1964) at Wagon Bed Spring. This outcrop is the sample location of Sample 20140822JC-5. The tuff hosts clinoptilolite and heulandite.

Figure 42. Outcrop of pale yellow tuff with local light orangish iron oxide staining and scattered small vugs. This is the outcrop of Sample 20140828BG-4 taken from the Wagon Bed Formation (unit 3 of Van Houten, 1964).

Figure 43. Light tan to yellow, weakly limonite stained zeolitic tuff from unit 3 of the Wagon Bed Formation (Van Houten, 1964) in a slumped succession of interbedded sandstone and zeolitic tuff. Sample 20140828JC-1 was collected from this outcrop. The tuff hosts heulandite and clinoptilolite.

occurrences in the White River Formation in this region or throughout most of Wyoming, a few samples were available to us and were examined for zeolite potential.

One sample of tuffaceous sandstone from the White River Formation collected in the western Beaver Rim section indicated possible trace amounts of the zeolites offretite and possibly clinoptilolite. XRD methods identified the possibility, but due to high clay contents and peak overlaps, specifically those below 9° 2θ, additional XRD and other analytical methods are required to verify this observation. Sample 14BR05 (Dishpan Butte area), collected by the University of Wyoming, exhibited cation ratios consistent with offretite (Passaglia and others, 1998) and clinoptilolite in the range of CaO statistical methods (Hawk, 1974). Many other samples were examined by XRD, but none matched patterns of known zeolite minerals.

Teacup Butte, sec. 1, T. 32 N., R.90 W., Fermont County

Lander and Hay (1993) note the presence of clinoptilolite at several horizons in the lower White River Formation at this location. Love (1970) described the roughly 148 m (485 ft) section as a succession of interbedded white, gray, olive, brown, and tan sandstones, siltstones, and claystones with abundant calcareous and tuffaceous (biotite) material. This supports the suggestion that these zeolites formed in an open system (Lander and Hay, 1993).

Split Rock Formation

Love (1961, 1970) describes the dominant lithology in the upper porous sandstone sequence of the Split Rock Formation as medium- to coarse-grained gray to buff, massive to coarsely cross-bedded sandstone. Remarkably pure bluish-white pumicite beds are present in the upper porous sandstone sequence. The shards, which are the major constituent, are curved or rectangular and pink or colorless. One such pumicite near Split Rock in sec. 31, T. 29 N., R. 89 W., was sampled but did not contain zeolite minerals.

Sweetwater Arch (Granite Mountains and vicinity)

Split Rock Formation

In a table listing deposits categorized as being at least 30 cm (1 ft) thick and consisting of at least 75 percent clinoptilolite, Sheppard (1976; table 7-2) cited in King and Harris (2002), lists a "tuff in the Split Rock Formation of Miocene age." King and Harris (2002) could not confirm this assertion, nor could we. It is unclear but possible that Sheppard (1976) was referring to the pumicites mentioned by Love (1970). We cannot support that assertion as no significant zeolite occurrences were found in the Split Rock Formation during the course of this investigation, neither in the Split

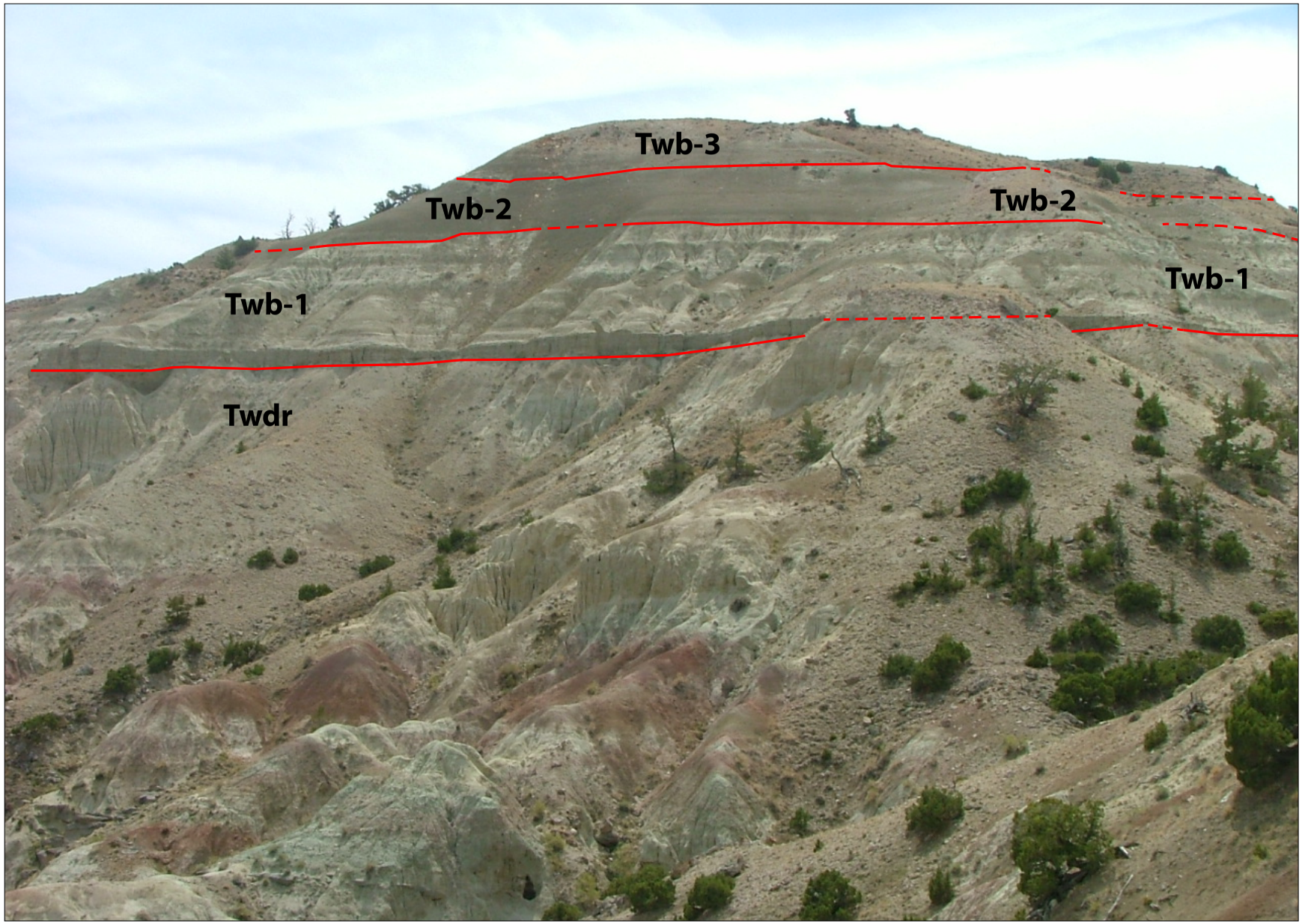

Figure 44. Badland topography in the Wind River Formation (Twdr) and unit 1 of the Wagon Bed Formation (Twb-1) in the Government Slide Draw area, sec. 18,

Figure 45. Heulandite-bearing, greenish-gray tuff (Sample 20120810BG-4) with extensive iron oxide staining of unit 3 (Van Houten, 1964) near Government Slide Draw, Fremont County.

Rock area nor any other Split Rock locations sampled. Trace amounts of what may be a sodium-bearing zeolite (erionite or heulandite, or both) were present in a single sample (see below) and identified using XRD methods. This finding should be further investigated prior to any reporting or additional investigation of zeolite occurrence in Split Rock Formation outcrops. The sample from this investigation is 20150702DB-1.

Dry Creek Road, sec. 30, T. 31 N., R. 89 W., Natrona County

This sample was collected from a distinct double-banded layer of white to pale-tan, tuffaceous sandstone 0.5 m (2 ft) thick with obvious lighter bands of more tuffaceous material on the top and bottom margins of each layer. This sample was taken from the lower of the two bands (approximately 5-10 cm thick) that weathers into small angular clumps. It is bounded on the bottom by brown to tan, calcified sandstone containing abundant white calcifications up to 15 cm in length. XRD identified only a possible trace of sodium-bearing erionite.

Despite the lack of obvious zeolites found in the Split Rock Formation during this investigation, other workers have reported favorable locations to investigate possible zeolitic alterations in tuffaceous rocks of the Split Rock Formation. Love (1970) describes tuffaceous units including "Bluish-white pumicite" of marker bed "P."

In the Split Rock area of southwest Natrona County (sec. 31, T. 29 N., R. 89 W.), a sample of very light weight, blue-gray tuff (similar in character to pumicites described by Love, 1970) tested negative for zeolite minerals; the diffractogram indicated mostly amorphous material, likely due

Figure 46. This sample location (Sample 20120810BG-3) is also from unit 3 and is similar to Sample 20120810BG-4, but lacks the iron oxide staining on weathered surfaces.

to the high concentration of vitric glass shards. This bed is approximately 1.5 m (5 ft) thick and overlies a tan, fine- to very fine-grained tuffaceous sandstone, which is devoid of minerals other than quartz and albite.

Moonstone Formation

Numerous samples collected from the Moonstone Formation during this investigation contain zeolite group minerals. Erionite, offretite, clinoptilolite, and heulandite were found to occur within the various members of the Moonstone Formation described by Love (1961, 1970). Zeolites occur at several intervals within the Moonstone Formation and at multiple stratigraphic depths. Erionite and offretite phases were identified by XRD methods and further defined by Mg/(Ca+Na) and K(+Sr+Ba)/Mg ratios as described by Passaglia and others (1998) from whole rock geochemistry. Those samples containing clinoptilolite and heulandite were identified by XRD methods and differentiated into relative concentrations by CaO abundance statistical methods described by Hawkins (1974) from whole rock geochemistry.

The aerial extent of the Moonstone Formation in the Granite Mountains area is relatively limited. Its western extent lies at the foot of the Precambrian outcrops in central T. 30 N., R. 90 W., and is bounded on the east at the western outcrops of crystalline basement rocks in west-central T. 30 N., R. 88 W. The northernmost mapped outcrops lie in T. 30 N., R. 89 W., and only minor outcrops occur in northernmost T. 29 N., R. 89 W. (Love, 1970; fig. 47).

Lone Mountain and Lankin Creek areas, secs. 16, 27, and 30, T. 30 N., R. 89 W., Natrona County

Love (1961) reports that unit 22 of the Moonstone Formation contains erionite-Ca, erionite-K, and heulandite. He describes the unit as a tan, tuff, part laminated,

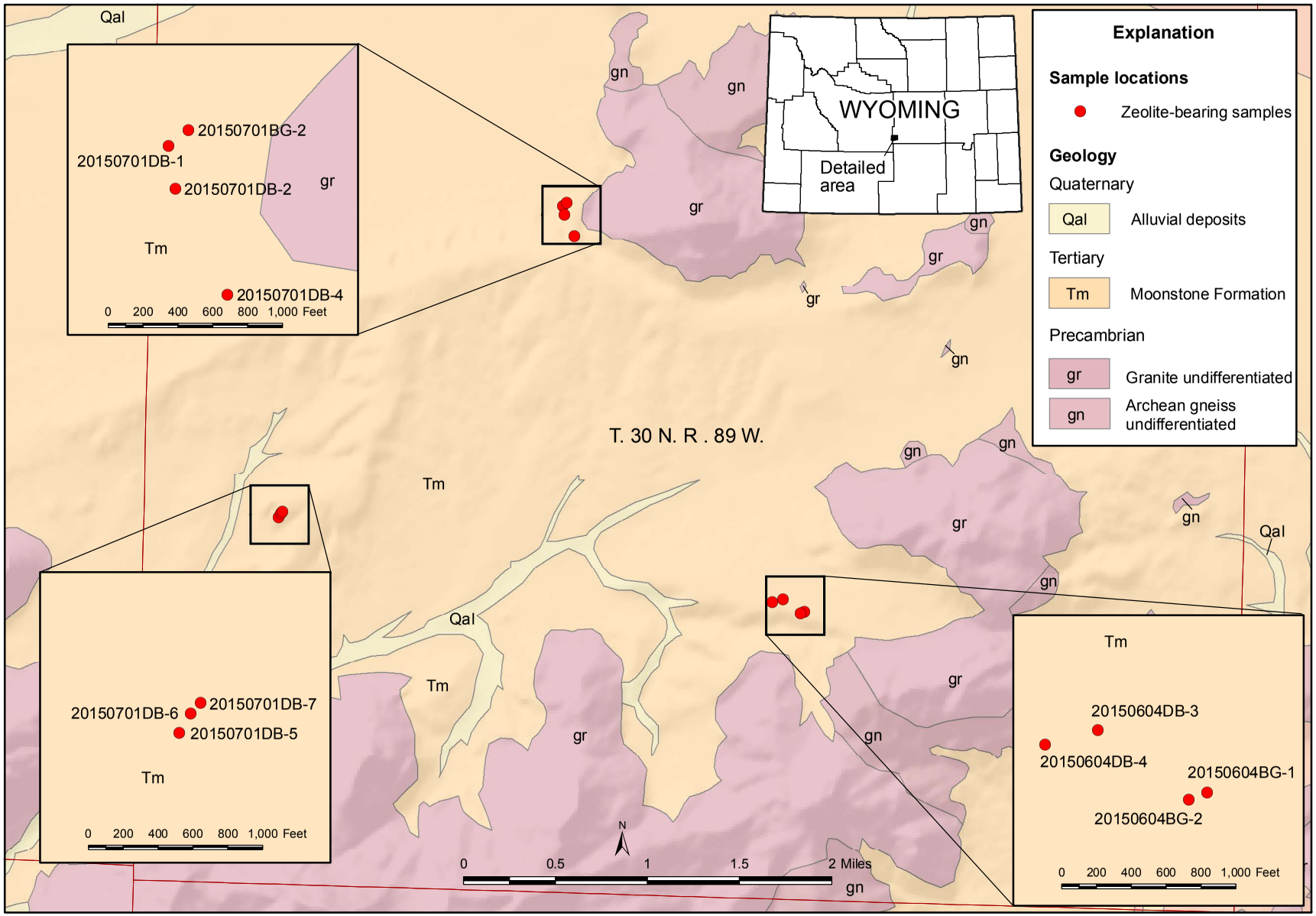

Figure 47. Geologic map of a portion of the central Granite Mountains area in the general vicinity of the Miocene Moonstone Formation exposures. Map modified from Sutherland and Hausel (2003).

part massive, soft although it forms the tops of cliffs, porous, very light weight, with abundant glass shards near top, and approximately 2.7 m (9 ft) thick. Samples from section 16 (immediately west of Lone Mountain) from this investigation include:

20150701BG-2: Tuffaceous sandstone, yellowish gray, subrounded fine- to angular and subangular coarse-grained, poorly sorted, well indurated, calcareous cement; grains include quartz, minor biotite, iron oxides, sparse apatite, and potassium feldspar (figs. 48 and 49).

Sample 20150701DB-2 comes from the top of a normal graded sequence of tuffaceous conglomerate to tuffaceous fine- to very fine-grain sandstone. This sample is the upper fine- to very fine-grain, ledge forming, tan to medium tan bed, containing abundant quartz and lithic fragments (<1 mm). Fragments are very angular. This unit is approximately 4 m (13 ft) thick; the upper portion sampled is variable in thickness, but less than 1 m (3 ft) thick at the sample location.

One sample (20150701DB-5) collected in section 30, and believed to be from unit 22, is described as a ledge-forming, tuffaceous sandstone, massive bedded in most places with laminar bedding in the top meter, tan to light-tan, averaging 3-4 m (10-13 ft) thick. This bed overlies a laminar bedded unit that exhibits distinct soft sediment deformation locally.

Unit 23 of the Moonstone Formation as reported by Love (1961) contains erionite, though additional XRD methods

Figure 48. Moonstone Formation outcrop of Sample 20150701BG-2, believed to be of unit 22 of Love (1961).

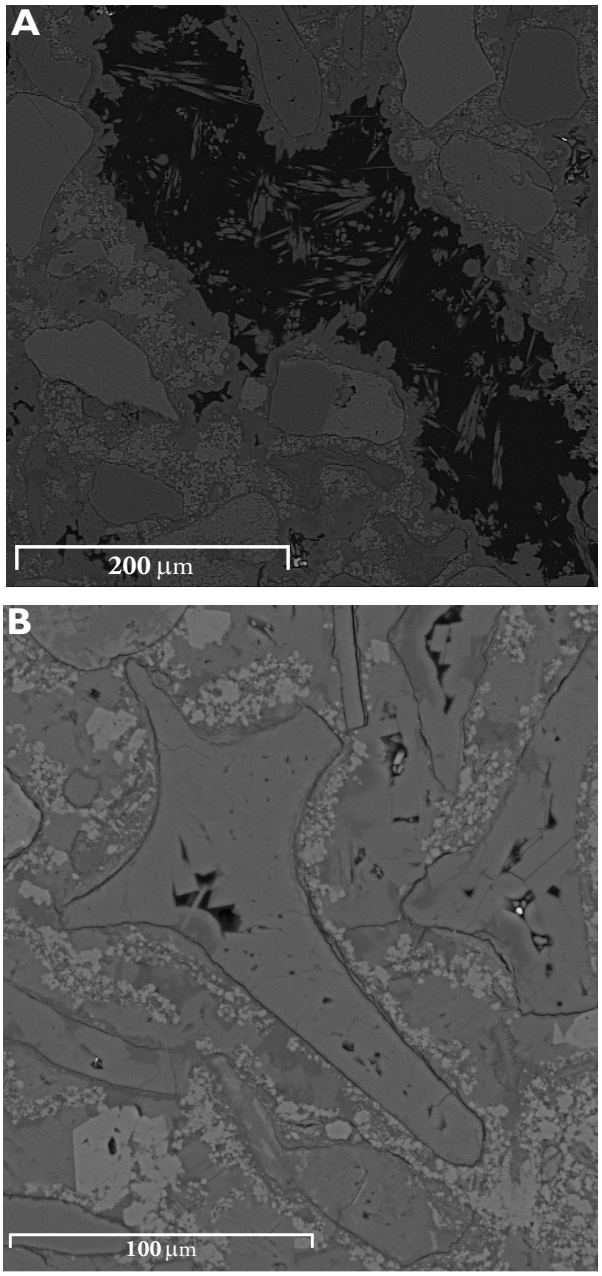

Figure 49. Sample 20150701BG-2 SEM observations: SEM methods identified erionite as thin mineral fibers within pore spaces of the sample. Alteration and etching of glass shards is common in this sample and clearly visible in this SEM electron backscatter image. Matrix of the rock is a mix of $CaCO_3$ and glass shards with erionite intergrowths. A) Erionite crystals in a relatively large pore space. B) Erionite-dominated pseudomorphs of glass shard. Erionite crystals in both A and B are enriched in K, whereas matrix is enriched with respect to Ca and Na while depleted in K. Bright spot just right of center is iron oxide.

are required to differentiate between clinoptilolite and erionite in this member of the formation (i.e. Bish and Chipera, 1991). Love (1961) describes unit 23 as an 8.5 m (28 ft) thick, light gray to white, very limy and very soft tuff that forms "slope above cliff," with "abundant small irregular brown chalcedony nodules that are gray on fractures." Sample 20150701DB-6 (fig. 50) was found to contain erionite, clinoptilolite, and minor amounts of heulandite. The sample is from a massive bedded, 30 cm (1 ft) thick layer of fine- to very fine-grain, tuffaceous sandstone located 1.5 m (5 ft) above Sample 20150701DB-5 (unit 22). It was collected within a several meter thick section of slope forming, tan beds of tuffaceous clay and sandstones, the top surface of which weathers into small tan nodules (mm- to cm-scale).

Figure 50. Outcrop of unit 23 (Love, 1961) of the Moonstone Formation, sec. 30, T. 30 N., R. 89 W., Natrona County. Sample 20150701DB-6 was collected here and contains erionite, clinoptilolite, and minor heulandite.

The bottom of unit 25 of the Moonstone Formation lies approximately 9 m (30 ft) above the top of unit 22 and is reported by Love (1961) to contain more than 50 percent clinoptilolite and lesser fractions of heulandite. Love (1961) describes the tuff of unit 25 as white to rusty-tan in color, very soft, slope-forming, and containing numerous small, irregularly shaped limy and chalcedonic nodules. Also in the unit are larger limestone concretions and "bulbous masses 10 ft (3 m) long and 3 ft (0.9 m) thick with radial structure," as well as local lenses of a "chalky white tuff" (Love, 1961).

Two samples collected from unit 25 of the Moonstone Formation during this investigation contain zeolite minerals. Sample 20150701DB-4 (figs. 51 and 52) was collected near the base of Lone Mountain in section 16, T. 30 N., R. 89 W. This sample is a resistant, white to light tan, very fine-grain, tuffaceous sandstone, less than 1 m (3 ft) thick, and weathers into blocky fragments. This sample location sits approximately 6 m (20 ft) below the ridge top, which is unit 26 described by Love (1961).

Sample 20150701DB-7 was collected in the NW1/4 NE1/4 of section 30 T. 30 N., R. 89 W., approximately one mile north of Lankin Creek. This outcrop is a massive bedded tuffaceous sandstone, 1 m (3 ft) thick, white, fine- to very fine-grained, containing abundant shards and small flecks of biotite (fig. 53). This unit crops out directly below a slightly more resistant, brown to tan, wavy bedded unit approximately 2 m (7 ft) thick. Above the wavy bedding is a thick, approximately 6 m (20 ft), laminar bedded unit of similar color and character. This is the bottom most portion of unit 25 from Love (1961).

Sample 20150604BG-2 was collected from what is most likely unit 42 of Love (1961) and was found to contain minor amounts of erionite and heulandite. Love describes this unit as a 25 ft (7.6 m) thick soft, olive-drab tuffaceous sandstone, nodular and "slabby" in part. At this location, the outcrop is a tuffaceous sandstone, pale yellow, well indurated, very fine- to fine-grained, well sorted subangular to subrounded sand component, non-calcareous cement; sand-sized grains include quartz, biotite, chert, possible garnet, glass shards, and secondary iron oxide staining (fig. 54).

Sample 20150604BG-1 was collected approximately 5 m (16 ft) stratigraphically up-section from Sample 20150604BG-2. This outcrop is believed to be unit 44 of Love (1961), which he describes as a 3 m (10 ft) thick succession of both sandstone and tuff, white to light tan, soft, and interbedded with pumicite and claystone. Sample 20150604BG-1 is generally similar in character to that of

Figure 51. Outcrop of unit 25 (Love, 1961) of the Moonstone Formation, sec. 30, T. 30 N., R. 89 W., Natrona County. Sample 20150701DB-4 was collected here and contains minor heulandite.

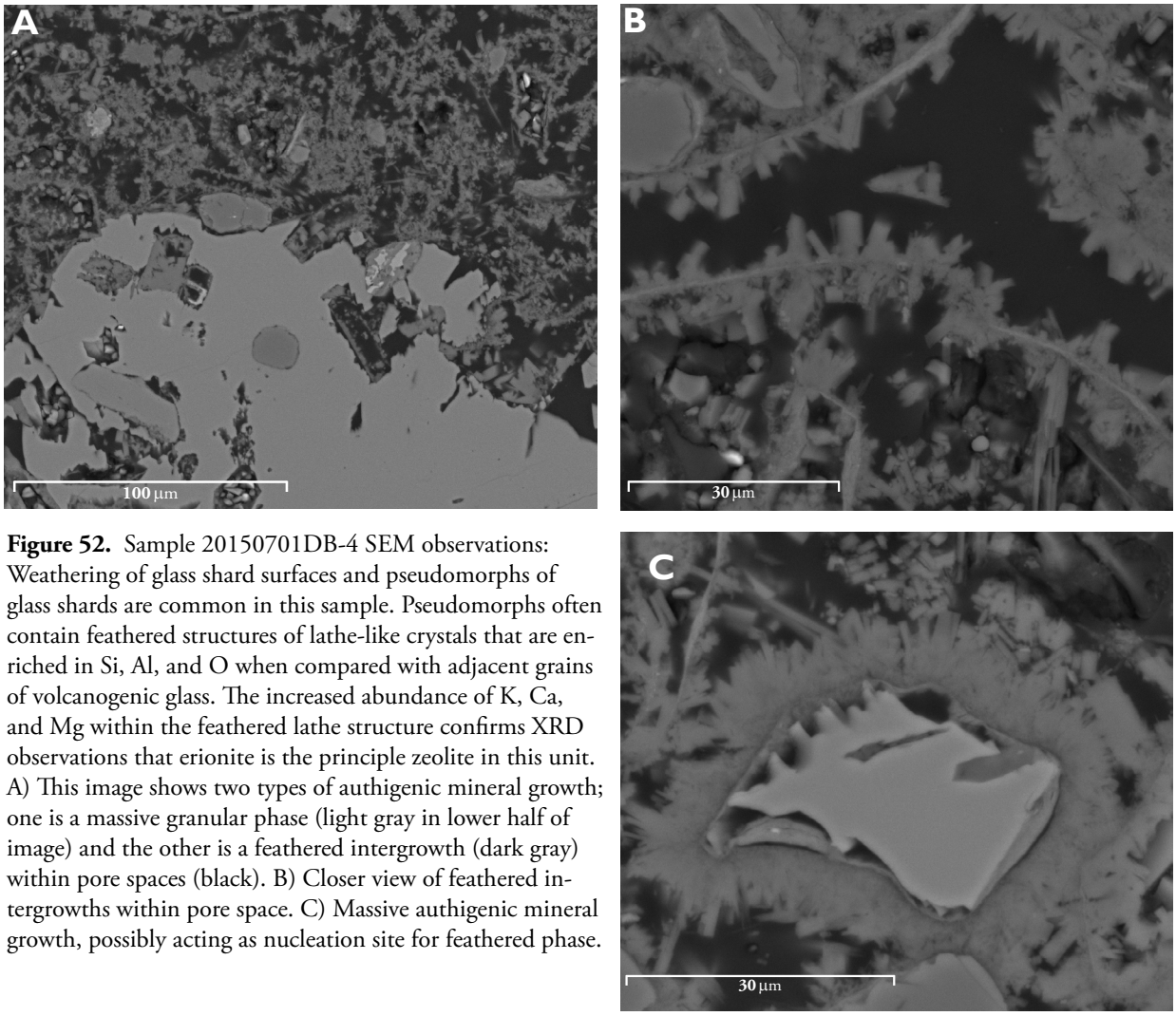

Figure 52. Sample 20150701DB-4 SEM observations: Weathering of glass shard surfaces and pseudomorphs of glass shards are common in this sample. Pseudomorphs often contain feathered structures of lathe-like crystals that are enriched in Si, Al, and O when compared with adjacent grains of volcanogenic glass. The increased abundance of K, Ca, and Mg within the feathered lathe structure confirms XRD observations that erionite is the principle zeolite in this unit. A) This image shows two types of authigenic mineral growth; one is a massive granular phase (light gray in lower half of image) and the other is a feathered intergrowth (dark gray) within pore spaces (black). B) Closer view of feathered intergrowths within pore space. C) Massive authigenic mineral growth, possibly acting as nucleation site for feathered phase.

Figure 53. Outcrop of the base of unit 25 of Love (1961). Sample 20150701DB-7 was collected here and found to host a minor amount of heulandite.

Sample 20150604BG-2 but lacks a laminar characteristic. Erionite and offretite are present in this sample, mostly as matrix material interstitial to fine to very fine grains of quartz, biotite, chert, glass shards, iron oxides, and possibly granite (fig. 55).

Also from what is believed to be unit 44, Sample 20150604DB-3 was taken from a location approximately 220 m (720 ft) to the northwest of Sample 20150604BG-1 (see above). This sample also contains small amounts of interstitial erionite and offretite (fig. 56). This sample is a laminar to lenticular bedded, white to tan, tuff or pumicite bed, directly overlapping a brown to tan sandstone unit containing abundant conglomeratic lenses. This unit is low density, sparkly, and has minor biotite. The laminar bed with the least amount of sandstone material was sampled along the top of a ridge of good exposure.

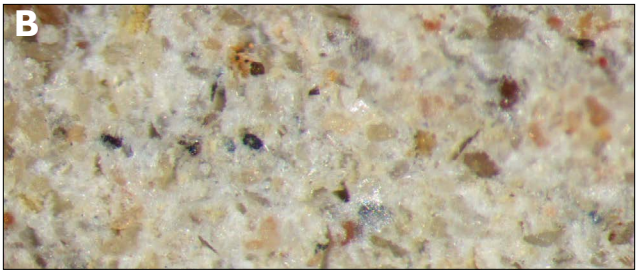

Figure 54. A) This location hosts minor amounts of heulandite and erionite in the matrix of this tuffaceous sandstone. Sample 20150604BG-2 was collected here and is consistent with Love's (1961) description of unit 44. B) Close-up view of Sample 20150604BG-2 showing tuffaceous matrix (white), subrounded detrital grains, and local angular elongate glass shards; width of view is 3 mm.

Sample 20150604DB-4 is from a thin (0.3 m or less), white to yellow, limey, tuffaceous bed making up the lower portion of unit 44. The bed is laminar but exhibits an undulatory character in some places due to possible algal matting or bedding ripple processes. Overlying this bed is a distinct resistant, gray tuffaceous sandstone, approximately 15 cm (0.5 ft) thick. All other tuffaceous beds within unit 44 overlie this sample location. Offretite and erionite are present as matrix material in this sample (fig. 57).

Bug Formation

The known extent of the Pliocene-Pleistocene Bug Formation covers 3 square miles in southwestern Natrona County (fig. 58). The Bug Formation consists of interbedded limestone, claystone, tuff, shale, and volcanoclastic sandstone and conglomerate (Love, 1970). Pebbles within Bug conglomerate are predominantly andesite and other volcanic rock types derived from the Rattlesnake Hills volcanic system. The fossil diatom assemblage of the Bug Formation indicates that it was, at least in part, deposited in a saline lacustrine environment (Love, 1970). At its type section in SW¼, SE¼, Sec. 5, T. 30 N., R. 87 W., the Bug

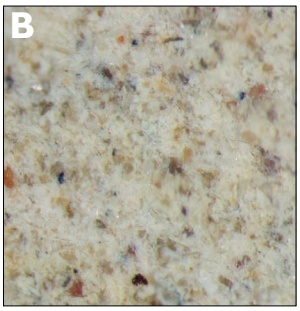

Figure 55. A) This location lies within unit 44 of Love (1961), and its description is similar to that of Sample 20150604BG-2. B) Close-up view shows a greater amount of tuffaceous (erionite/offretite-bearing) matrix; width of view is 3 mm.

Formation is more than 36 m (118 ft) thick; the maximum thickness of the Bug probably does not exceed 38 m (125 ft; Love, 1970). Surdam (1972) reported clinoptilolite in tuff within the Bug Formation, and Sheppard (1976) includes the formation in a table listing deposits categorized as being at least 30 cm (1 ft) thick and consisting of at least 75 percent clinoptilolite. While we did not observe a bed of clinoptilolite-rich tuff as indicated by Sheppard (1976), we did detect minor amounts of that zeolite mineral in a sample (20140909JC-1) of light green, fine- to medium-grained, rounded tuffaceous sandstone as matrix material interstitial to quartz, biotite, and hornblende (fig. 59).

Lysite Mountain area

Lysite Mountain is a high elevation erosional surface in the eastern Owl Creek Mountains resting unconformably on Mesozoic sediments of the southeastern Bighorn Basin in southeastern Hot Springs, southeastern Washakie, and northeastern Fremont Counties (fig. 60). Two sequences of middle and late Eocene rocks are present in the vicinity of Lysite Mountain. Love and Christiansen mapped the Eocene-aged rocks in the vicinity of Lysite Mountain as the Wagon Bed Formation. Bay (1969) provided the most thorough description of the Eocene sedimentary rocks in the area and divided them into informal *lower* and *upper sequences*. The lower sequence is roughly equivalent to the Aycross Formation in age, and the upper sequence is roughly equivalent in age to the Tepee Trail Formation. All

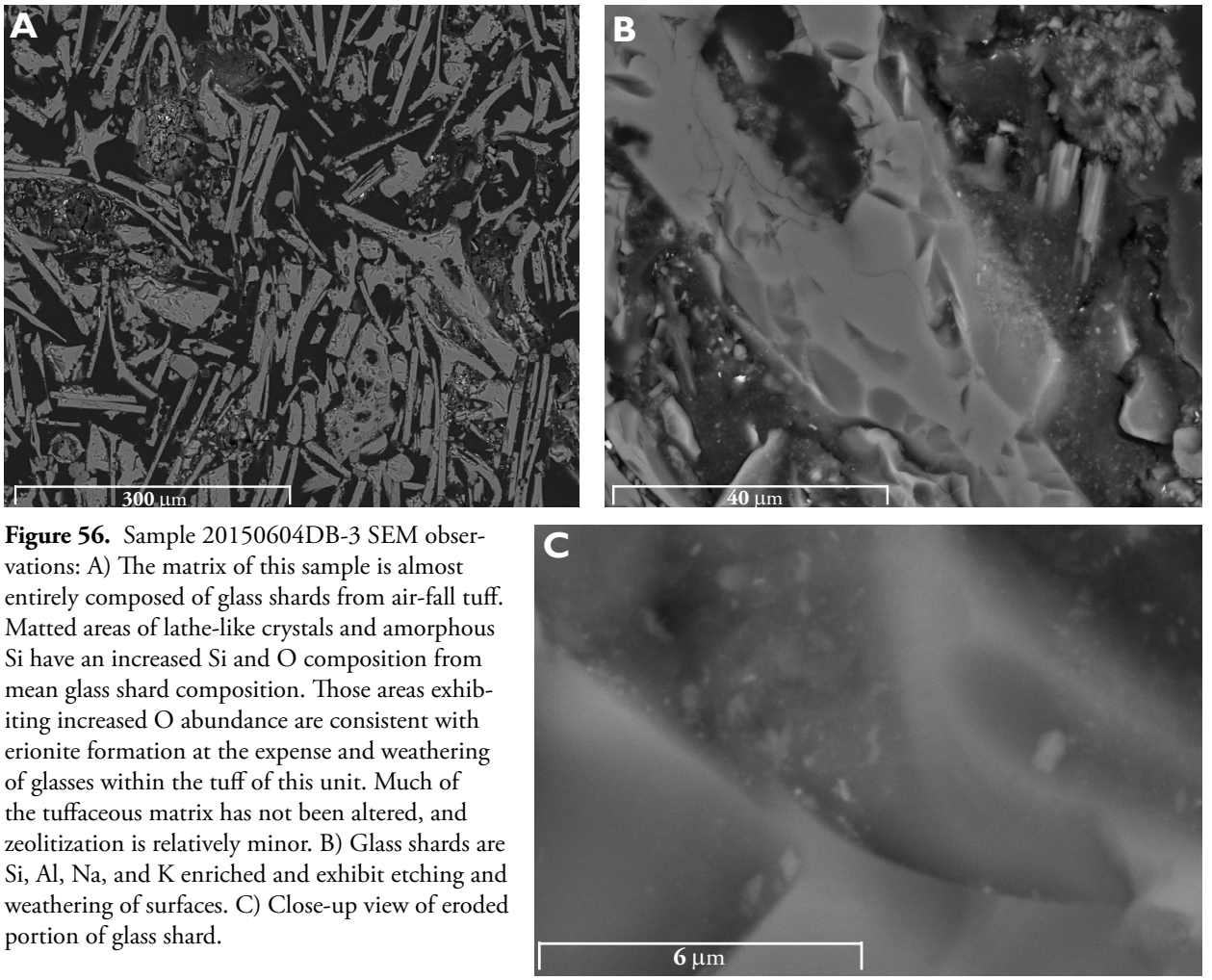

Figure 56. Sample 20150604DB-3 SEM observations: A) The matrix of this sample is almost entirely composed of glass shards from air-fall tuff. Matted areas of lathe-like crystals and amorphous Si have an increased Si and O composition from mean glass shard composition. Those areas exhibiting increased O abundance are consistent with erionite formation at the expense and weathering of glasses within the tuff of this unit. Much of the tuffaceous matrix has not been altered, and zeolitization is relatively minor. B) Glass shards are Si, Al, Na, and K enriched and exhibit etching and weathering of surfaces. C) Close-up view of eroded portion of glass shard.

Figure 57. Outcrop of Moonstone Formation, unit 44 (Love, 1961). A sample of tuffaceous sandstone from this location (20150604DB-4) was found to host minor amounts of offretite and erionite.

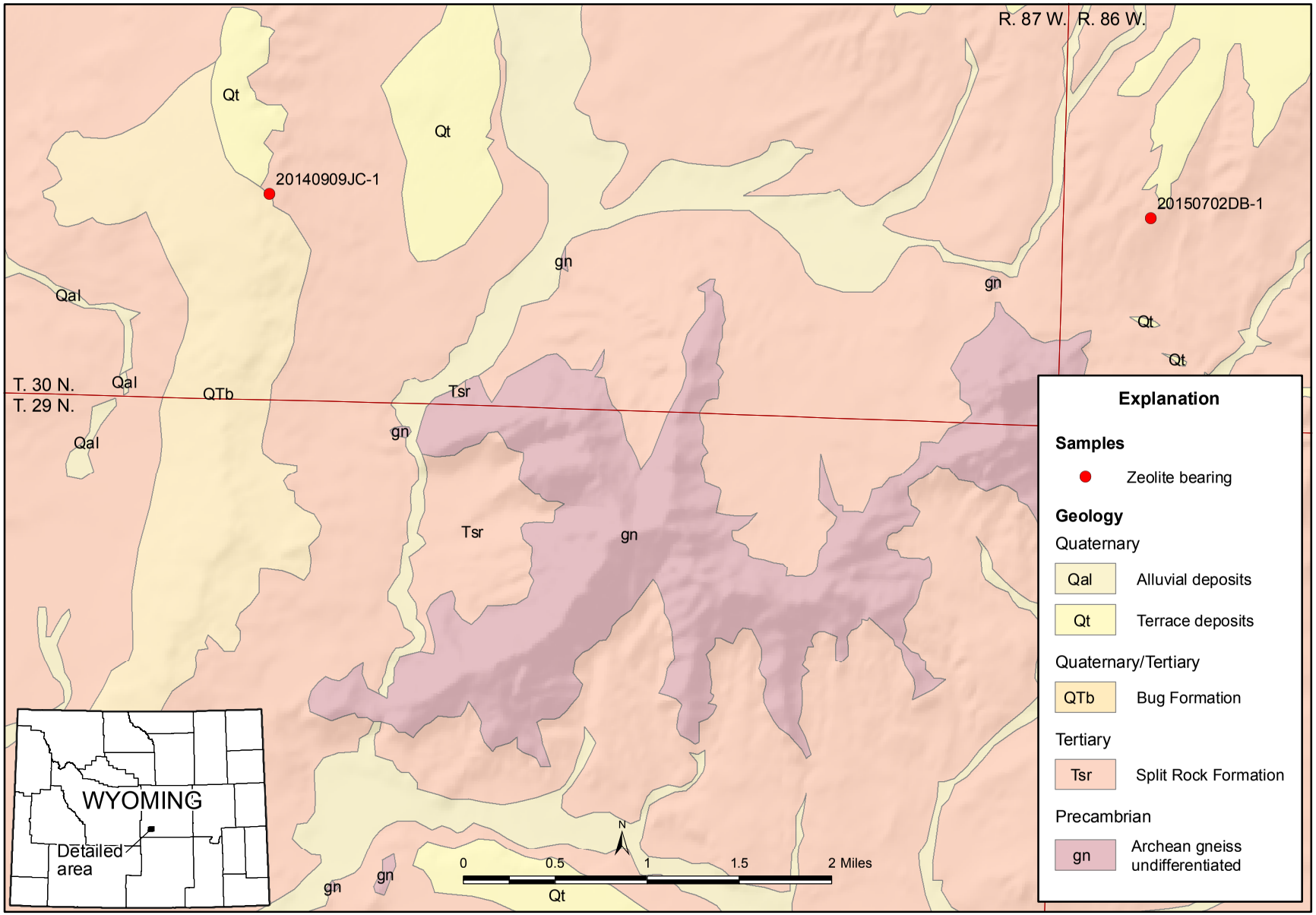

Figure 58. Geologic map of a region of the eastern Granite Mountains showing locations of zeolite-bearing samples collected in the Moonstone (Tms) and Bug (Tb) Formations. Map modified from Love and Christiansen (1985, 2014 release).

Figure 59. Outcrop of light green lithic quartz sandstone of the Bug Formation. The sandstone is medium-grained and rounded with a tuffaceous matrix. Clinoptilolite is hosted in the sandstone. This outcrop is the sample location of 20140909JC-1.

units are middle and upper Eocene, and are generally also time equivalents of the Wagon Bed, Washakie Bridger, and much of the Green River Formations (fig. 11).

The lower sequence is commonly tuffaceous and composed of pale-red to greenish-gray siltstone, sandstone, claystone, organic sediments, analcimolite, conglomerate, tuff, and limestone. At its thickest point, the lower sequence is nearly 152 m (500 ft) thick. The contact between the lower sequence and the underlying Mesozoic and Paleozoic sediments is an angular unconformity (fig. 61).

Like the lower sequence, the upper sequence is commonly tuffaceous. Principle lithologies include greenish-gray to yellowish-gray sandstone, siltstone, limestone, claystone, tuff, conglomerate, and analcimolite. The upper sequence ranges in thickness from 91 to nearly 305 m (300-1,000 ft) thick. The upper sequence disconformably overlies the lower sequence (Bay, 1969). Analcime was first observed around Lysite Mountain by Tourtelot (1946). Bay (1969) additionally identified clinoptilolite and mordenite in both the lower and upper sequences, as well as erionite in the upper sequence. Analcime is the only zeolite Bay (1969) observed in the western portion of the Lysite Mountain area; clinoptilolite, mordenite, and erionite were reported in the eastern half of the study area.

Bay (1969) primarily focused on the lower sequence in the western portion of his study area. Samples of the upper sequence on the west side of Lysite Mountain do not host zeolites; the primary authigenic mineral in tuffaceous sediments is apparently potassium feldspar.

Sampling from this investigation generally agreed with reported zeolite occurrences in the Lysite Mountain area. Lower sequence units contain mostly orthoclase and microcline, with lesser amounts of clinoptilolite and heulandite. Upper units contained clinoptilolite and heulandite, with lesser amounts of authigenic feldspars.

Hawks Butte area, sec. 35, T. 42 N., T. 90 W., Hot Springs County

Hawks Butte is a prominent escarpment exposing lower sequence rocks of Bay (1969) on the northeastern side of Lysite Mountain (fig. 62). Rocks of the lower sequence unconformably overlie pre-Tertiary rocks. Minor amounts of clioptilolite and heulandite were identified in a sample of tan to white biotitic tuff (20150820DB-2) collected approximately 1.25 km west of Hawks Butte. Zeolite phases in this sample are subordinate to quartz and orthoclase. This unit weathers into irregular flakey chunks with a few dispersed green to pale green-gray spots, less than 1 cm in diameter (fig. 63). This is the first white tuff bed (going up

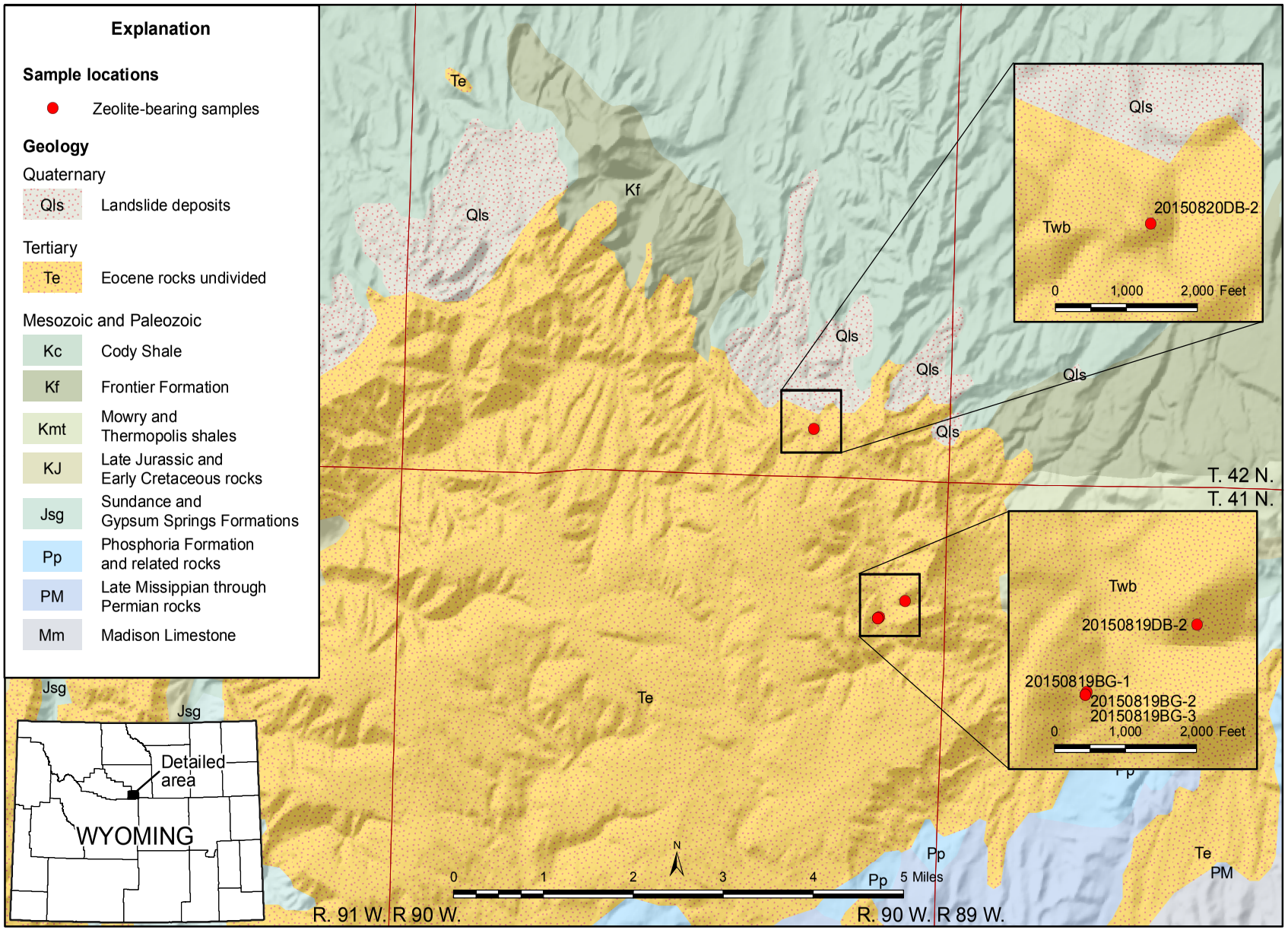

Figure 60. Geologic map of the Lysite Mountain area. Modified from Love and Christensen (1985); Bay's (1969) nomenclature is used for the Eocene Wagon Bed time equivalents (Tels for lower sequence and Teus for upper sequence). Map modified from Love and Christiansen (1985, 2014 release).

Figure 61. East end of Lysite Mountain, southern Washakie County. Eocene beds of the lower sequence (Tels of Bay, 1969) resting unconformably on red beds of the Triassic Chugwater Formation. Slumping (a form of mass wasting that results in large blocks of rock formations dropping or sliding) of the Tertiary and Triassic red beds in the lower portion of the picture, has resulted in the apparent placement of Chugwater red beds above those of the lower sequence (see upper left of photo).

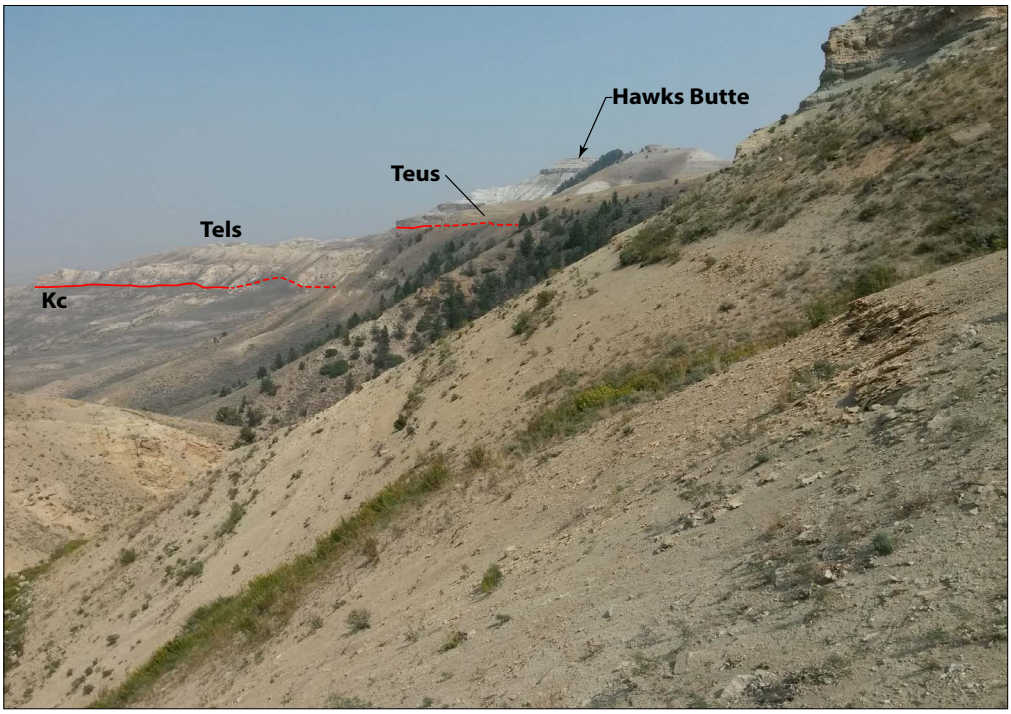

Figure 62. View (looking east) of Hawks Butte at the northeast end of Lysite Mountain in sec. 36, T. 42 N., R. 90 W, southeastern Hot Springs County. Upper sequence rocks (Teus of Bay, 1969) lie disconformably on those of the lower sequence (Tels).

section) overlying graded beds of cross-bedded sandstone and conglomerate units at the base of the lower sequence. The unit underlies tuffaceous sandstone that is pale-tan (fig. 64).

Battle Mountain area, sec. 12, T. 41 N., R. 90 W., Hot Springs County

Upper sequence rocks are locally exposed on the east side of the greater Lysite Mountain area. Battle Mountain is situated at the northeast corner of the greater Lysite Mountain area, from which it is set apart by Bates Creek. Clinoptilolite was identified in three samples within a sequence of tuffs at least 2 m (6.5 ft) thick. Sample 20150819BG-1 is a pale yellowish green porous tuff, which is relatively free of accessory minerals other than some secondary transparent, euhedral quartz crystals in cavities and cracks (fig. 65). Sample 20150819BG-2 underlies the above described tuff and occurs about 15 m (50 ft) west. This tuff is orangish white with local patchy orange staining, a very fine-grained sand component with sparse coarse-grained clay or tuff fragments, or both, and is well indurated with noncalcareous cement. Iron oxide minerals and staining (particularly in fractures) is common as are scattered flakes of biotite.

Sample 20150819BG-3 is texturally similar to Sample 20150819BG-2 but lacks the iron oxide influenced color (see fig. 65). This tuff is light greenish gray with a very minor sand component of very fine- to medium-grained, angular to subangular grain size, good induration, and noncalcareous cement. Accessory minerals in this tuff include biotite, glass shards, and iron oxides (notably lacking in quartz grains).

Sample 20150819DB-2 contains a minor amount of clinoptilolite and was collected about 550 m (1,800 ft) across the Bates Creek valley (east side) and approximately 23 m (75 ft) up-section from the location describe above (Sample 20150819BG-1). This sample is a white-tan to pale green tuff approximately 3 m (10 ft) thick.

Figure 63. White tuff of the upper part of the lower sequence rocks of Lysite Mountain (Bay, 1969). This unit hosts a minor amount of clinoptilolite and heulandite (Sample 20150820DB-2).

The four samples described above are located approximately one mile south of "stratigraphic section G" of Bay (1969).

Maimes Canyon, T. 41 N., R. 91 W., Hot Springs County

Maimes Canyon is on the western edge of Lysite Mountain in eastern Hot Springs County. The Eocene upper and lower sequences (Bay, 1969) are exposed within the canyon. The Eocene upper sequence is moderately well to well exposed, and includes a prominent cliff-forming basal sandstone, overlain by interbedded mudstone, sandstone, and tuff. To the southwest of the location, Bay (1969) observed significant analcime mineralization in the lower portion of the Eocene lower sequence, but did not present data for rocks of the upper sequence in this part of Lysite Mountain. On the eastern portion of Lysite Mountain, Bay (1969) identified analcime, clinoptilolite, and mordenite throughout the Eocene rocks as well as erionite in the upper sequence. Samples of the upper sequence from Maimes Canyon collected by the WSGS did not contain zeolites; one sample of poorly exposed tuff in the lower sequence contains possible minor clinoptilolite, but XRD data are insufficient for a positive identification.

Bridger Creek Road, sec. 16, T. 40 N., R. 91 W., Fremont County

Several small outcrops of presumably Wagon Bed sit unconformably on the Triassic Chugwater Formation in this area (fig. 66). Sample 20070928BG-1 is a resistant light gray, semi-blocky tuffaceous mudstone very fine-grained sandstone and contains a possible minor amount of clinoptilolite.

Southeast Wyoming

Shirley Basin

The Tertiary units of the Shirley Basin include the Wind River, Wagon Bed, White River, and Arikaree Formations (Harshman, 1972). Harshman (1968, 1972) labeled Middle and Late Eocene rocks as the Wagon Bed Formation, contrary to Van Houten's (1964) assertion that sedimentary units deposited in separate structural basins should be assigned to separate stratigraphic units. Rather, stratigraphic nomenclature in the Shirley Basin reflects similarity in geology age with units formally recognized in other

Figure 64. Outcrop of the lower sequence (Bay, 1969) rocks showing the location of Sample 20150820DB-2. This unit is in the lower part of the lower sequence rocks (Tels).

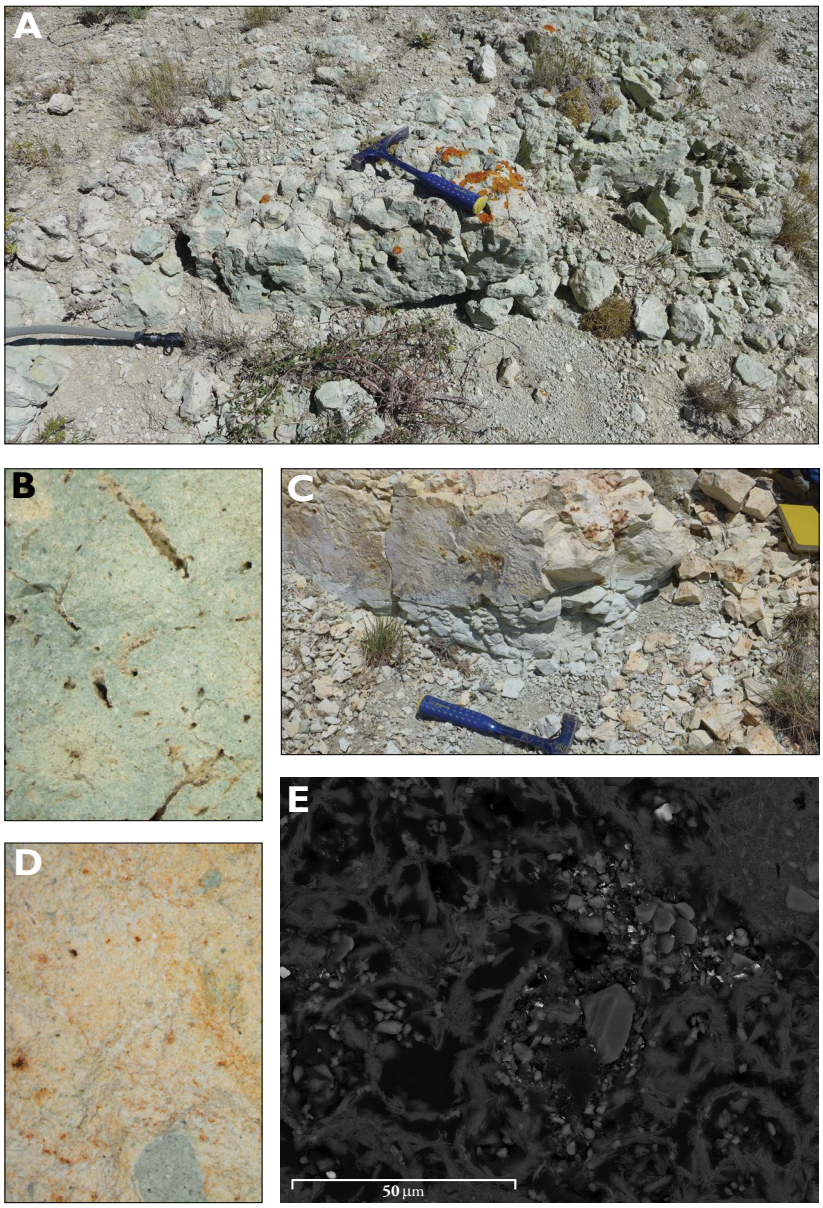

Figure 65. A) Tuff outcrop in the Battle Mountain area (northeast region of the Lysite Mountain area). Clinoptilolite and heulandite were identified in this sample (20150819BG-1). B) Close-up of Sample 20150819BG-1 showing irregular vuggy porosity. C) Weathered outcrop of Sample 20150819BG-1 and 20150819BG-2. D) Close-up of Sample 20150819BG-2 showing two modes of zeolite occurrence in this outcrop. E) SEM observations of Sample 20150819BG-2: In agreement with XRD observations, SEM work showed two varieties of Si, Al, O enriched grains that appear to be authigenic; one is a feathered crystal structure built from individual lathes and fiber-like grains relatively enriched in K, Ca, and Ba, and a second variety composed of individual grains that monoclinic and occur in aggregate mats or as single grains, not enriched in K or Ba, but still having Ca. Clinoptilolite and heulandite are predicted by XRD. Ba more readily occurs within heulandite framework than clinoptilolite, though the solid solution series of the heulandite group (includes clinoptilolite) does not rule out Ba enriched clinoptilolite in this sample.

areas (Harshman, 1972). The Wagon Bed Formation is present in the eastern and western parts of Shirley Basin, but pre-Oligocene erosion removed Wagon Bed sediments in the central portion of the basin.

Sheppard reported via personal communication to Harshman in 1967 that samples of the Wagon Bed Formation from Shirley Basin did not contain zeolite minerals (Harshman, 1972, p. 25); Sheppard also reported that the Wagon Bed Formation in the Shirley Basin never experienced the alkaline conditions needed for zeolite authigenesis.

Wagon Bed Formation

Western Shirley Basin, SE¼, sec. 24, T. 27 N., R. 82 W.

The Wagon Bed Formation is exposed at this locality (Jones and Gregory, 2011), and is composed of interbedded ledge-forming muddy sandstone to sandy mudstone, and slope-forming, locally bentonitic mudstone. Within the ledge-forming beds, sand is typically subangular to angular, medium- to very coarse-grained, and arkosic. Zeolites are not present in samples collected at this location.

Little Medicine Road, Eastern Shirley Basin, sec. 5, T. 27 N., R. 77 W., Carbon County

Jones and Gregory (2011) mapped the Wagon Bed Formation at this location (fig. 67). Near the base of the Wagon Bed Formation here is white, poorly indurated, extensively fractured limestone 1 - 1.5 m (3 - 5 ft) thick. Above this limestone, the Wagon Bed is dominantly composed of white to gray, muddy, coarse-grained, angular to subangular arkosic sandstone. At least one minor mudstone bed is present near the top of the Wagon Bed outcrop at this location. This mudstone is white to pale yellow, tuffaceous, and hosts minor mordenite (fig. 68). The

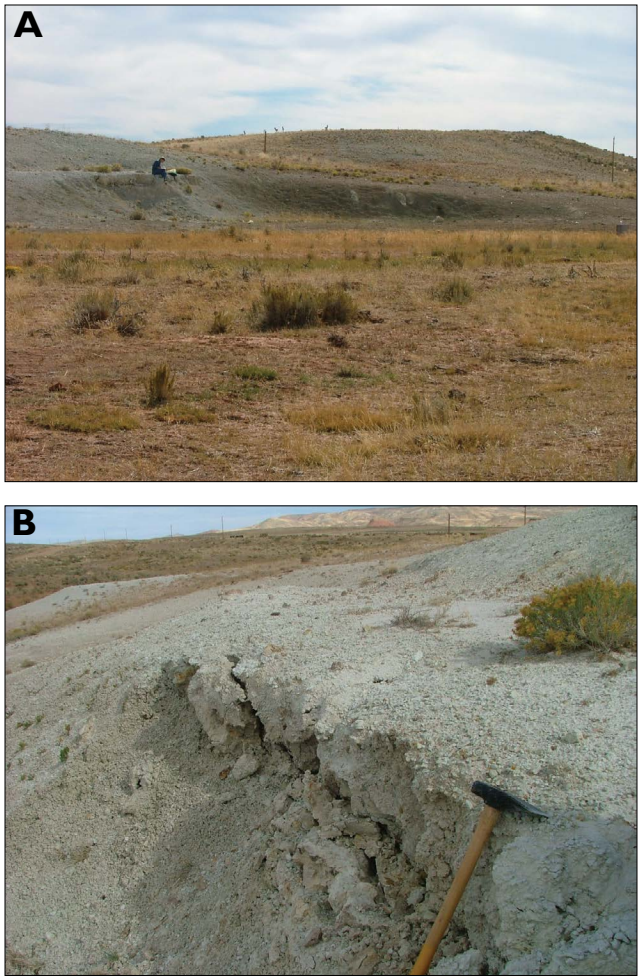

Figure 66. Sample 20070928BG-1. A)Eocene sediments (mapped as Wagon Bed Formation by Love and Christensen, 1985) at this location in northeastern Fremont County rest unconformably on Triassic red beds just east of Bridger Creek Road. B) Blocky tuffaceous sandstone at this location hosts minor amounts of heulandite. The southwestern extent of Lysite Mountain can be seen in the upper right skyline.

Wagon Bed Formation disconformably overlies the Mowry Formation here. Locally, erosion has removed a relatively small area of the Wagon Bed Formation to expose the underlying Mowry Shale, which is composed of siliceous, iron-rich shale and mudstone. Though analcime is found in the Mowry at multiple locations across Wyoming (e.g. King and Harris, 2002), no zeolites are present in a sample taken from the Mowry in this area.

White River Formation

The White River Formation is a widespread accumulation of various lithotypes, primarily tephra-based off-white siltstones, bentonitic claystones (Denson and Bergdahl, 1961), along with associated fluvial deposits of reworked volcaniclastics. This formation was deposited in a time of relative tectonic stability following extensive erosion of Laramide uplifts. The White River Formation forms prominent relatively flat-topped mesas all along the front range and many intermontane basins (fig. 69). Snoke (1993) points out that no evidence for contemporaneous volcanism exists in Wyoming, suggesting that the vitric material came from magmatism in the Great Basin. The dominant geologic setting during White River deposition was fluvial influenced, and thus tuffaceous material accumulated in mostly open systems rather than closed (lacustrine) systems, such as those described by Surdam and Sheppard (1978). Although the White River Formation in Wyoming is largely barren with respect to zeolites, in places there are significant, albeit not economic, deposits.

Douglas area, Tps. 31 and 32 N., Rgs. 70 and 71 W., Converse County

Lander and Hay (1993) document two areas of significant zeolite (clinoptilolite) mineralization resulting from the combination of optimum hydrologic conditions and abundant dacitic and rhyolitic tuffs and tuffaceous sediments in the White River Formation southeast of Douglas. The locations are in the Wulff Ranch (T. 32 N., R. 71 W.) and the Dilts Ranch (T. 31 N., R. 70 W.). The mineral was identified in composite sections and reportedly occurs at several horizons over an interval of about 150 m (500 ft). They suggest that a systematic increase in Ba and Sr content in clinoptilolite with depth demonstrates that the altering fluids were influenced by the underlying strata, including the crystalline basement rocks (Lander and Hay, 1993).

Browns Park Formation

The Miocene Browns Park Formation is predominantly volcaniclastic sediments, including conglomerate, tuffaceous sandstone and siltstone, and tuffs, along with some interbedded limestone (Ebens, 1966). This formation reportedly contains zeolitic tuffs in the Saratoga, Pick Ranch, Pick Bridge, and Poison Basin areas (King and Harris, 2002).

Beaver Creek area, secs. 18 and 19, T. 17 N., R. 86 W.; secs. 13, 14, 23, and 24, T. 17 N., R. 87 W., Carbon County

King and Harris report as much as 90 percent clinoptilolite and minor heulandite at this site. This sample was collected at an unknown location by a third party and analyzed at the WSGS in the 1980s by XRD. Based on field investigations conducted in 2006, the claim cannot be supported by this author. Two promising tuff samples were collected in 2006 in this area, but both were devoid of zeolite minerals. It is possible that a zeolite-rich tuff exists in one of the other sections listed above (from King and Harris, 2002),

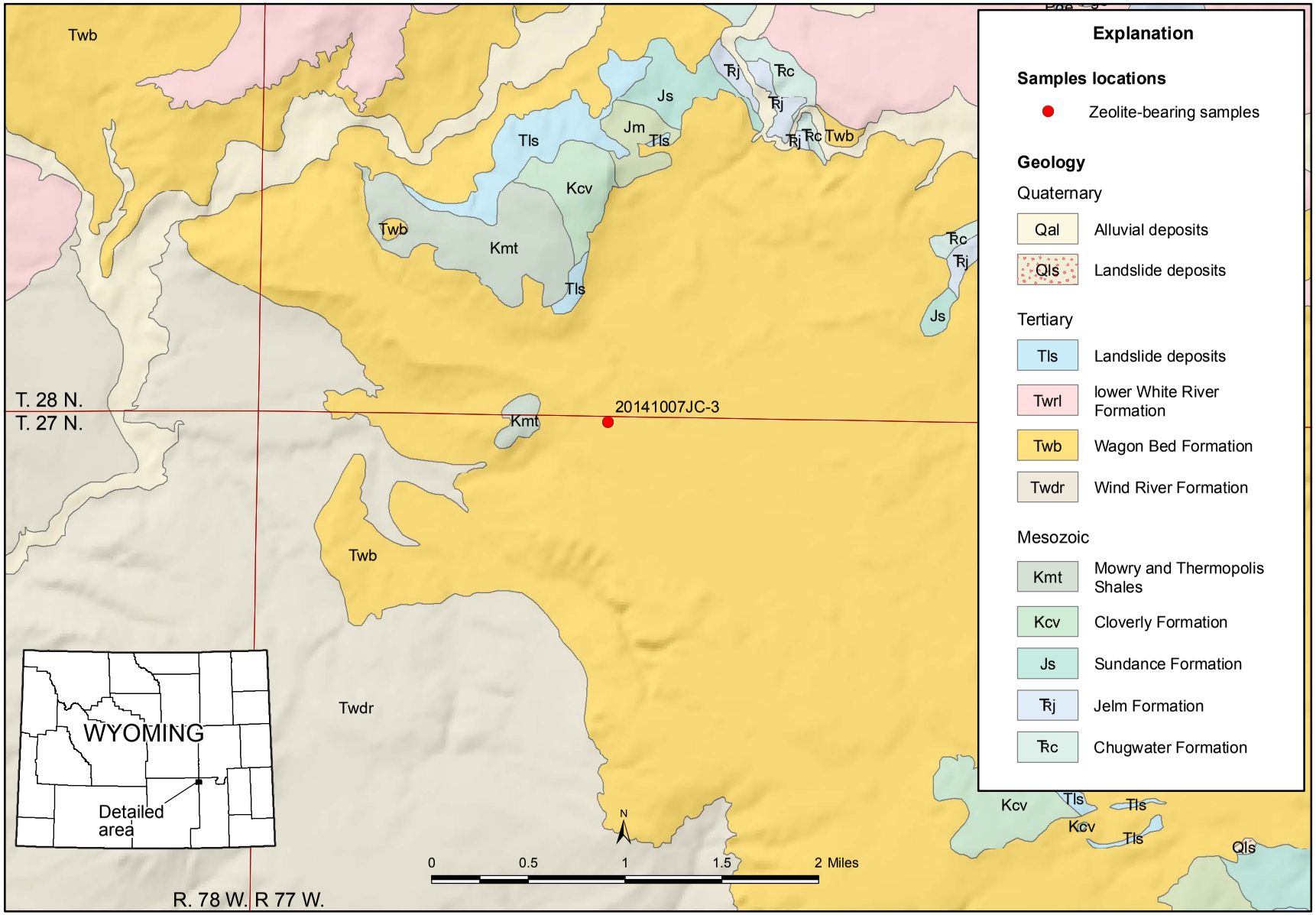

Figure 67. Map of the northern Shirley Basin showing the location of Sample 20141007JC-3. Map modified from Jones and Gregory, 2011.

Figure 68. Sample 20141007JC-3. Gray to yellowish-brown, limonite stained mudstone. No outcrop is present at the sample location, but pebbles of this mudstone cover the ground. This mudstone hosts minor amounts of mordenite.

but confirmation cannot be made based on recent investigations. King and Harris (2002) note several other minor occurrences (table 4), which were not prioritized in this investigation.

Western Wyoming

Greater Yellowstone area and Jackson Hole

Zeolite occurrences were not found during the course of this investigation in the greater Yellowstone area or Jackson Hole. Though volcanogenic sources contributed material to sedimentary units across the region, none were sampled in this study. Most occur within federal lands of Grand Teton and Yellowstone National Parks and were not easily accessible for sampling nor would any occurrences

Figure 69. Chalk Mountain (White River Formation) in the Shirley Basin, sec. 31, T. 28 N., R. 80 W., and sec. 6, T. 27 N., R. 80 W., Carbon County.

Table 4. Miscellaneous natural zeolite occurrences in northern Wyoming. Numbers in parentheses refer to select minor occurrences in King and Harris (2002).

Location Name (Location Number)	Legal Location	County	Geologic Unit	Zeolite(s) Present	Reference
Middle Fork of Chugwater Creek (1)	sec. 25, T. 19 N., R. 71 W.	Albany	Mowry Shale	Phillipsite	Davis, 1967a,b
Historic Wilkinite mining area (14)	secs. 3, 4, and 5, T. 22 N., R. 79 W.	Carbon	Steele Shale; Mesaverde Formation	Analcime	King and Harris, 2002
Douglas area	Tps. 31 and 32 N., Rgs. 70 and 71 W.	Converse	White River	Clinoptilolite	Lander and Hay, 1993
Pick Bridge (12)	sec. 10, T. 18 N., R. 84 W.	Carbon	Browns Park	Clinoptilolite	King and Harris, 2002
Poison Basin (13)	sec. 36, T. 13 N., R. 93 W.	Carbon	Browns Park	Heulandite	Gruner and others, 1956

be considered economic. It is possible that depositional or post-depositional conditions, or both, were correct for zeolite formation in the many tuffs outcropping in the area. Additionally, alteration of intrusive and extrusive volcanic rocks in the greater Yellowstone area may have resulted in zeolite mineral formation. For additional information on minor occurrences in western and northern Wyoming, see table 5.

ACKNOWLEDGMENTS

The authors would like to thank the following people and organizations for their support and contributions to the successful completion of this report: the Wyoming State Legislature for initiating and funding this project; State Geologist and WSGS Director Thomas Drean, along with Alan Ver Ploeg, Seth Wittke, and David Lucke for their management oversight; administration manager Kathy Olson for financial and budgetary management and guidance; accounting personnel Brandee Smith and Shari Williamson for their equipment, purchasing and budgeting assistance; James Rodgers for his expertise in creating and enhancing our illustrations, tables, and figures; and Christina George for the layout, design, and production of this report. We are grateful to Wayne Sutherland for invaluable discussions of the relevant geology and rock units, technical, and editorial review; and to Elizabeth Cola for assistance with technical review and helpful geologic discussions. We are also indebted to Dr. Susan Swapp of the University of Wyoming, Department of Geology and Geophysics, for her assistance and guidance in microbeam analysis.

Table 5. Miscellaneous natural zeolite occurrences in southeastern Wyoming. Numbers in parentheses refer to select minor occurrences in King and Harris (2002).

Location Name (Location Number)	Legal Location	County	Geologic Unit	Zeolite(s) Present	Reference
Cowley area (6)	sec. 31, T. 58 N., R. 95 W.	Big Horn	Mowry Shale (bentonite)	Analcime	Davis, 1967a,b
Greybull area (2, 3)	T. 53 N., R. 92 W.	Big Horn	Mowry Shale (bentonite)	Analcime	Slaughter and Early, 1965
Hyattville area, (4, 5)	sec. 32, T. 49 N., R. 90 W.	Big Horn	Mowry Shale (bentonite)	Analcime	Davis, 1967a,b
North Butte (8)	SW1/4 sec. 13, T. 44 N., R. 76 W.	Campbell	Wasatch	Heulandite, Clinoptilolite	Vine and Tourtelot, 1973; Minobras, 1975
Southern Bear Lodge Mountains (15)	T. 52, R. 63, 64 W.	Crook	Bear Lodge igneous intrusive complex	Analcime	White, 1980; O'toole, 1981; Wilkinson, 1982; Jenner, 1984
Barlow Canyon, Devils Tower, Missouri Buttes areas	T. 53-54 N., R. 65-66 W.	Crook	Tertiary igneous rocks	unspecified	Halvorson, 1980
Mineral Hill (19)	sec. 32, T. 51 N., R. 60 W.	Crook	Tertiary igneous rocks	Analcime; thomsonite	Ray, 1979; Welch, 1974
Duling Hill (20)	secs. 23, 26, 34, and 35, T. 50 N., R. 62 W.	Crook	Tertiary igneous rocks	Analcime; unspecified	Elwood, 1978
Upper North Fork of Owl Creek, and Cottonwood Creek (40)	NE¼ of T. 44 N., R. 102 W.	Hot Springs	Wiggins Formation	Mordenite; clinoptilolite	Sundell, 1985
Pedro area	NW T. 45 N., R. 62 W.; NE T. 45 N., R. 63 W,	Weston	Pierre Shale (Pedro bentonite)	Clinoptilolite	Bramlette and Posjnak, 1933; Sheppard, 1971a; Slaughter and Early, 1965; Davis, 1971a,b, 1976

We are extremely grateful to the numerous Wyoming ranchers, farmers, ranch managers, and other landowners who graciously granted us permission to either cross their property or investigate the geology on it. They include: Robert Orchard, Vance Lundgren, Thomas McGuire, Don Schramm of the Rock Springs Grazing Association (and their members), Mr. and Mrs. Mike McCoy, and Greg Gardener. We are also greatly indebted to Nolan McWherter and Teresa Bowerman of the Anadarko Corporation for allowing us to investigate so many areas of the Washakie and Green River Basins.

SUMMARY

Zeolites are vital in a wide variety of applications, including the agriculture, petroleum, wastewater, and air purification industries, among others. Natural zeolites are attractive alternatives to synthetic zeolites due to their availability in large volume and generally lower production costs. The applicability of natural zeolites grows as technology advances. Wyoming hosts potentially commercial-grade natural zeolite deposits, which have only been developed on a small scale. This investigation confirms and expands the information on known natural zeolite occurrences in Wyoming, adds information on some known or suspected occurrences, and provides information on some previously unknown occurrences. Grab samples collected during this study are a starting point for future research and exploration. No economic evaluations or projections for any deposit or occurrence were made on the basis of our findings, and our data serve only as a general aid to exploration. This report is supplemented by additional data (geochemistry and raw XRD files) available online or by contacting the WSGS.

REFERENCES

Ackley, M.W., Rege, S.U., and Saxena, H., 2003, Application of natural zeolites in the purification and separation of gases: Microporous and Mesoporous Materials, v. 61, 1-3, p. 25-42.

Altare, C.R., Bowman, R.S., Katz, L.E., Kinney, K.A., and Sullivan, E.J., 2007, Regeneration and long-term stability of surfactant-modified zeolite for removal of volatile organic compounds from produced water: Microporous and Mesoporous Materials, v. 105, i. 3, p. 305-316.

Ames, L.L., 1967, Zeolitic removal of ammonium ions from agriculture wastewaters: Proceedings, 13th Pacific Northwest Industrial Waste Conference, Washington State University, Pullman, p. 135-152.

Andronikashvili, T., Kardava, M., Korkzakhia, T., and Gamisonia, M., 2010, The influence of organ-zeolitic fertilizers on yield, formation of the assimilating apparatus, and cobbing of maize: in Petrov, O.E., and Tzvetanova, Y.K., editors, Zeolite 2010, 8th International Conference on the Occurrence, Properties, and Utilization of Natural Zeolites, p. 41-42.

Ball, A.S., 2006, Energy inputs in soil systems in Biological Approaches to Sustainable Soil Systems, Taylor & Francis Publishers, Boca Raton, London, New York, p. 79-89.

Barrington, S.F., and El Moueddeb, K., 1995, Zeolite as pig manure additive to control odor and conserve N: Canadian Society of Agricultural Engineering Paper no. 95-510, Saksatoon, Canada.

Bay, K.W., 1969, Stratigraphy of Eocene sedimentary rocks in the Lysite Mountain area, Hot Springs, Fremont, and Washakie counties, Wyoming: Laramie, University of Wyoming, Ph.D. dissertation, 181 p.

Bergreo, D., 1997, Effect of natural clinoptilolite or phillipsite in the feeding of lactating dairy cows in Kirov, G., Filizova, L., Petrov, O., editors, Natural Zeolites, Sofia '95, p. 67-72.

Bish, D.L., and Chipera, S.J., 1991, Detection of trace amounts of erionite using X-ray powder diffraction; erionite in tuffs of Yucca Mountain, Nevada, and central Turkey: Clays and Clay Minerals, 39(4), p. 437-445.

Boles, J.R., 1968, Zeolites and authigenic feldspar along a part of the Beaver Rim, Fremont County, Wyoming: Laramie, University of Wyoming, M.S. thesis, 64 p., 2 plates.

Boles, J.R., and Surdam, R.C., 1971, Authigenesis of the Wagon Bed Formation, central Wyoming: Contributions to Geology, v. 10, no. 2, p. 141-144.

Boles, J.R., and Surdam, R.C., 1973, A summary of authigenic aluminosilicates in the Green River and Wind River Basins of Wyoming: Wyoming Geological Association 25th Field Conference Guidebook, p. 149-152.

Boles, J.R., and Surdam, R.C., 1979, Diagenesis of volcanogenic sediments in a Tertiary saline lake; Wagon Bed Formation, Wyoming: American Journal of Science, v. 279, no. 7, p. 832-853.

Bradley, W.H., 1945, Geology of the Washakie Basin, Sweetwater and Carbon counties, Wyoming, and Moffat County, Colorado: U.S. Geological Survey Oil and Gas Investigations Map OM-32, scale 1:190,080.

Bramlette, M.N., and Posnjak, E., 1933, Zeolitic Alteration of Pyroclastics: The American Mineralogist, v. 18, no. 4, p. 167-171.

Breck, D.W., 1974, Zeolite molecular sieves – structure, chemistry, and use: John Wiley and Sons, Inc., New York, New York, 771 p.

Chipera, S.J., Smith, M.E., Counce, D., Ehler, D., Longmire, P., and Taylor, T., 2006, Use of zeolites as selective sorbates for radiological decontamination applications, in R.S. Bowman and S.E. Delap, editors, Zeolite '06 – 7th International Conference on the Occurrence, Properties, and Utilization of Natural Zeolites, p. 84-85.

Coombs, D.S., Ellis, A.J., Fyfe, W.S., and Taylor, A.M., 1959, The zeolite facies, with comments on the interpretation of hydrothermal synthesis: Geochemica et Cosmochemica Acta, v. 17, 1-2, p. 53-107.

Curry, H.D., and Santini, K., 1986, Zeolites in the Washakie Basin, (abs.): Wyoming State Geological Survey Public Information Circular 25, p. 107-108.

Davis, J.C., 1967a, Petrology of the Mowry Shale: Laramie, University of Wyoming, Ph.D. dissertation, 141 p.

Davis, J.C., 1967b, Measured sections of the Mowry Shale, Wyoming State Geological Survey Mineral Report (unpublished) MR 67-2, 59 p.

De Gennaro, R., Cappelletti, P., Cerri, G., de Gennaro, M., Dondi, M., Grazian, S.F., and Langella, A., 2006, Expanded lightweight aggregates production using Italian zeolitized volcanoclastic materials and industrial wastes, in R.S. Bowman and S.E. Delap, editors, Zeolite '06 – 7th International Conference on the Occurrence, Properties, and Utilization of Natural Zeolites, p. 94-95.

Deer, W.A., Howie, R.A., and Zussman, J., 1967, An introduction to the rock forming minerals: John Wiley and Sons, Inc., New York, New York.

Doula, M.K., 2009, Simultaneous removal of Cu, Mn and Zn from drinking water with the use of clinoptilolite and its Fe-modified form: Water research, v. 43, no. 15, p. 3659-3672.

Doula, M.K., and Dimirkou, A., 2008, Use of an iron-over-exchanged clinoptilolite for the removal of Cu 2+ ions from heavily contaminated drinking water samples: Journal of hazardous materials, v. 151, no. 2, p. 738-745.

Ebens, R.J., 1966, Stratigraphy and petrography of Miocene volcanic sedimentary rocks in southeastern Wyoming and North-central Colorado: Laramie, University of Wyoming, Ph.D. thesis, 129 p., 2 plates.

Elwood, M.W., 1978, Geology of the Black Buttes, Crook County, Wyoming: Rapid City, South Dakota School of Mines and Technology, M.S. thesis, 123 p.

Eyde, T.H., and Holmes, D.A., 2006, Zeolites: in Kogel, J.E., Trivedi, N.C., Barker, J.M., and Krukowski, S.T., editors, Industrial Minerals and Rocks, 7th Edition, SME, Littleton, Colorado, p. 1039-1064.

Flanigen, E.M., and Mumpton, F.A., 1977, Utilization of Natural Zeolites, in F.A. Mumpton, editor, Mineralogy and Geology of Natural Zeolites, Mineralogical Society of America, v. 4, p.165-176.

Fu, F., Wang, Q., 2011, Removal of heavy metal ions from wastewaters: a review: Journal of environmental management 92.3, pp. 407-418.

Gottardi, G., 1989, The genesis of zeolites: European Journal of Mineralogy, v. 1, p. 479-487.

Gottardi, G., and Galli, E., 1985, Natural zeolites: Springer-Verlag, New York, New York, 409 p.

Gruner, J.W., Smith, D.K., Jr., and Knox, J.A., 1956, Annual Report for April 1, 1955 to March 31, 1956, Part II: U.S Atomic Energy Commission Technical Report RME-3137 (part II), p. 6.

Harris, R.E., 1995, Natural Zeolites in southwestern Wyoming: Wyoming Geological Association 1995 Field Conference Guidebook, p. 113-123.

Harshman, E.N., 1968, Geologic map of the Shirley Basin area, Albany, Carbon, Converse, and Natrona counties, Wyoming: U.S. Geological Survey Miscellaneous Geologic Investigations Map I-539, scale 1:48,000.

Harshman, E.N., 1972, Geology and uranium deposits, Shirley Basin area, Wyoming: U.S. Geological Survey Professional Paper 745, 82 p.

Hauri, F., 2006, Natural zeolite from southern Germany: Applications in concrete, in R.S. Bowman and S.E. Delap, editors, Zeolite '06 – 7th International Conference on the Occurrence, Properties, and Utilization of Natural Zeolites, p. 130-131.

Hawkins, D.B., 1974, Statistical analyses of the zeolites clinoptilolite and heulandite: Contributions to Mineralogy and Petrology, 45(1), p. 27-36.

Hay, R.L., 1978, Geologic occurrences of zeolites, in L.B. Sand and F.B. Mumpton, editors, Natural zeolites – Occurrence, properties, use: Pergamon Press, New York, New York, p. 135-143.

Hay, R.L., and Sheppard, R.A., 1977, Zeolites in open hydrologic systems, in F.A. Mumpton editor, Mineralogy and geology of natural zeolites: Mineralogical Society of America Short Course Notes, v. 4, p. 93-102.

Hemken, R.W., 1983, Effect of clinoptilolite on lactating dairy cows fed a diet containing urea as a source of protein in Pond, W.G., and Mumpton, F.A., editors, Zeo-Agriculture: Use of natural zeolite in agriculture and aquaculture, p. 171-176.

Hofstetter, K.J., Hitz, C.G., Baston, V.F., and Malinauskas, A.P., 1983, Radionuclide analyses taken during preliminary coolant decontamination at Three Mile Island: America Nuclear Society Journal, v. 63, no. 3, p. 461-469.

Holmes, D.A., 1994, Zeolites: in Carr, D.D., editor, Industrial Minerals and Rocks, SME, Littleton, Colorado, p. 11129-1158.

High, Lee R., Jr., and Picard, M.D., 1965, Sedimentary petrology and origin of analcime-rich Pogo Agie Member, Chugwater (Triassic) Formation, west-central Wyoming: Journal of Sedimentary Petrology, v. 35, no. 1, p. 49-70.

Iijima, A., 1980, Geology of natural zeolites and zeolitic rocks, in L.V.C. Rees, editor, Proceedings of the Fifth International Conference on Zeolites: Heyden, London, U.K., p. 103-118.

Inglezakis, V.J., Doula, M.K., Aggelatou, V., and Zorpas, A.A., 2010, Removal of iron and manganese from underground water by use of natural minerals in batch mode treatment: Desalination and Water Treatment, v. 18, no. 1-3, p. 341-346.

Jana, D., 2007, A new look to an old pozzolan: clinoptilolite – a promising pozzolan in concrete, in Proceedings of the 29th ICMA Conference on cement microscopy, Quebec City: Curran Associates, Inc., p. 168-206.

Jayaraman, A., Hernandez-Maldonado, A.J., and Yang, R.T., 2004, Clinoptilolites for nitrogen/methane separation: Chemical Engineering Science, v. 59, no. 12, p. 2407-2417.

Jenner, G.A., Jr., 1984, Tertiary alkalic igneous activity, potassic fentinization, carbonatitic magmatism, and hydrothermal activity in the central and eastern Bear Lodge Mountains, Crook County, Wyoming: Grand Forks, University of North Dakota, M.S. thesis, 232 p.

Johannsen, A., 1914, Petrographic analysis of the Bridger, Washakie, and other Eocene Formations of the Rocky Mountains: American Museum of Natural History Bulletin, v. 33, p. 209-222.

Jones, N.R., and Gregory, R.W., 2011, Preliminary Geologic Map of the Shirley Basin 30' x 60' Quadrangle, Carbon, Natrona, Albany, and Converse counties, Wyoming: Wyoming State Geological Survey, Open File Report 11-8, scale 1:100,000.

Kallo, D., 1995, Wastewater purification in Hungary using natural zeolites: Natural Zeolites, v. 93, p. 341-350.

Kallo, D., and Sherry, H.S., editors, 1988, Occurrence, properties, and utilization of natural zeolites: Akademiai Kiado, Budapest, Hungary, 857 p.

Keller, W.D., 1952, Analcime in the Popo Agie member of the Chugwater Formation Wyoming: Journal of Sedimentary Petrology, v. 22, no. 2, p. 70-82.

King, J.K., and Harris, R.E., 2002, Natural zeolites in Wyoming [Revised]: Wyoming State Geological Survey Open File Report, 90-4, 51 p.

Kistner, F.B., 1973, Stratigraphy of the Bridger Formation in the Big Island-Blue Rim area, Sweetwater County, Wyoming: Laramie, University of Wyoming, M.S. thesis, 174 p.

Lander, R.H., and Hay, R.L., 1993, Hydrogeologic control on diagenesis of the White River sequence: GSA Bulletin, v. 105, p. 361-376.

Leggo, P.J., 2014, The organo-zeoliltic-soil system: a comprehensive fertilizer: in Dakovic, A., Trgo, M., and Langella, A., editors, Zeolite 2014, 9th International Conference on the occurrence, properties, and utilization of natural zeolites, p. 115-116.

Loughbrough, R., 1993, Minerals for animal feed, in a stable market: Industrials Minerals, March, 1993, p. 19-33.

Love, J.D., 1961, Split Rock Formation (Miocene) and Moonstone Formation (Pliocene) in central Wyoming: U.S. Geological Survey Bulletin, 1121-I, 37 p.Love, J.D., 1970, Cenozoic geology of the Granite Mountains area, central Wyoming: U.S. Geological Survey Professional Paper 495-C, 154 p., scale 1:125,000.

Love, J.D., and Christiansen, A.C., 1985, Geologic map of Wyoming: United States Geological Survey (Wyoming State Geological Survey release 2014), 3 pls., scale 1:500,000, color.

Matthew, W.D., 1909, The Carnivora and Insectavora of the Bridger Basin, middle Eocene: Memoirs of the American Museum of Natural History, v. 9, pt. 6, p. 291-567.

Mercer, B.W., Ames, L.L., Touhill, J.C., Van Slyke, W.J., and Dean, R.B., (1970) Ammonium removal from secondary effluents by selective ion-exchange: Water Pollution Control Federation Journal, v. 42, no. 2, part 2, p. R55-R107.

Milojevic-Rakic, M., Vasiljevic, B.N., Jovic, A., Kragovic, M., Cvetanovic, K., Damjanovic, L.J., and Dondur, V., 2014, Cetylpyridinium chloride functionalized clinoptilolite as efficient adsorbant for pesticide removal: in Dakovic, A., Trgo, M., and Langella, A., editors, Zeolite 2014, 9th International Conference on the occurrence, properties, and utilization of natural zeolites, p. 149-150.

Minobras, 1975, Wyoming industrial minerals: Minobras, Dana Point, California, 65 p.

Mumpton, F.A., editor, 1977, Mineralogy and geology of natural zeolites: Mineralogical Society of America Short Course Notes, v. 4, 233 p.

Mumpton, F.A., 1999, La roca magica: Uses of natural zeolites in agriculture and industry: Proceedings of the national academy of Sciences, v. 96, no. 7, p. 3463-3470.

Murphey, P.C., and Evanoff, E., 2008, Stratigraphy, fossil distribution and depositional environments of the upper Bridger Formation (middle Eocene), southwestern Wyoming: Wyoming State Geological Survey Report of Investigation 57, 107 p.

Murphey, P.C., Lester, A., Bohor, B., Robinson, P., Evanoff, E., and Larson, E., 1999, 40Ar/39Ar dating of volcanic ash deposits in the Bridger Formation (middle Eocene) of southwestern Wyoming (abstract): Geological Society of America Abstracts with Programs, v. 31, no. 7, p.233.

National Academy of Sciences website, March 2016, http://www.pnas.org/content/96/7/3471.full#sec-1.

O'Toole, F.S., 1981, Petrology of the Cenozoic phonolites and related rocks of the Houston Creek area, Bear Lodge Mountains, Wyoming: Grand Forks, University of North Dakota, M.S. thesis, 112 p.

Passaglia, E., Artioli, G., and Gualtieri, A., 1998, Crystal chemistry of the zeolites erionite and offretite: American Mineralogist, 83(5-6), p. 577-589.

Rakic, V., Simic, A., Zivanovic, I., Markivic, J., Dzeletovic, Z., and Krogstadt, T., 2014, Clinoptilolite as a fertilizer carrier: the effect on pasture yield and quality: in Dakovic, A., Trgo, M., and Langella, A., editors, Zeolite 2014, 9th International Conference on the occurrence, properties, and utilization of natural zeolites, p. 193-194.

Ray, J.T., 1979, Petrology of the Cenozoic rocks of the Tinton district, Black Hills, South Dakota – Wyoming: Grand Forks, University of North Dakota, M.S. thesis, 122 p.

Roehler, H.W., 1972, Zonal distribution of montmorillonites and zeolites in the Laney Shale Member of the Green River Formation in the Washakie Basin, Wyoming: Geological survey research 1972, U.S. Geological Survey Bulletin 800-B, p. 121-124.

Roehler, H.W., 1973a, Stratigraphy of the Washakie Formation in the Washakie Basin, Wyoming: U.S. Geological Survey Bulletin 1369, 40 p.

Roehler, H.W., 1973b, Stratigraphic divisions and geologic history of the Laney Member of the Green River Formation in the Washakie Basin, southwestern Wyoming: U.S. Geological Survey Bulletin 1372-E, 28 p.

Roehler, H.W., 2004, Geologic map of the Kinney Rim 30' x 60' quadrangle, Sweetwater County, Wyoming and Moffat County, Colorado: Wyoming State Geological Survey Open File Report 04-5, scale 1:100,000, color.

Sand, L.B., and Mumpton, F.A., editors, 1978, Natural Zeolites – Occurrence, properties, use: Pergamon Press, New York, New York, 546 p.

Seifi, L., Torabian, A., Kazemian, H., Bidhendi, G.N., and Azimi, A.A., 2010, Kinetic study of petroleum monoaromatics uptake on the surface-modified granulated natural zeolite nanoparticles: in Petrov, O.E., and Tzvetanova, Y.K., editors, Zeolite 2010, 8th International Conference on the Occurrence, Properties, and Utilization of Natural Zeolites, p. 237-238.

Seki, Y., Onuki, H., Okumura, K., Takashima, I., 1969, Zeolite distribution in the Katayama geothermal area, Onikobe, Japan. [Katayama geothermal area]: Japan Journal of Geology and Geography, v. 40, p. 2-4.

Sheppard, R.A., 1971a, Clinoptilolite of possible economic value in sedimentary deposits of the conterminous United States: U.S. Geological Survey Bulletin 1332-B, 15 p.

Sheppard, R.A., 1971b, Zeolites in sedimentary deposits of the United States - A review, in R.F. Gould, editor, Molecular Sieve Zeolites I: American Chemical Society Advances in Chemistry, no. 101, p. 279-310.

Sheppard, R.A., 1973, Zeolites in sedimentary rocks: U.S. Geological Professional Paper 820, p. 689-695.

Sheppard, R.A., 1976, Zeolites in sedimentary deposits of the northwestern United States – Potential industrial minerals, in 11th Annual Industrial Minerals Forum: Montana Bureau of Mines and Geology Special Publication 74, p. 69-84.

Slaughter, M., and Early, J.W., 1965, Mineralogy and geological significance of the Mowry bentonites, Wyoming: Geological Society of America Special Paper 83, 116 p.

Snoke, A.W., 1993, Geologic history of Wyoming within the tectonic framework of the North American Cordillera, in Snoke, A.W., Steidtman, J.R., and Roberts, S.M., editors, Geology of Wyoming: Geological Survey of Wyoming Memoir 5, p. 2-56.

Sundell, K.A., 1985, The Castle Rocks chaos – a gigantic Eocene landslide-debris flow within the southeastern Absaroka Range: University of California, Santa Barbara, Ph.D., 286 p.

Surdam, R.C., 1972, Economic potential for zeolite-rich sedimentary rocks in Wyoming: Earth Science Bulletin, Wyoming Geological Association, v. 5, no. 1, p. 5-8.

Surdam, R.C., and Sheppard, R.A., 1978, Zeolites in saline, alkaline lake deposits, in L.B. Sand and F.A. Mumpton, editors, Natural Zeolites – Occurrence, Properties, Use: Pergamon Press, New York, New York, p. 353-371.

Surdam, R.C., and Parker, R.D., 1972, Authigenic aluminosilicate minerals in the tuffaceous rocks of the Green River Formation, Wyoming: Geological Society of America Bulletin, v. 83, no. 3, pp. 689-700.

Sweeney, T.F., 1983, Effect of dietary clinoptilolite on digestion and rumen fermentation in steers in Pond, W.G., and Mumpton, F.A., editors, Zeo-Agriculture: Use of natural zeolite in agriculture and aquaculture, p. 177-187.

Thompson, R.M., and White, V.L., 1954, Geology of the Riverton area, central Wyoming: Oil and gas investigations map, 0127, U. S. Geological Survey, Reston, Virginia.

Torabian, A., Kazemian, H., Seifi, L., Bidhendi, G.N., Azimi, A.A., and Ghadiri, S.K., 2010, Removal of petroleum aromatic hydrocarbons by surfactant-modified natural zeolite: The effect of surfactant: Clean – Soil, Air, Water, v. 38, issue 1, p. 77-83.

Tourtelot, H.A., 1946, Tertiary stratigraphy in the northeastern part of the Wind River Basin, Wyoming: U.S. Geological Survey Oil and Gas Investigations Preliminary Chart OC-22.

Uzal, B., and Turanli, L., 2006, Blended cements containing high volume of natural zeolites: superplasticizer requirement and compressive strength of mortars: in R.S. Bowman and S.E. Delap, editors, Zeolite '06 – 7th International Conference on the Occurrence, Properties, and Utilization of Natural Zeolites, p. 236-237.

Van Houten, F.B., 1964, Tertiary geology of the Beaver Rim area, Fremont and Natrona counties, Wyoming: U.S. Geological Survey Bulletin 1164, 99 p., scale 1:62,500.

Vaughn, D.E.W., 1978, Properties of natural zeolites, in L.B. Sand and F.B. Mumpton, editors, Natural Zeolites – Occurrence, Properties, Use: Pergamon Press, New York, New York, p. 353-371.

Vine, J.D., and Tourtelot, E.B., 1973, Geochemistry of lower Eocene sandstones in the Rocky Mountain region: U.S. Geological Survey Professional Paper 789, 36 p.

Virta, R.L., and Flanagan, D.M., 2014, Zeolites in U.S. Geological Survey Minerals Yearbook 2014 (advance release), p. 83.1-83.3.

Waterman, D.F., Harmon, R.J., Hemken, R.W., and Langlois, B.E., 1983, Milking frequency as related to udder health and milk production: Journal of Dairy Science, v. 66, 2, p. 253-258.

White, S.F., 1980, Petrology of the Cenozoic rocks of the Lytle Creek area, Bear Lodge mountains, Wyoming: M.S. thesis, University of North Dakota, Grand Forks, 69 p.

Wilkinson, M., 1982, Petrology and alteration in the core of the Bear Lodge Tertiary intrusive complex, Bear Lodge Mountains, Crook County, Wyoming: M.S. thesis, University of North Dakota, Grand Forks, 127 p.

Wolfbauer, C.A., 1972, Chemical petrology of non-marine carbonates in the western Bridger Basin, Wyoming: Laramie, University of Wyoming, Ph.D., 80 p.

Appendix 1 - Zeolite Applications

ANIMAL FEED

The agriculture industry is the number one consumer of natural zeolite (Virta and Falanagan, 2014) where it is used as an additive to feed for livestock such as cattle, poultry, and swine. Natural zeolites' primary values are for promoting growth and for carrying nutrients. Zeolites act as buffers in the digestive system (rumen) of animals, storing nutrients and later releasing them via ion exchange, primarily with sodium and potassium. The animal can then extract more dietary benefit from the same amount of feed than with no zeolite added, as some nutrients would pass without being utilized (Loughbrough, 1993). Natural zeolites, such as clinoptilolite, have been shown to buffer ammonium (NH_4) levels in the rumen of cattle, lowering the risk of toxicity by preventing a rise of pH and ammonia (NH_3) levels in the animals' blood serum (Bergreo, 1997). Lower ammonium levels in the rumen of livestock have been linked to more efficient use of dietary protein (Waterman and others, 1983). Natural zeolites have also been shown to promote increased rumen acetate production, which is the precursor to milk fat, promoting increased production from dairy cows (Sweeney and others, 1983). Another benefit of natural zeolite as an additive to cattle feed is in the increase of fecal dry matter (Sweeney and others, 1983). The environment of large, crowded feedlots is improved by decreasing the moisture available for microbial growth, leading to improved animal health and lower disease communication. Natural zeolites have shown similar promise for the poultry and swine industries as well (Barrington and El Moueddeb, 1995).

ODOR CONTROL

In addition to odor control in livestock industries, natural zeolites can absorb odors, such as ammonia and other aromatics, primarily in the agriculture industry. As described above, ammonia molecules are stored inside the framework of the zeolite pore structure, essentially neutralizing the odor-causing compound. Another primary user is the pet litter industry, which ranks fifth in domestic uses of natural zeolites (Virta and Falanagan, 2014). Most pet litter manufacturers combine natural zeolites with other ingredients such as bentonite or similar material, which also has the ability of fluid absorption. Other domestic products that employ natural zeolites as odor absorbers include carpet powders and other household odor eliminators or odor absorbers.

WATER PURIFICATION

Natural zeolites have the capability to remove metals and other contaminants from water in numerous settings, including surface waters, groundwater, drinking water, and wastewater. Mumpton (1999) cites several examples of large municipalities that have made beneficial use of clinoptilolite in treating drinking water by taking advantage of the mineral's affinity for the removal of ammonium and ammonia. Sewage can be treated with natural zeolite to extract ammonium and increase oxygen consumption, which helps dehydration prior to its use in fertilizers (Ames, 1967; Mercer and others, 1970; Kallo, 1995). Depending on the particular application, natural zeolites are often pretreated for a particular purpose to remove metal contaminants such as arsenic, cadmium, chromium, copper, iron, manganese, lead, and zinc (Fu and Wang, 2011; Inglezakis and others, 2010; Doula, 2009; Doula and Dimirkou, 2008). Other water treatment applications for natural zeolite include acid heavy metal removal from acid mine drainage, lead removal from drinking water, and hazardous material spill cleanup and containment.

GAS ADSORPTION AND AIR FILTRATION

Many natural zeolites offer vast potential for gas filtration and separation by way of adsorption. Where compositional purity is not as high a priority, natural zeolites have the advantages of abundant supply and lower cost than the more expensive synthetic zeolites. For certain industrial applications such as air separation, natural zeolites are well suited for removing nitrous oxide (N_2O) from air, while they are outperformed by synthetic zeolites for other applications, such as bulk oxygen (O_2) separation (Ackley and others, 2003). With pretreatment and purification of natural zeolites, nitrogen and methane can be separated effectively (Jayaraman and others, 2004). Dewatering of natural gas streams such as methane in hydrocarbon refining can also be accomplished effectively using natural zeolites. Chabazite-rich tuff has been used on an industrial scale to remove hydrochloric acid (HCl) from hydrogen (H_2) streams, water from chlorine streams, and carbon dioxide (CO_2) stack emissions (Mumpton, 1999).

NATURAL ZEOLITES AND FERTILIZERS

In agriculture, natural zeolites can increase the effectiveness of fertilizers and reduce the overall costs of soil amendments. When combined with fertilizers, natural zeolites improve soil moisture retention and control the rate of release of nutrients from fertilizers into the soil. Natural zeolites also prevent the accumulation of undesirable microbes that result from excessive use of nitrogen, phosphorous, and potassium fertilizers, commonly referred to as NPK fertilizer (Ball, 2006). If left unchecked, such microbes eventually deteriorate soil structure and diminish water retention, which necessitates the addition of organic matter for the soil to remain productive. Clinoptilolite used to treat wastewater to remove ammonium ions can

be mixed with organic matter to create a biofertilizer. Biofertilizer added to soil results in the exchange with potassium in the soil; enhanced growth and higher plant quality was observed as a result (Leggo, 2014). Additionally, nitrogen can be retained for longer periods of time using clinoptilolite to bind and preserve it in soil fortified with cattle manure. Manure used for fertilization, when combined with clinoptilolite, has been demonstrated to help soil retain beneficial nitrogen and lead to a higher build-up of protein in crops (Rakic and others, 2014).

Natural phillipsite has also shown positive results in agricultural research. Andronikashvili and others (2010) report maize crop yield increases of 14 percent when fertilized with an "organo-zeolitic" fertilizer made up of a 1:1 ratio granular phillipsite (0.5-1.0 mm) and poultry droppings. Significant increases in the amount of green mass (surface area of leaves) was also observed with organo-zeolitic fertilizers added to soils compared to crops grown without fertilization or with only mineral fertilizers added to the soils.

FUNGICIDE/PESTICIDE CARRIERS

Pesticides are necessary for the cultivation of large quantities of crops, but their repeated application can degrade the quality of soils. Natural zeolites have been used to remove pesticides from soils to prevent their deleterious accumulation. To maximize the hydrophobic surfaces within the zeolite structure, the clinoptilolite is treated with cetylpyridinium chloride (CPC). The zeolite's ability to adsorb the pesticide glyphosate is increased by the surface modification (Milojevic-Rakic and others, 2014).

PETROLEUM SORBENTS

Synthetic zeolites generally outperform natural zeolites in the adsorption of typically larger petroleum molecules such as hazardous monoaromatics, including benzene, toluene, ethylbenzene, and xylene (commonly referred to as BTEX) from various aqueous solutions. However, natural zeolites that have been pretreated with a surfactant (surfactant modified zeolites or SMZ) have demonstrated increased promise with advances in research and development (Seifi and others, 2010). Torabian and others (2010) varied experimental conditions and showed modified clinoptilolite sorption capacity to be competitive with that of powder activated carbon (PAC), primarily by adjusting pH conditions during testing. Altare and others (2007) also showed SMZ to be a possible medium for the removal of BTEX from oil and gas field wastewater. Most of these tests have been at laboratory scale, and further testing will be needed to demonstrate their viability for widespread application in industry.

MISCELLANEOUS OTHER USES

Natural zeolites are efficient desiccants, and numerous commercial products are available for industrial scale or household usage. Research laboratories that require certain materials or specimens to be kept in a moisture-free environment often use a form of raw or modified natural zeolite. Catalysis is another of natural zeolites' applications where purity of catalyst is not of high priority, however, most industrial processes employ synthetic forms for maximum efficiency.

Aquaculture makes use of natural zeolites in several ways. Ammonium can be removed from water in aquariums, hatcheries, and ammonia in transport containers (Mumpton, 1999). Accumulating fecal matter and excess fish food in hatcheries produces excessive ammonium, and its removal is vital to the health of the fish. Other aquaculture uses include the generation of oxygen for aeration systems and in dietary supplements (Mumpton, 1999).

CEMENT

Cement for making concrete is produced by fine grinding and co-mixing Portland cement with certain additives, particularly various natural aluminosilicates collectively called pozzolan. Traditional sources of pozzolan are sand, silt, clay, and tuffaceous deposits. Pozzolan reacts in the presence of water to form compounds just as pure Portland cement does; but, being natural material, it does not require the energy input or entail the production of CO_2 that the manufacture of Portland cement does. The ancient Romans used tuffaceous material from the Neapolitan yellow tuff near Pozzuoli, Italy.

The efficacy of tuffaceous material as pozzolan results from zeolite minerals, such as clinoptilolite, in the tuffs. Uzal and Turanli (2006) experimented with natural clinoptilolite (80-85 percent zeolite) as a replacement for Portland cement in 10 percent steps from 5 to 55 percent by weight. They found that at 35 percent clinoptilolite, the blended cement attained compressive strength equal to that of Portland cement alone; and at 55 percent clinoptilolite, reached compressive strength within 10 percent of Portland cement alone, but only after a long curing. These results are significantly better than those attained with cement blends containing other pozzolan, which are commonly limited to 30 percent by weight. Because manufacture of Portland cement produces high volumes of CO_2, large proportions of zeolite in the cement mixture can significantly reduce these emissions. Concrete with a large zeolite component is used in Germany, Switzerland, and France (Hauri, 2006). In Italy, zeolite has been blended with waste from the production of other zeolite-based products to produce expanded, lightweight aggregate (de Gennaro and others, 2006).

Industry continues to find ways to take further advantage of natural zeolites as an additive to cement mixtures. Natural zeolites have been used to maximize qualities such as compressive strength and durability (Jana, 2007). Benefits also include lowering the overall weight of cement and as an additive to the cement as a lightweight aggregate.

RADIOACTIVE MATERIALS AND FALLOUT

Natural zeolites can have an affinity for radionuclides such as ^{45}Ca, ^{51}Cr, ^{60}Co, ^{90}Sr, and ^{137}Cs (Mumpton, 1999). Cation exchange is the property of natural zeolite minerals, primarily clinoptilolite, that is useful in the treatment of radioactive waste solutions. Radioactive water from Three Mile Island was treated with a mixture of synthetic and natural zeolites to remove ^{90}Sr and ^{137}Cs (Hofstetter and others, 1983). Once the zeolite materials are loaded with radionuclides, they are typically encased in a solid glass, a process called vitrification, prior to disposal. After nuclear weapons tests in the Bikini Islands in the 1950s, soils were treated with clioptilolite to reduce ^{90}Sr and ^{137}Cs levels in plants there. In some of the areas affected by the 1986 Chernobyl disaster, natural zeolites were used to treat soils to minimize the presence of ^{137}Cs in pasture plants and subsequently livestock. Natural zeolites were also used as a dietary supplement in certain livestock and even reindeer, as they readily incorporate radionuclides such as ^{90}Sr and 137Cs, so that they could be excreted by the animals more quickly (Mumpton, 1999).

Radioactive contamination, the result of accidental spills or acts of terrorism, requires a way to decontaminate buildings, structures, and equipment. At Los Alamos National Laboratories, Chipera and others (2006) tested zeolite as a decontamination agent. They developed a strippable coating that is applied directly to contaminated objects. The coating contains a zeolite, which acts as a repository for radionuclides. After exposure, the coating is removed and safely discarded. Cesium uptake was 90 to 100 percent with clinoptilolite and 98 to 100 percent when mordenite and chabazite were added. These natural zeolites were more effective than synthetic zeolites that were similarly tested.

Appendix 2 - Geochemical Analyses

Table 6. Whole rock geochemistry of zeolite-bearing samples collected during this investigation (<0.01 means a concentration below the lower detection limit of 0.01 percent, but not necessarily absent from the sample).

SAMPLE	SiO_2 (%)	Al_2O_3 (%)	Fe_2O_3 (%)	CaO (%)	MgO (%)	Na_2O (%)	K_2O (%)	Cr_2O_3 (%)	TiO_2 (%)	MnO (%)	P_2O_5 (%)	SrO (%)	BaO (%)	LOI (%)	Total (%)
20070928BG-1	64.5	11	0.99	5.3	0.78	1.92	2.75	<0.01	0.26	0.06	0.06	0.21	0.57	11.15	99.55
20120810BG-3	43.2	7.76	0.96	18.55	1.15	0.66	1.65	<0.01	0.08	0.22	0.13	0.14	0.28	23.7	98.48
20120810BG-4	57.3	13.25	3.23	2.81	1.19	1.69	3.34	<0.01	0.36	0.03	0.08	0.12	0.13	16.1	99.63
20140820BG-2	59.8	10.1	1.4	11.1	1.05	1.52	3.2	<0.01	0.3	0.12	0.19	0.06	0.06	11.95	100.85
20140820BG-3	65.1	12.55	0.75	1.71	0.34	4.3	1.69	<0.01	0.13	0.01	0.04	0.05	0.13	14.05	100.85
20140820BG-4	71.4	11	2.08	1.71	0.83	3.19	2.14	<0.01	0.26	0.02	0.1	0.04	0.09	9.03	101.89
20140820BG-5	63.7	13.2	1.37	1.58	0.7	4.38	1.65	<0.01	0.17	0.01	0.04	0.05	0.13	14.6	101.58
20140820JC-1	68.9	12.05	1.46	1.73	0.66	4.11	2.56	<0.01	0.26	0.01	0.11	0.04	0.13	9.83	101.85
20140820JC-2	65	12.7	1.68	1.68	0.74	4.13	2.19	<0.01	0.22	0.01	0.06	0.05	0.12	11.8	100.38
20140822JC-5	61.5	14.95	3.14	1.48	0.62	1.97	7.1	<0.01	0.29	0.01	0.17	0.2	0.17	8.7	100.3
20140828BG-4	61.3	13.3	1.86	4.03	1.87	0.98	2.54	<0.01	0.4	0.04	0.06	0.37	0.35	14.2	101.3
20140828BG-6	60.5	13.8	2.36	3.28	2.2	1.15	2.13	<0.01	0.41	0.02	0.09	0.42	0.34	15.1	101.8
20140828BG-7	66.2	12.5	1.29	2.97	1.02	1.21	1.8	<0.01	0.25	0.01	0.03	0.22	0.18	13.55	101.23
20140828JC-1	59.5	13.95	2.01	2.3	2.16	1.89	2.19	<0.01	0.42	0.01	0.08	0.42	0.4	15.25	100.58
20140828JC-2	59.9	13.85	7.44	2.03	0.58	1.49	4.89	<0.01	0.2	0.01	0.04	0.21	0.3	9.82	100.76
20140909JC-1	68.4	11	2.39	3.63	1.47	1.43	4.19	<0.01	0.35	0.04	0.09	0.14	0.2	7.89	101.22
20141007JC-3	68.9	13.45	2.45	1.11	0.38	1.04	2.3	<0.01	0.37	0.02	0.02	0.02	0.13	9.88	100.07
20141020JC-3	53.3	15.45	3.29	4.47	3.65	3.8	5.32	0.01	0.6	0.05	0.04	0.03	0.04	9.94	99.99
20141022BG-1	29.4	7.14	2.55	22.5	6.85	1.13	1.2	0.03	0.21	0.28	0.1	0.05	0.08	27.5	99.02
20141023BG-1	64	11.8	2.37	6.69	1.79	2.68	1.88	0.01	0.38	0.06	0.33	0.1	0.16	7.06	99.31
20141023BG-3	64.2	3.29	0.71	9.18	5.48	0.78	0.7	<0.01	0.13	0.03	0.06	0.05	0.06	15	99.67
20141023BG-6	68.6	13.4	2.63	2.81	1.48	3.18	2.88	0.01	0.43	0.03	0.15	0.06	0.09	4.39	100.14
20141023JC-3	62.1	9.63	2.17	8.63	1.49	2.44	2.18	0.01	0.41	0.1	0.28	0.06	0.12	9.45	99.07
20141023JC-4	57.9	11.05	2.47	9.63	1.65	1.95	3.58	0.01	0.4	0.16	0.18	0.05	0.1	10.55	99.68
20141105BG-2	59.8	18.6	1.64	1.38	1.17	1.82	6.31	0.01	0.87	0.01	0.08	0.02	0.07	8.08	99.86
20141105BG-3	73.3	10	1.67	2.48	0.93	2.04	2.36	<0.01	0.3	0.02	0.11	0.04	0.11	7.34	100.7
20141105BG-4	69.5	10.95	1.43	2.16	0.92	3.49	2.11	<0.01	0.28	0.03	0.06	0.05	0.14	9.65	100.77
20141105BG-5	68	12.2	1.41	1.43	0.81	4.27	2.25	<0.01	0.27	0.01	0.1	0.06	0.16	10.25	101.22
20141105BG-6	67.5	11.45	1.59	2.43	0.93	3.82	2.45	<0.01	0.29	0.04	0.09	0.05	0.12	10.05	100.81
20141105BG-7	72.1	10.6	1.62	1.91	1.02	2.51	2.57	<0.01	0.3	0.01	0.08	0.04	0.13	7.89	100.78
20141105BG-8	70.4	10.3	3.55	1.53	1.18	3.03	2.19	<0.01	0.27	0.03	0.12	0.04	0.11	7.63	100.38
20141105JC-1	32.5	7.42	2.93	9.3	5.58	1.47	2.45	0.01	0.29	0.05	0.52	0.07	0.09	33.5	96.18
20141105JC-2	49	12.8	3.78	7.48	4.94	1.82	3.86	0.01	0.64	0.07	0.09	0.08	0.07	17.15	101.79
20141105JC-3	37.1	8.58	3.32	8.34	7.56	1.42	2.76	0.01	0.36	0.05	0.03	0.06	0.05	28.5	98.14
20141105JC-4	64.8	11.15	2.79	3.53	1.88	1.6	2.51	0.01	0.39	0.01	0.16	0.09	0.14	9.57	98.63
20141105JC-5	64	13	2.74	2.11	1.69	2.6	2.41	<0.01	0.34	0.01	0.1	0.07	0.14	10.05	99.26
20141105JC-6	72.4	10.05	1.63	2.7	1.1	1.06	1.99	<0.01	0.27	0.01	0.08	0.18	0.22	8.3	99.99
20141105JC-7	62.2	14.85	3.45	3.04	1.69	3.81	2.78	0.01	0.49	0.02	0.36	0.06	0.09	5.91	98.76
20141105JC-8	71.9	10.55	1.68	1.58	0.92	2.96	2.39	0.01	0.3	0.03	0.1	0.04	0.13	7.7	100.29

Table 6 continued.

SAMPLE	SiO_2 (%)	Al_2O_3 (%)	Fe_2O_3 (%)	CaO (%)	MgO (%)	Na_2O (%)	K_2O (%)	Cr_2O_3 (%)	TiO_2 (%)	MnO (%)	P_2O_5 (%)	SrO (%)	BaO (%)	LOI (%)	Total (%)
20141105JC-9	66.4	13.1	2.96	2.5	1.44	3.56	2.71	0.01	0.46	0.04	0.13	0.06	0.14	6.03	99.54
20141105JC-10	71.4	10.75	1.6	1.08	0.87	3.26	2.2	<0.01	0.27	0.02	0.09	0.04	0.12	8.64	100.34
20141105JC-11	66.2	12.3	0.79	0.86	0.5	4.75	1.92	<0.01	0.16	0.01	0.04	0.06	0.18	12.85	100.62
20141106BG-1	64.4	14.3	2.87	1.27	1.23	5.27	2.51	0.01	0.45	0.01	0.14	0.03	0.05	6.93	99.47
20141106BG-2	68.8	12	2.6	1.59	1.47	2.65	2.71	0.01	0.42	0.01	0.18	0.07	0.2	7.68	100.39
20141106BG-3	66.6	11.95	0.85	0.86	0.55	4.53	1.89	<0.01	0.13	<0.01	0.04	0.05	0.13	12.6	100.18
20141106BG-4	64.5	12.65	1.48	1.34	0.68	4.31	2.14	<0.01	0.19	0.01	0.05	0.05	0.15	13.25	100.8
20141106BG-5	66.1	12.15	0.82	1.03	0.32	4.64	2.05	<0.01	0.11	<0.01	0.03	0.04	0.13	13.1	100.52
20141106BG-6	71.1	11.1	1.63	1.99	0.85	3.37	2.15	<0.01	0.26	0.02	0.08	0.04	0.11	8	100.7
20141106BG-7	69.3	11.5	1.06	1.29	0.54	3.79	2.31	<0.01	0.16	0.01	0.17	0.04	0.1	10.75	101.02
20141106BG-8	68.5	10.95	1.05	2.58	0.57	3.75	2.1	<0.01	0.21	0.04	0.07	0.04	0.11	10.7	100.67
20141106BG-9	71.4	11.2	1.37	2.33	0.71	2.94	2.3	0.01	0.27	0.04	0.08	0.04	0.1	8.39	101.18
20141106BG-10	72.2	10.7	1.15	1.42	0.65	3.49	2	<0.01	0.2	0.01	0.04	0.03	0.09	9.55	101.53
20141106JC-1	63.6	12.9	3.64	4.2	1.96	2.38	3.88	0.01	0.45	0.03	0.18	0.03	0.07	7.77	101.1
20141106JC-2	43.9	8	1.83	21.3	1.8	1.95	1.65	0.01	0.31	0.09	0.17	0.09	0.08	19.35	100.53
20141106JC-3	72.6	10.2	1.66	2.59	0.9	2.53	2.39	0.01	0.34	0.02	0.13	0.05	0.28	6.52	100.22
20141106JC-4	66.6	14.25	3.57	0.94	1.79	3.56	4.45	0.01	0.48	0.02	0.17	0.02	0.05	5.03	100.94
20141106JC-5	66.3	12.65	0.7	1.07	0.43	5.05	1.7	<0.01	0.1	0.02	0.05	0.06	0.15	13.3	101.58
20141106JC-6	70.6	11.15	0.84	1.39	0.37	3.82	1.94	<0.01	0.24	<0.01	0.04	0.04	0.18	11.1	101.71
20141106JC-7	65.6	12.55	2.13	2.47	1.21	3.34	2.6	<0.01	0.29	0.03	0.1	0.04	0.12	10.3	100.78
20141106JC-8	64.3	12.75	1.02	1.35	0.54	4.8	1.89	<0.01	0.16	0.01	0.04	0.05	0.12	14.2	101.23
20141106JC-9	64.3	12.5	2.89	2.66	1.65	3.58	2.37	0.01	0.35	0.03	0.16	0.04	0.09	9.97	100.6
20141106JC-10	64.4	13.1	0.99	1.35	0.59	4.62	2.05	<0.01	0.21	0.01	0.04	0.05	0.14	13	100.55
20150604BG-1	58.6	13.1	3	4.08	2.79	0.56	2.28	<0.01	0.36	0.03	0.05	0.04	0.02	15.85	100.76
20150604BG-2	75.4	11	2.35	1.88	0.76	2.15	3.72	<0.01	0.33	0.03	0.07	0.05	0.07	3.57	101.38
20150604DB-3	70.7	11.85	2.34	1.08	0.48	1.68	5.81	<0.01	0.28	0.03	0.03	0.01	0.07	6.99	101.35
20150604DB-4	55.8	12.2	3.07	2.2	1.9	3.04	4	<0.01	0.32	0.03	0.03	0.05	0.29	17.6	100.53
20150701BG-2	51.2	6.3	1.45	18.65	0.77	1.01	1.89	<0.01	0.2	0.05	0.03	0.08	0.06	17.8	99.49
20150701DB-1	63.3	10.05	2.26	8.05	1.76	1.78	2.66	<0.01	0.3	0.04	0.04	0.05	0.07	10.35	100.71
20150701DB-2	68.5	10.85	2.33	5.15	1.2	1.98	3.4	<0.01	0.31	0.04	0.04	0.05	0.07	7.55	101.47
20150701DB-4	68.4	10.35	1.41	4.88	0.95	0.9	2.98	<0.01	0.28	0.01	0.06	0.13	0.1	10.75	101.2
20150701DB-5	70.6	10.2	2.23	3.02	1.64	1.47	3	<0.01	0.32	0.02	0.07	0.07	0.07	8.12	100.83
20150701DB-6	69.7	11.45	1.29	2.43	1.29	2.23	3.87	<0.01	0.26	0.01	0.02	0.12	0.09	8.65	101.41
20150701DB-7	69	9.96	2.12	3.35	2.06	1.42	3.34	<0.01	0.32	0.03	0.07	0.06	0.06	9.18	100.97
20150702DB-1	56.4	9.58	0.93	12.4	0.88	1.54	3.89	<0.01	0.14	0.07	0.03	0.02	0.06	14.2	100.14
20150819BG-1	75.4	8.67	1.5	2.06	1.26	0.7	1.72	<0.01	0.2	0.01	0.02	0.2	0.36	8.81	100.91
20150819BG-2	62.9	12.9	1.31	2.96	1.81	0.63	2.72	<0.01	0.1	<0.01	0.02	0.32	0.64	14.05	100.36
20150819BG-3	63.3	13.5	1.75	2.57	2.23	1	3.74	<0.01	0.22	0.01	0.02	0.25	0.42	11.25	100.26
20150819DB-2	54.8	11.65	1.86	11.05	1.5	1.33	2.77	0.01	0.29	0.08	0.22	0.22	0.19	14	99.97
20150820DB-2	64.2	15.35	1.86	1.36	1.43	1.75	7.69	<0.01	0.19	0.02	0.11	0.09	0.18	5.93	100.16

Table 7. Rare earth element geochemistry of zeolite-bearing samples collected during this investigation (ppm = parts per million; <0.001 means the concentration of that element in the sample is below the lower detection limit of 0.001 ppm but not necessarily absent from the sample).

SAMPLE	Sc (ppm)	Y (ppm)	La (ppm)	Ce (ppm)	Pr (ppm)	Nd (ppm)	Sm (ppm)	Eu (ppm)	Gd (ppm)	Tb (ppm)	Dy (ppm)	Ho (ppm)	Er (ppm)	Tm (ppm)	Yb (ppm)	Lu (ppm)
20070928BG-1	3.6	17.5	30.7	51.5	5.81	21.7	3.97	0.53	2.92	0.46	2.82	0.56	1.65	0.24	1.57	0.24
20120810BG-3	3.1	14.4	32.8	57	5.6	20.2	3.41	0.38	2.67	0.41	2.51	0.52	1.56	0.25	1.63	0.25
20120810BG-4	4	17.5	39.7	76.9	8.2	29.1	4.64	1.17	3.38	0.51	3.07	0.63	2.07	0.32	2.21	0.35
20140820BG-2	3.7	11.2	32.4	60.6	6.52	24.5	4.19	0.83	3	0.4	2.22	0.41	1.05	0.15	0.91	0.14
2014-FLBG-3	3.1	20.1	35.1	69.3	7.49	27.6	4.9	0.6	3.66	0.54	3.44	0.71	2.18	0.33	2.16	0.33
20140820BG-4	4.8	14.2	36.1	67.3	7.11	26	4.37	0.69	3	0.44	2.59	0.49	1.57	0.24	1.63	0.25
20140820BG-5	4.2	15.2	44	84.9	8.99	33.1	5.47	0.81	3.82	0.53	3.14	0.56	1.64	0.22	1.44	0.22
20140820JC-1	5.1	17.6	35.6	65.9	7.15	27	4.66	0.69	3.7	0.55	3.15	0.62	1.9	0.27	1.75	0.26
2014-FLJC-2	3.6	14.6	41.2	75.6	7.98	29	4.7	0.7	3.25	0.48	2.8	0.53	1.56	0.21	1.41	0.21
20140822JC-5	8.3	4.5	50.3	62.6	5.08	16.5	2.42	0.81	1.42	0.2	1.1	0.2	0.61	0.09	0.7	0.11
20140828BG-4	5.6	12.9	59	109.5	11.15	40.1	5.42	0.9	3.42	0.48	2.5	0.48	1.43	0.19	1.25	0.18
20140828BG-6	6.2	13.3	48.9	93.2	9.44	34.4	5.47	1.1	3.71	0.52	2.93	0.53	1.47	0.2	1.28	0.19
20140828BG-7	5.5	3.4	32.7	58.3	5.66	18.9	2.63	0.65	1.39	0.17	0.8	0.14	0.34	0.05	0.34	0.06
20140828JC-1	5.4	19.2	36.6	62.3	7.33	27.6	4.95	0.89	4.05	0.57	3.11	0.61	1.63	0.21	1.35	0.21
20140828JC-2	3.8	2.9	15	30.6	3.34	13.2	2.28	0.62	1.13	0.15	0.77	0.14	0.39	0.06	0.4	0.07
20140909JC-1	5.2	12.2	25.2	47.5	5.5	21	3.76	0.72	2.79	0.4	2.28	0.44	1.26	0.19	1.26	0.19
20141007JC-3	5.1	9.5	24.2	45	4.43	15.8	2.61	0.47	1.89	0.28	1.73	0.34	1.07	0.16	1.09	0.18
20141020JC-3	7.4	5.2	12.3	23	2.41	8	1.16	0.22	0.86	0.13	0.9	0.2	0.64	0.11	0.81	0.13
20141022BG-1	4	17.7	26.3	47.1	4.96	18.8	3.22	0.56	2.55	0.38	2.4	0.51	1.71	0.26	1.9	0.31
20141023BG-1	8.7	13.7	36.8	70.1	7.25	27.3	4.55	1.02	3.15	0.45	2.5	0.49	1.38	0.2	1.34	0.2
20141023BG-3	1.8	4.7	7.3	16.05	1.87	7.5	1.45	0.33	1.08	0.16	0.92	0.18	0.51	0.08	0.49	0.07
20141023BG-6	7.8	12.4	31.4	58.4	6.34	24.3	4.11	0.91	2.94	0.41	2.33	0.44	1.28	0.19	1.18	0.18
20141023JC-3	6.4	17.3	32.5	62	6.62	25.2	4.33	0.83	3.29	0.48	2.76	0.54	1.76	0.24	1.68	0.26
20141023JC-4	6.4	16.5	36.3	67.8	7.04	26.4	4.27	0.89	3.23	0.45	2.57	0.52	1.58	0.23	1.56	0.24
20141105BG-2	8.5	12.4	57.9	114	12.35	45.7	7.05	1.11	3.85	0.52	2.72	0.48	1.41	0.21	1.36	0.21
20141105BG-3	3.7	10.4	25.2	46.6	5	18.7	3.35	0.52	2.32	0.34	1.94	0.38	1.16	0.17	1.14	0.16
20141105BG-4	3.9	8.2	25.1	46.8	4.81	17.2	2.81	0.46	1.86	0.27	1.52	0.3	0.96	0.14	0.98	0.15
20141105BG-5	4.2	15.4	39	72.1	7.76	28.9	4.93	0.72	3.46	0.49	2.8	0.54	1.59	0.22	1.39	0.21
20141105BG-6	3.7	13.2	30.5	56.7	5.86	21.2	3.5	0.6	2.59	0.4	2.4	0.48	1.55	0.23	1.64	0.25
20141105BG-7	5	12.2	32.1	58.6	6.19	22.6	3.77	0.64	2.63	0.39	2.22	0.45	1.36	0.2	1.38	0.2
20141105BG-8	4.9	22.2	36.1	67.7	7.41	27.6	5.04	0.79	3.65	0.58	3.33	0.74	2.21	0.33	2.17	0.32
20141105JC-1	6.7	15.7	26.9	53.1	5.74	22	4.03	0.74	2.92	0.45	2.59	0.54	1.69	0.24	1.57	0.24
20141105JC-10	3.4	11.3	32.2	58.1	6.11	22.1	3.74	0.61	2.33	0.35	1.99	0.4	1.25	0.18	1.22	0.18
20141105JC-11	1.8	14	43.7	79.4	8.13	28.5	4.45	0.65	2.81	0.42	2.4	0.5	1.52	0.23	1.6	0.24
20141105JC-2	9.6	23.4	37.8	77.7	9.18	36.4	6.87	1.22	4.85	0.72	3.99	0.8	2.33	0.33	2.16	0.31
20141105JC-3	7	10.9	26.9	52.3	5.53	20.9	3.58	0.58	2.34	0.36	1.97	0.44	1.14	0.15	1.02	0.14
20141105JC-4	7.5	19.9	40.5	74.7	8.16	30.4	5.14	0.88	3.71	0.54	3.13	0.69	2.07	0.29	2.07	0.32
20141105JC-5	6.4	22.7	46.6	87.8	9.54	35	6.44	1.04	4.55	0.7	3.94	0.8	2.37	0.33	2.15	0.3
20141105JC-6	4.2	11.9	31.4	55.7	5.86	21.4	3.66	0.63	2.45	0.37	1.99	0.42	1.27	0.19	1.39	0.21
20141105JC-7	8.6	28.4	36.5	70.8	8.04	31.1	5.75	1.19	4.45	0.69	4.15	0.95	3.06	0.44	2.95	0.45
20141105JC-8	5.1	19.9	29.2	56.2	6.19	23.7	4.57	0.7	3.56	0.56	3.19	0.69	2	0.29	1.83	0.28

Table 7 continued.

SAMPLE	Sc (ppm)	Y (ppm)	La (ppm)	Ce (ppm)	Pr (ppm)	Nd (ppm)	Sm (ppm)	Eu (ppm)	Gd (ppm)	Tb (ppm)	Dy (ppm)	Ho (ppm)	Er (ppm)	Tm (ppm)	Yb (ppm)	Lu (ppm)
20141105JC-9	8.3	18	35.8	66	7.36	28	5.04	0.97	3.69	0.56	3.08	0.63	1.83	0.26	1.62	0.25
20141106BG-1	8.4	20.1	48.1	88.2	9.22	34.4	6.02	1.16	4.24	0.65	3.44	0.68	1.92	0.24	1.63	0.23
20141106BG-10	3.4	13.4	33.5	61.8	6.59	24.2	4.41	0.66	3.12	0.49	2.57	0.51	1.43	0.2	1.37	0.2
20141106BG-2	6.9	17.9	42.4	78	8.77	33	5.87	1.12	4.48	0.65	3.47	0.67	1.82	0.24	1.57	0.23
20141106BG-3	2	12.2	47.5	86.9	8.84	31.1	4.99	0.69	2.87	0.43	2.24	0.46	1.27	0.18	1.22	0.19
20141106BG-4	3.6	18.3	48.2	89.5	9.46	33.6	5.48	0.8	3.7	0.56	3.16	0.63	1.81	0.24	1.51	0.21
20141106BG-5	1.9	14.2	42.4	75.9	7.84	27.4	4.25	0.62	2.55	0.37	2.11	0.46	1.72	0.27	1.78	0.28
20141106BG-6	5	11.4	30.1	56	6.06	22.6	3.97	0.75	2.73	0.4	2.17	0.42	1.19	0.16	1.09	0.16
20141106BG-7	2.8	21.8	28.5	56.3	6.21	23.7	4.63	0.66	3.81	0.61	3.52	0.72	2.33	0.32	2.09	0.32
20141106BG-8	3.7	13.7	25.6	51	5.74	21.8	4.11	0.59	2.97	0.46	2.59	0.52	1.54	0.22	1.41	0.22
20141106BG-9	5	14.1	29.4	55.2	6.09	22.5	4.17	0.73	3.11	0.48	2.62	0.55	1.6	0.22	1.43	0.22
20141106JC-1	6.9	13.9	32.4	63.3	6.7	25.6	4.55	0.86	3.19	0.47	2.53	0.51	1.49	0.2	1.26	0.18
20141106JC-10	4.6	20	50.8	90.9	9.56	31.6	5.3	0.81	3.7	0.54	3.29	0.7	2.37	0.39	2.38	0.4
20141106JC-2	5.5	13.3	24.2	45.8	4.92	17.8	3.28	0.72	2.68	0.4	2.35	0.5	1.57	0.25	1.7	0.27
20141106JC-3	5.5	11.1	28.5	51	5.54	19.6	3.48	0.73	2.78	0.4	2.29	0.43	1.24	0.19	1.24	0.19
20141106JC-4	8.7	17.3	45.9	85.7	9	31.5	5.63	1.06	4.34	0.62	3.39	0.64	1.86	0.27	1.66	0.26
20141106JC-5	1.3	8.7	41.4	74.6	7.66	25.3	3.92	0.68	2.63	0.34	1.93	0.37	0.95	0.15	0.85	0.14
20141106JC-6	4.7	9	33.6	61.1	6.33	21.3	3.42	1.08	2.31	0.31	1.76	0.37	1.18	0.19	1.27	0.21
20141106JC-7	5.6	17.2	38	71.7	7.87	27.5	4.98	0.9	4.03	0.6	3.42	0.65	1.95	0.28	1.78	0.27
20141106JC-8	3.6	20.2	46.9	85.8	9.36	32.3	5.75	0.91	4.42	0.66	3.83	0.75	2.18	0.31	1.91	0.28
20141106JC-9	6.5	22.8	35.3	67.7	7.58	27.4	5.4	0.97	4.57	0.72	4.24	0.88	2.65	0.39	2.76	0.43
20150604BG-1	5	70.5	101.5	220	20.7	73.2	13.9	0.92	12.45	2.02	11.85	2.28	6.58	0.97	6.35	0.93
20150604BG-2	4	12.7	29.5	54.4	5.96	21.6	3.79	0.82	3.23	0.42	2.46	0.51	1.37	0.2	1.29	0.21
20150604DB-3	4	47	77.8	149.5	15.55	53.8	9.89	0.78	8.96	1.42	8.28	1.65	4.96	0.77	4.75	0.7
20150604DB-4	4	43.6	62.5	123	12.25	45	8.27	0.77	7.19	1.38	9.91	2.27	7.67	1.36	8.69	1.1
20150701BG-2	3	25.4	22.6	48.5	5.08	20.7	4.13	0.64	4.16	0.66	3.7	0.85	2.51	0.38	2.55	0.36
20150701DB-1	5	29.5	33.3	69.3	7.69	29.9	6.03	0.99	5.49	0.92	5.32	1.08	3.24	0.49	3.29	0.47
20150701DB-2	4	24.3	38.2	73	8.11	30	5.78	0.88	4.9	0.77	4.23	0.91	2.61	0.42	2.53	0.39
20150701DB-4	4	15.6	32.5	59.6	6.53	23.7	4.27	0.71	3.61	0.52	3.04	0.62	1.68	0.25	1.61	0.25
20150701DB-5	5	20.5	37.2	71.9	8.11	30.4	5.39	0.87	4.5	0.72	3.8	0.83	2.41	0.42	3.65	0.64
20150701DB-6	4	8.7	31.9	63	7.07	25.1	4.18	0.65	2.84	0.39	1.96	0.32	0.84	0.13	1.01	0.16
20150701DB-7	6	15.4	27.8	52	5.85	21.3	3.66	0.71	3.3	0.5	3.07	0.6	1.78	0.32	2.06	0.34
20150702DB-1	2	9.9	24.9	44.5	4.48	15	2.55	0.47	1.98	0.25	1.47	0.33	0.91	0.15	1.1	0.18
20150819BG-1	3	6.8	34.4	67	6.54	21.6	3.42	0.34	2.64	0.33	1.71	0.3	0.67	0.1	0.59	0.08
20150819BG-2	2	13.5	61.7	124	13.35	46.6	9.59	0.43	7.08	0.96	3.99	0.6	1.37	0.15	0.85	0.08
20150819BG-3	3	12.5	44.7	87.6	8.83	31.8	7.14	0.47	5.61	0.81	3.71	0.57	1.25	0.15	0.84	0.1
20150819DB-2	5	16.7	37	69.1	7.13	27	4.69	1.01	3.79	0.52	3.11	0.66	1.76	0.28	1.63	0.24
20150820DB-2	3	7.6	40.9	65.3	5.91	19.6	3.18	0.57	2.51	0.29	1.54	0.3	0.67	0.09	0.64	0.09

Table 8. Single element geochemistry of zeolite-bearing samples collected during this investigation (ppm = parts per million; <0.001 means the concentration of that element in the sample is below the lower detection limit of 0.001 ppm but not necessarily absent from the sample).

SAMPLE	Ag (ppm)	As (ppm)	Ba (ppm)	Bi (ppm)	Cd (ppm)	Co (ppm)	Cr (ppm)	Cs (ppm)	Cu (ppm)	Ga (ppm)	Ge (ppm)	Hf (ppm)	In (ppm)	Li (ppm)	Mo (ppm)	Nb (ppm)	Ni (ppm)	Pb (ppm)	Rb (ppm)	Re (ppm)	S(%)	Sb (ppm)	Se (ppm)	Sn (ppm)	Sr (ppm)	Ta (ppm)	Te (ppm)	Th (ppm)	Tl (ppm)	U (ppm)	V (ppm)	W (ppm)	Zn (ppm)	Zr (ppm)
20070928BG-1	0.05	2.4	4930	0.24	0.04	1.7	12	2.51	6.8	13.75	0.09	2.4	0.029	7.5	0.67	16.3	2.8	14.6	76.4	0.003	0.12	0.34	1	2	1620	0.97	<0.05	10.4	1.12	5.8	22	3	33	80.5
20120810BG-3	0.06	33.6	2560	0.23	0.18	2	6	1.41	7	11.25	0.07	2.8	0.026	6.4	0.59	13	2.7	20.6	47	<0.002	0.11	0.45	1	1.7	1145	0.97	<0.05	9.6	0.56	3.6	8	0.2	32	93.3
20120810BG-4	0.04	16.2	1120	0.19	0.12	10.4	4	4.04	7.8	15.75	0.13	6.8	0.031	6	3.07	19.9	9.4	20.1	103	0.002	0.01	0.63	2	1.4	918	1.39	<0.05	14.4	1.2	4.5	8	0.2	51	193
20140820BG-2	0.04	15	520	0.18	0.09	4.2	31	4.86	22.7	13.75	0.13	3	0.038	32.6	4.86	8.5	10.1	10.4	99.2	0.005	0.11	0.4	1	1.4	479	0.78	<0.05	9.3	0.51	1.5	29	1.2	35	82.3
20140820BG-3	0.06	1.7	1150	0.19	0.03	0.7	2	1.7	6	13.9	0.09	4.9	0.039	5.7	0.37	22.4	1	20.8	60.9	0.002	<0.01	0.26	1	2.3	357	1.54	<0.05	14.9	0.58	2.2	5	0.5	34	154
20140820BG-4	0.06	10.8	770	0.19	0.17	4.5	18	4.35	15.4	14.15	0.08	3.3	0.035	22.7	0.8	15.3	8	19.6	94	0.002	0.02	0.67	1	1.8	296	1.01	<0.05	12.2	0.8	2	25	0.9	58	101.5
20140820BG-5	0.04	0.5	1130	0.18	0.05	1.1	2	1.81	5.5	16.55	0.1	6.1	0.032	13.9	0.1	20.5	1.4	17.6	70.2	0.002	<0.01	0.23	1	2.4	393	1.56	<0.05	16.2	0.34	2.7	7	0.3	43	222
20140820JC-1	0.05	1.4	1170	0.19	0.08	4.1	20	3.97	12.5	14.55	0.11	3.3	0.039	17.1	0.24	19.2	6.9	20.1	97.4	0.002	0.01	0.32	1	3.2	348	1.19	<0.05	14.8	1.09	2.3	24	0.7	61	112
20140820JC-2	0.11	0.4	1170	0.18	0.05	2.8	12	3.32	21.3	15.15	0.07	4.1	0.032	12.6	0.14	17.6	5.6	23.3	114.5	0.002	<0.01	0.37	1	2	396	1.16	<0.05	13.9	0.58	1.7	17	0.9	57	141
20140822JC-5	0.06	5.3	1580	0.16	0.1	3	13	1.24	20.3	17.9	0.12	5.7	0.055	6.6	0.87	14.7	2.3	17.3	88.5	0.003	0.72	0.33	1	1.4	1545	0.99	0.05	17.1	0.6	1.4	19	0.3	21	218
20140828BG-3	0.12	2.5	1300	0.12	0.07	15.1	57	1.5	26.1	21.7	0.14	4	0.04	75.5	0.67	11.3	33	19.5	48.9	0.002	0.04	0.21	1	1.2	982	0.69	<0.05	9.8	0.27	1.8	89	0.8	64	147
20140828BG-6	0.03	2.2	3090	0.17	0.07	4	4	1.41	7.8	17.75	0.13	7.5	0.037	10.3	5.37	22	3.9	16.5	49.3	<0.002	0.01	0.44	1	1.8	3440	1.41	<0.05	7.6	0.63	0.8	15	0.4	42	294
20140828BG-7	0.05	5.6	1540	0.25	0.02	3.4	11	2.3	9.8	17.7	0.08	4.6	0.038	15.3	1.01	15.4	4.2	16.9	57.8	0.005	0.07	0.35	1	1.9	1710	1.33	<0.05	16.9	0.56	1.4	12	0.4	38	163
20140828JC-1	0.05	2.2	3570	0.18	0.05	2.7	5	1.18	7.8	16	0.09	7.3	0.032	8.6	3.16	20.7	2.9	18.7	47.6	0.003	0.13	0.46	1	1.6	3300	1.38	<0.05	5	0.61	0.8	16	0.3	51	289
20140828JC-2	0.1	15.2	2780	0.29	<0.02	3.4	21	8.7	32.8	19.95	0.12	3.5	0.03	12	4.87	7	1.9	14.9	119.5	0.003	0.21	0.57	4	1.4	1665	1.47	0.06	5.3	1.61	2.7	39	0.3	30	110.5
20140909JC-1	0.07	5.2	1780	0.16	0.08	4.7	18	4.05	9.5	14.4	0.1	2.5	0.027	42.1	0.25	10.6	7.9	13.5	100.5	0.002	0.01	0.62	1	1.2	1125	0.71	<0.05	7.3	0.74	4.5	107	0.8	39	75.6
20141007JC-3	0.07	1.8	1140	0.24	0.06	2.2	11	4.68	7.3	19.2	0.09	7	0.041	19.4	1.66	23.7	2.4	19.4	103.5	0.002	0.01	0.38	1	2.3	210	1.59	<0.05	15.3	1.14	5.1	24	1.6	40	250
20141020JC-3	0.13	5.2	360	0.48	0.4	5.4	58	10.3	28.2	23.3	0.12	2.4	0.073	111	3.2	16.1	21.3	20.9	133.5	0.004	0.08	0.82	1	2.8	269	1	0.09	1.9	0.95	1.9	110	1.3	82	75.7
20141022BG-1	0.02	<0.2	700	0.09	0.17	6.3	20	5.17	8.5	10.25	0.07	2.3	0.023	16.4	3.33	9.2	10.3	10.4	54.2	0.021	0.09	0.29	1	1.1	439	0.58	<0.05	6.6	0.28	2.1	27	1.2	42	82.5
20141023BG-1	0.07	2.5	1400	0.13	0.15	11.7	42	1.8	23.5	16.4	0.1	2.7	0.035	32.4	0.48	10.3	17.2	14.9	55.6	0.002	0.04	0.54	1	1.3	769	0.68	<0.05	11.4	0.29	4	66	1	51	109
20141023BG-3	0.03	8.2	520	0.08	0.05	1.9	11	1.71	3.9	4.18	0.05	0.5	0.014	55.9	3.64	3.1	4.3	3.9	28.5	0.002	0.03	0.3	1	0.5	441	0.19	<0.05	3.8	2.01	2.7	22	0.7	11	23.1
20141023BG-6	0.09	1	800	0.15	0.03	8	35	4.95	23.2	18.3	0.07	2.4	0.04	26.9	0.45	9.8	14.2	14.5	71.4	0.002	0.03	0.32	1	1.4	480	0.57	<0.05	7.4	0.34	2.4	58	1.4	56	86.4
20141023JC-3	0.09	2.5	1000	0.17	0.14	7.6	35	3.97	18.1	12.75	0.08	2.5	0.03	40.7	1.15	9.9	12.5	12.8	77.1	0.003	0.14	0.5	1	1.5	462	0.61	<0.05	8.9	0.33	4.8	44	1.9	43	95.5
20141023JC-4	0.13	1.4	840	0.19	0.14	5.7	28	4.46	16.1	16.4	0.11	2.7	0.035	40.2	0.34	11.2	9.3	15.5	112	0.002	0.03	0.42	1	1.9	435	0.73	<0.05	11.1	0.46	5.8	39	1.4	48	97.6
20141105BG-2	0.24	5	580	0.6	0.02	4.2	61	12.6	22	28.7	0.19	2.4	0.05	24.3	3.4	26.5	4.5	18.2	152.5	0.005	0.17	1.12	1	4.3	161.5	1.56	0.09	16.7	0.92	6.2	115	4.7	47	88.6
20141105BG-3	0.07	3.6	940	0.22	0.08	7	24	4.56	13.9	10.85	0.06	2.3	0.029	33.1	0.34	13.7	12.8	13.9	83.9	0.002	0.01	0.44	1	1.8	349	0.85	<0.05	9.3	0.71	2.2	30	2.1	43	77.4
20141105BG-4	0.08	1.1	1190	0.19	0.09	3.3	17	2.75	9.5	13.35	0.09	3	0.031	32.1	0.23	14.3	4.9	14.4	82.8	0.002	0.02	0.34	1	1.9	378	0.86	<0.05	8.4	0.42	2.5	24	0.7	40	115
20141105BG-5	0.12	1.7	1390	0.18	0.09	4.3	19	2.61	11.2	15.6	0.11	3.8	0.036	21.2	0.49	23.9	5.5	19	87.1	0.002	0.01	0.3	1	2.5	463	1.15	<0.05	12.7	0.44	2.3	21	0.7	44	132.5
20141105BG-6	0.52	3	1050	0.18	0.14	7.6	19	2.66	52.1	18.35	0.12	3.4	0.033	25	0.6	18.1	14.5	44.6	80.1	0.002	0.01	0.36	1	1.4	390	0.77	<0.05	9.1	0.51	3.1	25	1.6	52	137
20141105BG-7	0.09	2.3	1150	0.23	0.08	3.4	26	5.57	22.3	13.9	0.08	3.2	0.034	36.5	0.38	20.3	8.6	17.7	91.5	<0.002	0.02	0.36	1	1.7	369	0.88	<0.05	13	0.51	2.9	30	1	54	147.5
20141105BG-8	0.07	5.2	990	0.21	0.17	5.2	26	3.55	22.1	17.75	0.11	3.5	0.036	37.6	0.41	14.9	11.6	17.4	78.9	<0.002	0.01	0.55	1	1.9	341	0.91	<0.05	12.2	0.53	3.4	31	1.4	58	145
20141105JC-1	0.17	54	390	0.82	0.85	12.8	37	4.83	72.4	11	0.12	2.3	0.035	30.4	18.4	7.4	29.4	28	81.7	0.031	2.03	1.44	6	1.3	618	0.51	0.08	12.9	0.65	15.3	125	1.5	70	86.7
20141105JC-2	0.05	2	620	0.28	0.09	3.1	52	5.75	20.1	18.8	0.12	2.1	0.067	28.1	1.07	16.9	10.9	13.6	109.5	0.014	0.15	0.34	2	2.9	648	1.01	<0.05	13.4	0.65	5.6	66	1.7	42	76.1
20141105JC-3	0.11	12.3	510	0.52	0.45	9.1	42	7.28	42.8	12.8	0.09	1.6	0.051	233	7.25	10.3	23.7	16.8	115.5	0.027	0.59	0.74	3	1.8	592	0.61	0.17	4.9	0.59	3.1	94	1.2	79	55.8
20141105JC-4	0.06	4	1260	0.19	0.26	4.4	47	6.56	21.1	16.55	0.11	4.3	0.045	34	1.95	14.8	16.7	19.7	74.6	0.003	0.09	0.54	2	1.9	728	0.95	0.05	14	0.51	5.3	53	1.9	64	161
20141105JC-5	0.07	2.3	1230	0.24	0.08	4.9	25	5.56	20.1	19.3	0.11	5	0.046	28.4	0.53	21.1	11.8	18.7	101	<0.002	0.01	0.37	1	2.5	610	1.29	<0.05	15.6	0.55	2.8	32	1.3	60	174
20141105JC-6	0.09	1.7	2010	0.17	0.08	8	23	2.64	9.4	12.6	0.07	3	0.028	28.1	0.27	15.6	9.4	13.4	59.9	0.002	0.02	0.34	1	2	1570	0.91	<0.05	9.9	0.37	3	25	1.1	43	103.5
20141105JC-7	0.09	3	830	0.17	0.09	7.5	58	5.86	15.6	20	0.08	4.1	0.049	25.1	0.42	14.3	17.5	19.2	93.9	<0.002	0.01	0.31	2	2	492	1.03	<0.05	12	0.67	8.3	57	1.2	54	154
20141105JC-8	0.06	1.7	1150	0.19	0.11	4.3	28	4.45	14.9	13.7	0.09	3.7	0.036	33.9	0.25	22.8	9.5	15.7	91.6	<0.002	0.02	0.35	1	2.3	378	1.11	<0.05	12.4	0.44	3.1	29	0.9	45	127
20141105JC-9	0.11	2.2	1250	0.14	0.07	6.8	54	3.29	11.2	18.3	0.09	3.5	0.043	23.8	0.24	16.4	11.5	17.7	111	<0.002	0.01	0.42	2	2	497	1.04	<0.05	11.8	0.55	2.1	53	0.7	64	116
20141105JC-10	0.15	13.9	1000	0.16	0.06	8.2	20	2.82	49.4	13.3	0.1	3.1	0.027	30.3	0.39	15.8	18.6	33.7	85.9	<0.002	<0.01	0.75	1	1.3	362	0.78	<0.05	9.9	0.68	2.1	26	1.8	57	120
20141105JC-11	0.19	0.7	1580	0.14	0.05	1.6	5	1.21	8.1	14.45	0.12	4.5	0.034	8.6	0.17	29.9	2.4	17.6	77.7	<0.002	<0.01	0.23	1	1.4	491	1.48	<0.05	14.6	0.43	3.1	6	1	30	163
20141106BG-1	0.16	24.6	440	0.23	0.23	5.2	36	12.25	21.3	19.1	0.12	5.3	0.044	26.9	1.07	24.4	10.4	19.9	129.5	<0.002	0.42	1.32	3	2.3	216	1.26	<0.05	12.9	1.15	2.9	65	0.7	58	219
20141106BG-2	0.09	2.2	1650	0.18	0.13	5.8	42	4.61	18.3	16.3	0.13	4	0.034	26.5	0.32	16.4	12.6	16	120.5	<0.002	0.03	0.53	2	1.8	538	1.05	<0.05	12.7	0.66	2.2	45	0.7	45	168
20141106BG-3	0.23	5.5	1200	0.16	0.06	1.6	4	1.83	8.7	12.25	0.1	4.5	0.036	10.6	0.77	10.9	2.8	18.7	89.8	<0.002	0.01	0.37	1	1.5	434	1.48	<0.05	17.7	0.74	2.7	7	0.3	26	148
20141106BG-4	0.07	1.9	1340	0.18	0.03	1.4	4	1.78	10.4	13.95	0.1	5	0.032	10.5	0.22	21.7	2.2	19.7	102.5	<0.002	0.01	0.25	1	2.4	400	1.44	<0.05	17.9	0.77	1.8	10	1	33	170.5
20141106BG-5	0.11	7.3	1140	0.16	0.02	1.2	2	2.38	14.7	11.4	0.08	3.9	0.029	4.8	0.53	10.8	2.3	18.6	77.8	<0.002	<0.01	0.42	1	1.7	318	1.41	<0.05	16.1	0.94	2.4	5	0.3	30	141
20141106BG-6	0.08	1.6	990	0.13	0.04	5	26	3.09	15.9	11.5	0.08	3	0.032	19.6	0.25	12.3	9.6	20	76.2	<0.002	0.02	0.32	1	1.7	366	0.97	<0.05	11.6	0.39	1.4	26	1.2	49	94.5

Table 8 continued.

SAMPLE	Ag (ppm)	As (ppm)	Ba (ppm)	Bi (ppm)	Cd (ppm)	Co (ppm)	Cr (ppm)	Cs (ppm)	Cu (ppm)	Ga (ppm)	Ge (ppm)	Hf (ppm)	In (ppm)	Li (ppm)	Mo (ppm)	Nb (ppm)	Ni (ppm)	Pb (ppm)	Rb (ppm)	Re (ppm)	S(%)	Sb (ppm)	Se (ppm)	Sn (ppm)	Sr (ppm)	Ta (ppm)	Te (ppm)	Th (ppm)	Tl (ppm)	U (ppm)	V (ppm)	W (ppm)	Zn (ppm)	Zr (ppm)
20141106BG-7	0.06	6.5	890	0.19	0.11	3.7	11	2.77	12.9	14.05	0.08	3.2	0.028	14.4	1.02	14.6	6.3	16.9	77.6	<0.002	0.01	0.66	1	2.1	325	1.19	<0.05	12.9	0.45	2	16	0.4	35	111
20141106BG-8	0.07	0.7	1010	0.19	0.05	2.5	15	2.74	15.2	12.9	0.1	3.4	0.028	15.8	0.14	17.7	5.1	17	78.2	<0.002	0.01	0.28	1	2.2	317	1.23	<0.05	13.5	0.3	1.6	18	0.7	47	101
20141106BG-9	0.05	0.9	910	0.17	0.09	3.8	24	3.35	9.2	12.4	0.08	3.2	0.033	17.9	0.27	16.6	7.1	16.4	81.6	<0.002	0.01	0.31	1	2.2	323	1.08	<0.05	12.6	0.42	1.9	25	0.9	46	103.5
20141106BG-10	0.05	1.8	780	0.16	0.05	3.1	15	3.54	7.8	12.35	0.09	3	0.024	19.7	0.2	13.2	6	18.9	81.6	<0.002	0.01	0.55	1	1.8	280	1.22	<0.05	15.5	0.4	2.3	20	0.9	37	93
20141106JC-1	0.21	2.9	620	0.23	1.59	8.5	44	6.04	24	17.35	0.13	3.3	0.042	33.3	0.48	11.8	20.9	14.7	108	<0.002	0.01	0.47	2	1.7	248	0.77	0.05	9.9	0.49	2.1	61	0.8	48	122
20141106JC-2	0.14	3.4	760	0.09	0.1	5	35	3.78	15.9	10.3	0.11	2.5	0.028	39.1	0.27	8.2	9.6	11.9	53.2	<0.002	0.01	0.25	1	1.1	924	0.46	<0.05	8.5	0.28	8.1	40	0.7	28	93.6
20141106JC-3	0.11	4.4	2660	0.14	0.2	5.9	32	3.34	14.2	13.35	0.16	3.7	0.03	35.7	0.3	11.4	10.4	13.4	93.1	<0.002	0.05	0.49	1	1.5	424	0.95	<0.05	8.5	0.6	1.8	38	0.7	38	148
20141106JC-4	0.09	2.1	500	0.29	0.16	7.6	42	11.4	27.7	19.75	0.18	4.3	0.048	37.8	0.29	17.1	20.3	21.3	164	<0.002	0.03	0.45	1	2.2	158.5	1.15	0.05	15.8	0.73	2.5	60	1	66	175.5
20141106JC-5	0.22	5.7	1360	0.16	0.04	2.5	2	0.89	8.4	10.5	0.17	4.4	0.031	5.9	0.26	7.5	3.5	15.8	68.9	<0.002	0.05	0.25	1	0.8	496	1.37	<0.05	15.3	0.49	1.8	5	0.2	19	130.5
20141106JC-6	0.09	43.5	1620	0.14	0.03	1.5	11	2.74	4.9	10.55	0.16	6.1	0.039	14.4	0.57	26.2	3.5	13.2	55.4	<0.002	0.02	0.51	<1	1.5	350	1.11	<0.05	9.4	0.53	1.8	20	2.2	13	182
20141106JC-7	0.08	4	1090	0.21	0.07	4.1	25	4.11	17.9	14.25	0.16	4.2	0.038	20.6	0.23	17	9.8	20.1	113	<0.002	0.01	0.36	1	2.1	366	1.24	<0.05	15.1	0.48	2.3	28	1.1	50	134
20141106JC-8	0.08	0.9	1130	0.19	0.02	0.7	4	1.35	6.9	15.9	0.16	5.7	0.032	8.1	0.08	30.9	1.8	17.1	92.9	<0.002	0.02	0.18	1	2	415	1.52	<0.05	17.7	0.36	2.1	8	0.6	35	208
20141106JC-9	0.1	1.4	850	0.2	0.35	4.6	32	5.29	18.1	17.8	0.13	4.2	0.042	36	0.16	20.2	11	18.7	108.5	<0.002	0.09	0.39	1	2.3	373	1.29	<0.05	15.9	0.59	4.2	41	0.6	61	135.5
20141106JC-10	0.1	6.1	1330	0.21	0.04	1.7	6	2.1	7.7	12.45	0.15	5.2	0.037	9.4	0.44	25.3	2	23	84.5	<0.002	0.02	0.4	1	3.3	444	1.72	<0.05	20.2	0.48	2.5	19	1.3	34	159
20150604DB-3	<0.5	1.7	642	0.44	<0.5	1	10	4.02	5	18.7	<5	9.3	0.022	10	3	36.7	1	30	199	<0.001	0.01	0.1	0.4	7	88.2	2.8	0.01	35.4	0.18	7.12	14	2	53	327
20150604DB-4	<0.5	10.8	2700	0.57	<0.5	4	10	3.22	8	20.2	<5	11.1	0.061	30	<1	43.2	3	45	147.5	0.012	0.37	0.41	7.9	8	398	3.2	0.02	35.1	0.7	24.5	83	<1	93	407
20150604BG-1	<0.5	7.7	207	0.36	<0.5	2	10	2.13	11	16.9	<5	10.8	0.054	50	<1	45.8	4	40	89.9	0.001	0.02	0.49	2.2	8	352	3.2	0.02	50.8	0.29	5.6	418	1	73	384
20150604BG-2	<0.5	2	640	0.09	<0.5	3	20	2.06	6	13.5	<5	6.3	0.021	20	<1	11.9	6	15	83.6	<0.001	0.02	0.17	0.4	2	396	0.8	0.01	6.31	0.18	3.54	51	1	37	239
20150701DB-1	<0.5	2.5	579	0.09	<0.5	3	10	2.18	5	13.3	<5	8.5	0.04	40	<1	12.7	6	19	84.6	<0.001	0.01	0.29	0.7	2	395	0.9	0.01	16.65	0.08	5.81	48	1	49	331
20150701DB-2	<0.5	2.9	633	0.09	<0.5	3	20	2.55	7	14.4	<5	7.9	0.029	20	1	15.1	7	19	106	0.001	0.02	0.21	0.5	2	370	1.1	0.01	11.55	0.1	5.13	56	1	44	312
20150701DB-4	<0.5	3.2	917	0.14	<0.5	3	20	2.58	7	12.6	<5	6	0.023	10	1	11.6	5	14	84.8	0.001	0.01	0.16	0.6	2	1100	0.8	0.03	9.5	0.26	16.95	48	1	30	236
20150701DB-5	<0.5	4.3	638	0.07	<0.5	2	20	2.33	5	14.1	<5	9.7	0.026	30	<1	14.2	6	15	91.5	<0.001	0.03	0.2	0.8	2	610	1	<0.01	66.2	0.09	29.7	105	1	47	417
20150701DB-6	<0.5	5.4	836	0.12	<0.5	<1	10	2.81	4	13.7	<5	5.7	0.024	20	<1	14.3	3	13	115.5	0.001	0.01	0.75	0.5	3	939	1.2	0.01	30.9	1.38	16.75	37	<1	17	208
20150701DB-7	<0.5	4	528	0.11	<0.5	5	20	4.04	8	13.9	<5	7	0.028	40	<1	12.6	8	20	98.7	0.015	0.01	0.17	0.7	2	473	0.9	<0.01	19.3	0.25	17.7	49	1	49	289
20150701BG-2	<0.5	2.1	533	0.08	<0.5	1	10	1.35	4	9.2	<5	3.9	0.028	10	<1	8	3	15	56	0.001	0.01	0.15	0.8	2	673	0.6	0.02	10.35	0.13	13.95	32	1	27	164
20150702DB-1	<0.5	0.6	564	0.02	<0.5	1	10	2.94	4	11.9	<5	2.6	0.006	20	1	11.8	4	14	133	<0.001	0.01	0.08	0.2	1	161	1.1	<0.01	13.65	0.04	4.28	68	1	29	90
20150819DB-2	<0.5	1.9	1685	0.14	<0.5	4	30	2.14	10	14.5	<5	4.3	0.024	30	<1	10.4	10	15	61.3	<0.001	0.01	0.15	0.5	2	1765	0.8	0.01	7.06	0.26	3.98	92	<1	44	165
20150820DB-2	<0.5	2.5	1565	0.49	<0.5	4	10	3.08	13	16.3	<5	4.5	0.014	10	1	7	10	33	65.6	<0.001	0.06	0.27	0.3	1	769	1.6	0.01	5.89	0.33	0.87	31	1	41	172
20150819BG-1	<0.5	<0.1	3340	0.14	<0.5	3	20	2.02	8	15.3	<5	6.9	0.037	40	<1	22.6	10	17	47	<0.001	<0.01	<0.05	0.4	3	1615	2.2	0.01	10.3	0.18	0.44	35	3	51	229
20150819BG-2	<0.5	14.8	5850	0.29	<0.5	1	10	1.34	10	22.6	<5	8.5	0.076	10	2	29	12	29	43.9	0.009	0.1	0.39	0.7	6	2610	4.5	0.02	19	0.98	0.77	26	2	58	230
20150819BG-3	<0.5	0.3	3830	0.28	<0.5	4	30	1.89	14	22.5	<5	8	0.068	20	<1	35.8	22	30	63.3	0.003	0.02	0.07	0.6	5	1985	4	0.02	12.55	0.76	0.61	39	1	100	214

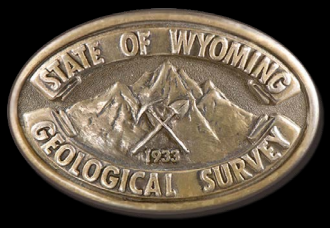

Interpreting the past, providing for the future